

CIRCUMSTELLAR DISKS AT WHITE DWARFS: OBSERVATIONS

J. Farihi¹

1. INTRODUCTION

A circumstellar disk or ring is particulate matter that surrounds a star and is primarily confined to the plane of stellar rotation. Thus, disks distinguish themselves from spherical clouds or envelopes of gas (and dust) that typically surround protostellar objects and evolved giant stars. Circumstellar disks appear at every stage of stellar evolution, though the origin of the orbiting material is not always clearly understood. Pre-main sequence stars accrete material from a disk that is the flattened remnant of the cloud out of which they formed. Disks found at young stars in subsequent evolutionary stages are the likely site of planet formation, migration, and sometimes destruction. Mature main-sequence stars exhibit dusty disks owing to recent or ongoing energetic collisions among orbiting asteroid or comet analogs, commonly referred to as the “Vega Phenomenon” (named after the first star observed to have orbiting, non-stellar material). Several first-ascent and asymptotic giant stars are also known to have circumstellar disks, though their origins are still debated with hypotheses ranging from debris in a cold cometary cloud to consumed stellar companions. For a thorough (pre-*Spitzer*) review, see Zuckerman (2001).

White dwarfs are a relatively recent addition to the list of stellar objects with circumstellar disks, as their intrinsic faintness and the infrared-bright sky have conspired to keep them hidden. The last six years have seen a profusion of white dwarf disk discoveries, due primarily to the 2003 launch and unprecedented infrared performance of the *Spitzer Space Telescope*, while ground-based projects with large sky coverage such as the Sloan Digital Sky Survey and the Two Micron All Sky Survey have also played important roles. Given the small radii of white dwarfs, and because circumstellar material derives its luminosity from the central star, disk observations at white dwarfs are challenging.

¹Department of Physics & Astronomy, University of Leicester, Leicester LE1 7RH, UK; jf123@star.le.ac.uk

2. HISTORY AND BACKGROUND

Developed in the fifties and sixties, the first photoelectric detectors for infrared¹ astronomy were revolutionary (McLean 1997), but restricted to luminous sources, especially at wavelengths beyond $3\mu\text{m}$ where the sky itself is bright and variable. Even so, the circumstellar disk at Vega, one of the brightest stars in the sky, was not discovered until 1983 with the launch of the *Infrared Astronomical Satellite (IRAS)*. Despite the unprecedented sensitivity and all-sky coverage of *IRAS*, the detection of dust at white dwarfs had to await the development of more sensitive infrared detectors and arrays.

2.1. Early Searches

Infrared excess emission associated with a star can arise from heated circumstellar dust or from a self-luminous companion. Owing to their compact nature, white dwarfs can be easily outshone by low mass stellar and brown dwarf companions. This fact led Probst (1981) to search a large sample of nearby white dwarfs for near-infrared *JHK* photometric excess to study the luminosity function of the lowest mass stars and brown dwarfs (Probst 1983; Probst & O’Connell 1982). This was the first search for infrared excess at white dwarfs, and Probst deserves the credit for an insight that is now taken for granted and which fostered an abundance of subsequent infrared work on white dwarfs.

The first mid-infrared search for excess emission from white dwarfs was similarly motivated by the potential identification of brown dwarf companions. Shipman (1986) carried out a cross correlation of *IRAS* catalog point sources with known, nearby white dwarfs, but the search did not produce any detections. This is perhaps unsurprising given that *IRAS* was only sensitive to point sources brighter than 500 mJy at its shortest wavelength bandpass of $12\mu\text{m}$, while the brightest white dwarf in the sky (Sirius B) should only be around 5 mJy at that wavelength.

2.2. The Discovery of Infrared Excess at G29-38

Inspired by the work of Probst and armed with a rapidly evolving set of infrared detectors atop Mauna Kea at the NASA Infrared Telescope Facility (IRTF), Zuckerman & Becklin

¹Here, the terms near-, mid-, and far-infrared refer to the wavelength ranges $1 - 5\mu\text{m}$, $5 - 30\mu\text{m}$, and $30 - 200\mu\text{m}$, though alternative divisions and definitions exist (McLean 1997).

(1987b) detected the first white dwarf with infrared excess that was not associated with a stellar companion; G29-38. Photometric observations at three bandpasses longward of $2\,\mu\text{m}$ revealed flux in excess of that expected for the stellar photosphere of this relatively cool, $T_{\text{eff}} = 11\,500\,\text{K}$ white dwarf (Figure 1). Because the prime motivation behind the observations was to search for substellar companions, the infrared excess was attributed to a spatially unresolved brown dwarf. Interestingly, circumstellar dust as warm as $1000\,\text{K}$ was not favored due to the likelihood of rapid dissipation due to ongoing accretion and radiation drag. Zuckerman & Becklin (1987b) prophetically noted that if a disk of material were orbiting close enough to reach such high temperatures, then spectral signatures of accretion should be seen (at the time, its atmospheric metals had not yet been detected).

Over the next few years, the infrared emission at G29-38 was studied intensely by many groups, and its unique properties sparked interest across many subfields of astrophysics research: brown dwarf and planet hunters, astroseismologists, infrared astronomers, and white dwarf pundits. Observational evidence gradually began to disfavor a brown dwarf as the source of infrared emission. First, some of the first near-infrared imaging arrays revealed G29-38 to be a point source in several bandpasses. Second, near-infrared spectroscopy measured a continuum flux source (Tokunaga et al. 1988), whereas a very cool atmosphere was expected to exhibit absorption features. Third, the detection of optical stellar pulsations echoed in the near-infrared were difficult to reconcile with a brown dwarf secondary (Patterson et al. 1991; Graham et al. 1990). Fourth, significant $10\,\mu\text{m}$ emission was detected at G29-38, a few times greater than expected for a cool object with the radius of Jupiter, essentially ruling out the brown dwarf companion hypothesis (Tokunaga et al. 1990; Telesco et al. 1990).

Some lingering doubt remained that G29-38 was indeed surrounded by very warm dust, but variations seen in radial velocity (Barnbaum & Zuckerman 1992) and pulse arrival times (Kleinman et al. 1994) were never successfully attributed to an orbiting companion. A decade after the discovery of its infrared excess, the optical and ultraviolet spectroscopic detection of multiple metal species in the atmosphere of G29-38 (Koester et al. 1997) made it clear the star is currently accreting from its circumstellar environs (Figure 2).

2.3. The Polluted Nature of Metal-Rich White Dwarfs

It would not be possible to tell the story of G29-38 and subsequent disk detections at white dwarfs without introducing the phenomenon of atmospheric metal contamination. The origin and abundances of photospheric metals in isolated white dwarfs has been an astrophysical curiosity dating back to the era when the first few white dwarfs were finally understood to be subluminescent via the combination of spectra and parallax (van Maanen

1919). In a half page journal entry, van Maanen (1917) noted that his accidentally discovered faint star with large proper motion had a spectral type of “about F0”, almost certainly based on its strong calcium H and K absorption features (Figure 3). Only four decades later did it become clear that vMa 2 was metal-poor with respect to the Sun (Weidemann 1960). Over the next decade and a half, it became gradually understood that white dwarfs (as a class) had metal abundances a few to several orders of magnitude below solar (Wehrse 1975; Wegner 1972).

Any primordial heavy elements in white dwarfs can only be sustained in their photospheres for the brief period while the degenerate is still rather hot and contracting, and then only to a certain degree (Chayer et al. 1995). For $T_{\text{eff}} < 25,000$ K, gravitational settling is enhanced by the onset of convection and heavy elements sink rapidly in the high surface gravity atmospheres of white dwarfs (Alcock & Illarionov 1980; Fontaine & Michaud 1979; Vauclair et al. 1979) leaving behind only hydrogen or helium. Downward diffusion timescales for heavy elements in cool white dwarfs are always orders of magnitude shorter than their evolutionary (cooling) timescales (Paquette et al. 1986), and thus external sources are responsible for the presence of any metals within their photospheres.

The term “metal-rich” is used (somewhat ironically) to refer to cool white dwarfs that have trace abundances of atmospheric heavy elements. These are either hydrogen- or helium-rich atmosphere white dwarfs whose optical spectra exhibit the calcium K absorption line; the same atomic transition that is strongest in the Sun. While iron and magnesium absorption features are detected in the optical spectra for a substantial fraction of these stars, and additional elements are seen in a few cases, all currently known metal-rich white dwarfs display the calcium K line.

[White dwarfs in binary systems may accrete heavy elements from a companion star via Roche lobe overflow or wind capture (e.g. cataclysmic variables), but the discussion here is restricted to white dwarfs that lack close stellar companions. The topic of gaseous accretion disks at white dwarfs resulting from binary mass transfer is not discussed here.]

2.4. Interstellar or Circumstellar Matter

There are two possible sources for the atmospheric metals seen in cool, single white dwarfs: accretion from the interstellar medium or from its immediate circumstellar environment. The latter case refers to material physically associated with the white dwarf and its formation (i.e. in simplest terms, a remnant planetary system) as opposed to a local accumulation of matter with distinct origins. In both cases, the accretion of heavy elements

necessary to enrich the white dwarf atmosphere may be accompanied by the formation of a circumstellar disk. Thus, for cool white dwarfs the phenomena of photospheric metals and circumstellar disks are likely to have a profound physical connection.

Historically, accretion from the interstellar medium was the most widely accepted hypothesis for the metals detected in cool white dwarfs. This was perhaps all or for the most part due to the fact that until 1983, all metal absorption features detected in cool white dwarfs were the result of relatively transparent, helium-dominated atmospheres (Sion et al. 1990b). Such stars (referred to here as type DBZ) have relatively deep convection zones and commensurately long timescales for the downward diffusion of heavy elements, up to 10^6 yr (Paquette et al. 1986). This allows for the possibility that their extant photospheric metals could be remnants of a interstellar cloud encounter several diffusion timescales prior (Dupuis et al. 1993a,b, 1992). However, the general lack of significant hydrogen in DBZ stars has been a continually recognized and glaring drawback for the interstellar accretion hypothesis (Aannestad et al. 1993; Wesemael 1979; Koester 1976).

The confirmation of the first cool, hydrogen atmosphere white dwarf with metal absorption (G74-7, type DAZ; Lacombe et al. 1983) presented a new challenge to the idea of interstellar cloud accretion. It took some time for robust stellar models to emerge, but it was basically understood that DA white dwarfs have relatively thin convection zones and correspondingly short metal diffusion timescales. These span a wide range from a matter of days in warmer stars like G29-38 all the way up to a few 10^3 yr for relatively cool stars such as G74-7 (Paquette et al. 1986). Compared to all previously known metal-enriched white dwarfs, it was clear that the first DAZ star had experienced a recent accretion event. This led to the idea that comet impacts could be responsible for the photospheric metals in polluted white dwarfs (Alcock et al. 1986).

The strength of the cometary impact model was that it capitalized on the the hydrogen-poor nature of the accreted material in the numerous DBZ stars (Sion et al. 1990a), yet it was difficult to reconcile with the lack of detected DAZ stars, as only G74-7 was known at the time (Alcock et al. 1986). This apparent dearth of DAZ stars was eventually understood as an observational bias due to the relatively high opacity of hydrogen atmospheres compared to those composed primarily of helium (Dupuis et al. 1993b; see Figures 2 and 3). The eventual detection of atmospheric metals in numerous cool, hydrogen-rich white dwarfs required the combination of large telescopes and high-resolution spectroscopy (Zuckerman & Reid 1998). While these detections presented a challenge to the interstellar accretion hypothesis, they failed to breathe new life into the cometary impact model. For example, the second DAZ white dwarf to be found, G238-44 (Holberg et al. 1997), has a metal diffusion timescale of only a few days, and an unlikely, continuous rain of comets is needed to account for its metal

abundance (Holberg et al. 1997).

2.5. G29-38 and the Asteroid Accretion Model

Thus did the study of metal-enriched white dwarfs come to somewhat of a historic crossroads circa 2003, a few months prior to the launch of the *Spitzer Space Telescope*. With the sole exception of G29-38 there was a distinct lack of reliable (infrared) data on the circumstellar environments of white dwarfs, yet a growing profusion of stars contaminated by metals, and problems with existing hypotheses (Zuckerman et al. 2003). Because of their long metal dwell times, the contamination measured in DBZ stars with trace hydrogen could be made consistent with interstellar accretion models. But the marked lack of marked lack of dense interstellar clouds within 100 pc of the Sun (i.e. the Local Bubble; Welsh et al. 1999, 1994) made this picture difficult to reconcile with the existence of DAZ stars. In particular, the necessity for ongoing, high-rate accretion of heavy elements at some DAZ stars (e.g. G238-44) rendered both the cometary impact and the interstellar cloud models unattractive and unlikely. Lacking a detailed model, Sion et al. (1990a) had speculated that asteroidal or planetary debris could be the ultimate source of the photospheric metals in hydrogen-poor DBZ white dwarfs.

In a short but seminal paper, Jura (2003) modeled the observed properties of G29-38 by invoking a tidally-destroyed minor planet (i.e. asteroid) that generates an opaque, flat ring of dust analogous to the rings of Saturn. Rather than impacting the star, an asteroid perturbed into a highly eccentric orbit makes a close approach to the white dwarf, passes within its Roche limit and is torn apart by tidal gravity. Ensuing collisions reduce the fragments to rubble and dust, and the resulting disk of material rapidly relaxes into a flat configuration owing to a range of very short ($P \sim 1$ hr) orbital periods. The closely orbiting dust is heated by the star producing an infrared excess, and slowly rains down onto the stellar surface, polluting its otherwise-pristine atmosphere with heavy elements. The bulk of a flat disk is shielded from the full light of the central star, allowing dust grains to persist for timescales longer than permitted by radiation drag forces. This model compared well to all the available infrared data on G29-38, including *Infrared Space Observatory (ISO)* 7 and $15\mu\text{m}$ photometry (Chary et al. 1999).

3. PRE-*SPITZER* AND GROUND-BASED OBSERVATIONS

3.1. Photometric Searches for Near-Infrared Excess

The infrared excess and photospheric metals in G29-38 gave astronomers an empirical model to test at other white dwarfs prior to the asteroid accretion model. Because the dust emission at G29-38 is prominent beginning at $2\,\mu\text{m}$ (i.e. the K band), an obvious starting point would be to search for white dwarfs with similar near-infrared excess detectable with ground-based photometry. As mentioned previously, the excess at G29-38 was found in just such a survey, but aimed at identifying unevolved, low mass companions such as brown dwarfs. Although the authors did not state the result, Zuckerman & Becklin (1992) found no candidate analogs to G29-38 among JHK photometry of roughly 200 white dwarfs searched for near-infrared excess. Although Zuckerman & Becklin continued to take similar data for white dwarfs over the next several years, very little was published on the topic until the *Spitzer* era.

Three photometric studies again aimed at identifying low mass stellar and brown dwarf companions to white dwarfs were published beginning in 2000. Green et al. (2000) surveyed around 60 extreme ultraviolet-selected white dwarfs at JK and identified a few stars with near-infrared excess consistent with stellar companions. These stars are too hot for any photospheric metals to be considered pollutants, and they did not search for mild K -band excesses that might be expected from circumstellar dust. Farihi et al. (2005a) published the cumulative results of a decade and a half of near-infrared observations of white dwarfs begun by Zuckerman & Becklin. Among 371 white dwarfs, the study included over two dozen white dwarfs with a K -band excess from cool secondary stars, but no candidates for dusty white dwarfs. However, only roughly one third of the sample stars had independent JK photometry while data for the remainder of the sample was taken from the Two Micron All Sky Survey (2MASS; Skrutskie et al. 2006).

Wachter et al. (2003) and later Hoard et al. (2007) published the results of a cross-correlation between the 2249 entries in the white dwarf catalog of McCook & Sion (1999) and the 2MASS point source catalog second and final data releases. This enormous undertaking found a few dozen previously unidentified white dwarfs with infrared excess owing to cool stellar companions. But although G29-38 satisfied their criteria for infrared excess, the search found no other candidates with similar colors; a startling result when taken at face value. However, the sensitivity limits of 2MASS, particularly in the K_s band, often prevent reliable flux estimates for white dwarfs. A typical catalog entry in McCook & Sion (1999) has $V \sim 15$ mag and near zero optical and infrared colors, so that its predicted near-infrared magnitudes should be similar. Unfortunately 2MASS K_s -band data becomes increasingly

unreliable for sources fainter than $K_s = 14$ mag, severely limiting a robust dust search at a large number of nearby white dwarfs (Farihi 2009).

3.2. Metal-Polluted White Dwarf Discoveries

Over a period of time spilling over into the first couple of years after the launch of *Spitzer*, there were two major surveys of white dwarfs using high-resolution optical spectrographs on the world’s largest telescopes. Zuckerman et al. (2003) published a survey of nearly 120 cool DA white dwarfs with the HIRES spectrograph on the Keck I telescope. The study specifically aimed to detect photospheric metals in $T_{\text{eff}} \lesssim 10,000$ K, hydrogen-rich white dwarfs and was highly successful. Overall, 24 new DAZ stars were identified via the calcium K-line, including 5 that were known to have detached, low mass main-sequence companions (Zuckerman et al. 2003). The study of Zuckerman et al. (2003) underscored the fact that photospheric metals in DA white dwarf produce weak optical absorption features that require high-powered instruments in order to be detected; nearly all of their detections had equivalent widths smaller than 0.5 \AA .

Less than two years later, Koester et al. (2005b) published a sub-sample of stars from the Supernova Progenitor Survey (SPY; Napiwotzki et al. 2003) which observed over one thousand white dwarfs with the UVES spectrograph on the Very Large Telescope (VLT) unit 2. This extensive survey aimed to identify radial velocity variable, double degenerate binaries and thus required high spectral resolution. But as a by-product, the search uncovered 18 new DAZ and nine new DBZ stars among warmer, $T_{\text{eff}} \gtrsim 10,000$ K white dwarfs, all displaying weak calcium K lines with equivalent widths less than 0.3 \AA (Koester et al. 2005a,b). Importantly, nearly 500 DA stars of various temperatures were searched for calcium K line absorption and upper limit abundances determined for null detections (Figure 4). These results provide a visually straightforward demonstration of the observational bias against the optical detection of metals in warmer white dwarfs.

3.3. The Spectacular Case of GD 362

The second white dwarf discovered to have circumstellar dust came 18 years(!) after G29-38 and resulted from two groups simultaneously recognizing the significance of its very metal-rich spectrum. Gianninas et al. (2004) reported the optical spectrum of GD 362 had the strongest calcium lines seen in any DA star to date (Figure 5), strong lines of magnesium

and iron, and nearly *solar* abundances of these elements². The authors concluded the cool star was too nearby to have attained its spectacular metal content from an interstellar cloud, but otherwise offered no explanation for their amazing find.

The significance of the spectacular pollution in this star was evident to at least two groups of astronomers, each involved in the early stages of *Spitzer* programs on white dwarfs. Using different observational methods, both teams simultaneously published evidence for a circumstellar disk at GD 362 in the same issue of the *Astrophysical Journal*. Chronologically, Kilic et al. (2005) observed the white dwarf first, using low-resolution near-infrared spectroscopy at $0.8 - 2.5 \mu\text{m}$. Their spectrum revealed continuum excess beginning near $2.0 \mu\text{m}$, matched well by adding 700 K blackbody radiation to the expected stellar flux. The authors inferred that the infrared emission is due to heated circumstellar dust but neither modeled nor constrained its physical characteristics or origin.

Becklin et al. (2005) performed ground-based, mid-infrared photometric observations of GD 362 and detected the source in the N' band ($11.3 \mu\text{m}$) at 1.4 mJy (Figure 6). Because the expected flux from the stellar photosphere at this wavelength is only 0.01 mJy, the detection by itself is strong evidence for warm dust. Becklin et al. (2005) also obtained near-infrared $JHKL'$ photometry, constraining the spectral energy distribution of the infrared excess, and revealing that the emitting surface area was too large for a substellar companion. They employed the flat dust ring model of Jura (2003) to the infrared emission at GD 362 and showed that the innermost dust is located within 10 stellar radii and has a temperature around 1200 K, where typical dust grains rapidly sublimate. Thus, the location of the dust was found to be consistent with a tidally disrupted minor planet, and the resulting circumstellar disk the probable source of the accreted metals.

The JHK photometry for GD 362 was probably insufficient to confidently establish the presence of circumstellar dust. While the K -band photometry reveals a 10% excess over the expected photospheric flux, the confidence was less than 3σ , and hence the need for the L' - and N' -band measurements. Whereas the spectroscopy constrains the shape of any excess, whether a continuum (e.g. dust) or having absorption features (e.g. substellar companions).

²I was on the phone to my collaborators within minutes of reading the GD 362 discovery paper, making sure the group planned to observe the star when it rose again a few months later.

3.4. Spectroscopic Searches for Near-Infrared Excess

The success of the near-infrared spectroscopic detection of excess emission at GD 362 was soon repeated. Kilic et al. (2006) detected a very strong continuum excess at the metal-rich white dwarf GD 56 (Figure 7), sufficient to produce a photometric excess in the H -band (Farihi 2009) and stronger overall than the near-infrared excesses at both G29-38 and GD 362. This discovery accompanied the first published survey for near-infrared excess that specifically targeted metal-rich white dwarfs. Among 18 DAZ stars, the search identified two additional targets with marginal K -band excesses; GD 133 and PG 1015+161. In both cases the potential excess was considered too uncertain due to relatively low signal-to-noise (S/N) or nearby sources of potential confusion (Kilic et al. 2006), and no conclusions were made for these stars. Using the same technique roughly one year later, Kilic & Redfield (2007) identified a continuum K -band excess at one more metal-enriched white dwarf, EC 11507–1519 (also Figure 7).

Generally, near-infrared data alone cannot distinguish between various dust emission models, as the excess at these wavelengths only represents ‘the tip of the iceberg’ (as shown later). The near-infrared excesses measured at GD 56 and EC 11507–1519 were attributed to $T \approx 900$ K dust rather than substellar companions, the distribution of the orbiting material was not modeled (Kilic & Redfield 2007; Kilic et al. 2006). Hence, the science that emerged from these few years of discoveries made in the near-infrared were generally qualitative and provided some statistical limits on the frequency of DAZ dust disk emission similar to that of G29-38. An identical search of 15 DBZ stars (Kilic et al. 2008) failed to produce any new dust disks, but again provided some limiting statistics on the frequency of metal-rich white dwarfs with warm circumstellar dust. With hindsight, there were as many as six white dwarfs with circumstellar dust that went unidentified in these near-infrared spectroscopic observations.

3.5. Spectroscopy at Longer Wavelengths

There are few sufficiently bright, metal-rich white dwarfs that can be observed from the ground in a variety of infrared modes. Tokunaga et al. (1990) obtained a noisy yet pioneering, IRTF low-resolution spectrum of G29-38 between roughly 3 and $4\mu\text{m}$ with an early generation near-infrared spectrometer. The authors concluded no spectral features were present, specifically not those typically seen in comets. By modern standards, the data quality was insufficient to draw a firm conclusion. Thus, many years later their experiment was repeated with an 8 meter telescope and 21st century instrumentation. No spectral features were detected (Figure 8), but the data were of sufficient quality to rule out a variety

of hydrocarbon emission features associated with comets, the interstellar medium, and a variety of nebulae (Farihi et al. 2008b).

4. THE INITIAL IMPACT OF *SPITZER*

Prior to the launch of *Spitzer*, there was only a single previously published, mid-infrared study of white dwarfs; an *ISO* search for dust emission at 11 nearby white dwarfs, six of which have metal-enriched photospheres (Chary et al. 1999). The *ISO* imaging exposures were executed in bandpasses centered near 7 and 15 μm , and included observations of G29-38, G238-44, and vMa2. Most of the white dwarfs were detected at 7 μm but only a few were sufficiently bright to be seen at 15 μm , yet all measured fluxes were consistent with photospheric emission with the sole exception of G29-38. These data eventually formed part of the basis for the flat dust ring model hypothesized by Jura (2003).

4.1. Infrared Capabilities of the *Spitzer Space Telescope*

Spitzer opened up a previously-obscured space to white dwarf researchers, and a few groups were primed to take advantage of its promised, unprecedented sensitivity to substellar companions and circumstellar dust at mid-infrared wavelengths. The entire observatory was cryogenically cooled to 5.5 K which prevented the facility from being a significant source of thermal background radiation for its instruments. *Spitzer* was launched in late 2003 with three instruments that had the capability to detect sources at the μJy level (Werner et al. 2004). The Infrared Array Camera (IRAC; Fazio et al. 2004a) is a dual-channel, near- and mid-infrared imager with filters centered at 3.6, 4.5, 5.8, and 7.9 μm . The Infrared Spectrograph (IRS; Houck et al. 2004) provided low and moderate-resolution spectroscopy between 5 and 40 μm , plus limited field of view imaging at 16 and 22 μm . The Multi-Band Imaging Photometer for *Spitzer* (MIPS; Rieke et al. 2004) produced imaging and photometry in three wide bandpasses at 24, 70, and 160 μm . At the time of writing, the cryogenic lifetime of the observatory has finished, and only near-infrared observations are possible during its warm mission.

4.2. First Results

Results from the first two years of *Spitzer* white dwarf observations did not emerge chronologically as they were proposed or obtained, and were heavily influenced by a rapidly

evolving field. At the time observing proposals from the general community were solicited in late 2003 (and before the deadline arrived in early 2004), only the DAZ study of Zuckerman et al. (2003) had been published, and highly metal-enriched atmosphere of GD 362 had not yet been discovered. The ground-based disk searches and further metal-rich white dwarf discoveries published in 2005 both had an understandable impact on evolving programs and proposals to use the observatory.

4.2.1. G29-38

Readers will not be surprised to learn that the most highly sought *Spitzer* white dwarf target was G29-38. Utilizing all three observatory instruments Reach et al. (2005a) imaged the prototype dusty white dwarf at 4.5, 7.9, 16, and $24\,\mu\text{m}$, and obtained a low-resolution spectrum between 5 and $15\,\mu\text{m}$. These data represented three major advances relative to previous infrared observations of G29-38. First, the 2% to 5% photometry at $3 - 8\,\mu\text{m}$ were by far the most accurate data obtained for the star. Second, the mid-infrared photometry included novel, longer wavelength coverage and the first observations at $\lambda \geq 10\,\mu\text{m}$ with total errors better than 20%. Third and most significant scientifically, the spectroscopy over a wide range of mid-infrared wavelengths at $S/N > 20$ was unprecedented.

Figure 9 displays these *Spitzer* data for G29-38, revealing both a strong thermal continuum of $T \approx 900\,\text{K}$, and a remarkable $9 - 11\,\mu\text{m}$ silicate dust emission feature. A comparison of the shape of its silicate emission to that observed in the interstellar medium, the envelope of the mass-losing giant star Mira, comet Hale-Bopp, and the zodiacal cloud was the first concrete evidence that the dust at G29-38 had a circumstellar, and hence planetary, origin. Notably, its spectrum does not exhibit signatures of polycyclic aromatic hydrocarbon (PAH) molecules, which often dominate the mid-infrared spectra of the interstellar medium (Draine 2003; Allamandola et al. 1989). The appearance of the $9 - 11\,\mu\text{m}$ feature (Figure 10) at G29-38 differs from interstellar silicates and also from silicates forming in the ejecta of Mira (particles that will eventually become part of the interstellar medium). Of the four distinct sources compared to G29-38, its emission most resembles the emission from the rocky particles of the zodiacal cloud.

Reach et al. (2005a) modeled both the warm thermal continuum and the silicate emission with an optically thin, circumstellar cloud (i.e. a spherical shell or flattened disk) of dust with an exponentially decreasing radial profile. The model invoked micron-sized olivine (plus some forsterite) dust to account for the strong emission feature and similarly small carbon grains to account for the thermal continuum. Silicates are common in the debris of short-period comets and asteroids in the Solar System, hence the dust at G29-38 is consis-

tent with planetary materials (Lisse et al. 2006). The authors did note that the lack of PAH features in the spectrum was potentially inconsistent with the presence of carbon grains at a ratio of 3:1 to the silicate grains, as in their model. It is likely that carbon for its featureless infrared spectrum, rather than a likely constituent of planetary debris, as externally polluted white dwarfs only rarely show signatures of carbon (Jura 2006).

The fundamental difference between this model and the disk model of Jura (2003) is the assumed optical depth of the disk material at various wavelengths. In the geometrically flat, vertically optically thick model of Jura (2003), the bulk of material is unseen and effectively shielded from stellar radiation. Such a disk is heated by absorption of ultraviolet radiation – often a major or the dominant source of radiant energy in white dwarfs – and the warmest dust grains are located within a few tenths of a solar radius. In order to absorb and re-emit up to 3% of the stellar luminosity as does G29-38, a flat disk must be seen in a near face-on configuration. For optically thick disk material, it is only possible to infer a minimum mass as most of the material is hidden by definition. In contrast, the optically thin model proposed by Reach et al. (2005a) yields a total disk mass from the infrared emission; for G29-38 this model predicts of order 10^{18} g of small dust grains, and potentially more mass contained in larger, inefficiently emitting, particles.

Critically, optically thin dust grains are warmed by the full starlight of the host star and located at a few to several solar radii in the case of G29-38. Poynting-Robertson (PR) or radiation drag will cause exposed dust particles to spiral in towards G29-38 on timescales of a few years (Reach et al. 2005a). Without a source of replenishment for this closely orbiting dust, it is difficult to reconcile optically thin emission at G29-38 over an 18 year period between its discovery and the first *Spitzer* observations.

4.2.2. GD 362

Naturally, the discovery of infrared excess on top of spectacular metal-enrichment at GD 362 made it an obvious *Spitzer* target. Jura et al. (2007b) conducted observations of GD 362 with IRAC 3 – 8 μm photometry, IRS 5 – 15 μm low-resolution spectroscopy, and MIPS 24 μm photometry. These observations detected a striking silicate feature sufficient in strength to influence the 7.9 μm IRAC photometry and by itself re-emit 1% of the stellar luminosity (Figure 11). While the 9 – 11 μm feature measured at G29-38 is quite strong, the emission detected at GD 362 is simply *towering*; among mature stellar systems, only the very dusty main-sequence star BD +20 307 (Song et al. 2005), has a comparably strong silicate emission feature. As in the case of G29-38, the 24 μm photometry indicates a lack of cool dust, and an outer...

Jura et al. (2007b) modeled the entire infrared emission with a more sophisticated version of the geometrically thin, vertically optically thick disk model used for G29-38. The model consisted of three radially concentric and distinct regions within a flat disk geometry: two inner, opaque regions and an optically thin outer region. The innermost region was required to be vertically isothermal, and the middle region was modeled to have a temperature gradient between its top and middle layers. The outermost region was then modeled to be the source of the silicate emission, and generally warmer than the middle region due to the change in optical depth Jura et al. (2007b). Importantly, the modeled disk at GD 362 had a *finite* radial extent, and was contained entirely within $1 R_{\odot}$ of the white dwarf where rocky bodies such as large asteroids should be tidally-destroyed (Davidsson 1999). Remarkably, a strictly flat disk model does not have sufficient surface area (i.e. cannot intercept enough starlight) to account for the prodigious, overall infrared emission from GD 362; an warp or slight flaring in the (outer) disk was necessary to reproduce the data.

Again, the main difference between the models of Jura et al. (2007b) and Reach et al. (2005a) is the relative transparency or opaqueness of the disks. For a star like GD 362 which contains more than 10^{22} g of metals in its convection zone (Koester 2009), it is all but certain the disk is more massive than the minimum 10^{18} g of optically thin material required to account for its silicate emission.

4.3. The First *Spitzer* Surveys of White Dwarfs

There were four programs approved in the first cycle of *Spitzer* that aimed to detect infrared excess at white dwarfs. Most of these programs actively sought an excess from substellar or planetary companions in addition to searching for dust similar to that seen at G29-38. On the one hand, the frequency of brown dwarfs and planets at the intermediate-mass, main-sequence progenitors of white dwarfs constrains theories of star and planet formation. The direct or indirect detection of such low-mass objects at A- and early F-type stars ranges from very difficult to impossible compared to their detection at the white dwarf descendants (Farihi et al. 2008b). On the other hand, one possible origin for the photospheric metals in cool white dwarfs is wind capture from an unseen, low-mass stellar or substellar companion (Zuckerman & Reid 1998; Holberg et al. 1997). Zuckerman et al. (2003) reported a 60% fraction of metal-enrichment among DA white dwarfs with close or very close (i.e. spatially unresolved from the ground or known radial velocity variables), low-mass, main-sequence companions. Therefore, *Spitzer* was primed to detect various astrophysical sources that might account for metal contamination observed in cool white dwarfs.

4.3.1. *An Unbiased Survey*

The largest *Spitzer* survey of white dwarfs to date was carried out in its first cycle and observed 124 stars selected for brightness at near-infrared wavelengths from their data in the 2MASS catalog (Mullally et al. 2007). No preference was given to metal-rich white dwarfs, but the brightness-selected sample included G29-38 and 11 other cool stars with photospheric metals. For reasons of efficiency, each of the targets was observed with IRAC at 4.5 and 7.9 μm only, as IRAC is capable of simultaneous exposures at one near- and one mid-infrared bandpass. Of the 12 externally polluted white dwarfs, only G29-38 (the IRAC photometry published by Reach et al. 2005a was a party of this survey) and LTT 8452 were found to have infrared excesses consistent with circumstellar dust (von Hippel et al. 2007). Perhaps even more profound is the result that of 112 white dwarfs not considered to be externally polluted, none had an infrared excess attributable to a disk. One must keep in mind that roughly one quarter of the stars in their search had effective temperatures above 25,000 K, and that the bulk of white dwarfs in the sample had not been observed with high-resolution spectroscopy necessary to detect modest metal abundances. Therefore some caution is warranted when interpreting this result, but tentatively speaking, no disks are detected at white dwarfs that are not metal-polluted.

The metal-enriched stars in their sample were rather diverse in effective temperature, calcium abundances, and basic atmospheric composition (i.e. both DAZ and DBZ stars), and the authors did not try to draw any statistical conclusions on the basis of these two disk detections. Nevertheless, they demonstrated that the opaque, flat disk model fit the available photometric data on all known white dwarfs with disks at the time of publication (G29-38, GD 362, GD 56, and LTT 8452; Figure 13). Importantly, the authors concluded that the analogy with planetary rings suggests viscous spreading lifetimes on par with the Gyr cooling ages of white dwarfs, and therefore such a disk does not require replenishment as in the optically thin dust model.

4.3.2. *Surveys of DAZ White Dwarfs*

Together, both Debes et al. (2007) and Farihi et al. (2008b) targeted 18 cool DAZ stars from Zuckerman et al. (2003) with IRAC imaging observations at all four wavelengths, including the prototype DAZ white dwarf G74-7. Given the proliferation of disk discoveries occurring at that time, it was fairly disappointing and somewhat surprising that neither of the two surveys identified any stars with infrared excess similar to G29-38 and other dusty white dwarfs. Debes et al. (2007) suggested that rapid dust depletion due to PR drag within the tidal disruption radius of the white dwarf could be responsible for the absence of

disks. The four DAZ stars observed by Debes et al. (2007) have temperatures below 9000 K and hence metal diffusion timescales longer than 100 yr (Koester & Wilken 2006); a ‘recent’ absence of dust is conceivable for these stars, if the accreted disk material was originally optically thin.

Farihi et al. (2008b) surveyed several DAZ stars warmer than 9,000 K and a few warmer than 10,000 K where the observed metal abundances essentially require ongoing accretion and for which an absence of orbiting material would be difficult to reconcile. They hypothesized that collisions between grains in an developing disk could rapidly destroy dust particles while preserving the circumstellar material – in gaseous form, primarily – necessary for the inferred, ongoing accretion. A simple calculation showed that optically thin material within the Roche limit of a white dwarf will collide on timescales 10 to 30 times faster than their PR timescales, and thus a ring of gaseous debris might develop instead of circumstellar dust (Farihi et al. 2008b).

4.3.3. *G166-58*

However, an apparent infrared excess was identified at the metal-rich white dwarf G166-58, yet only at the two longer IRAC wavelengths of 5.8 and 7.9 μm (Farihi et al. 2008b; Figure 14). At the time of discovery, the available IRAC mosaicking software was limited to creating images with 1''2 pixels, and the image of G166-58 overlapped somewhat with a background galaxy 5'' distant. The background source complicated the flux measurements of the star, especially at 7.9 μm where the galaxy appears brighter than the white dwarf. Both point spread function (PSF) fitting photometry and radial profile analyses supported the conclusion measured excess originated in the point-like image of the star.³

Due to the diffraction limit of the telescope and the fact that most galaxies have steeply rising (power law) SEDs that peak at far-infrared wavelengths, *Spitzer* images of G166-58 at 16 or 24 μm would almost certainly be confused with an even brighter galaxy. Yet despite the absence of warmer dust at this star, the flux decrease towards 7.9 μm is consistent with a disk contained within the tidal disruption radius. But it is the inner, dust-poor region that made this star unique upon discovery and begs for an explanation, which its discoverers lacked.

³In later software released by the *Spitzer* Science Center, the ability to construct images with 0''6 pixels firmly corroborated the point-like infrared excess at G166-58 (Farihi et al. 2010c).

4.3.4. Other *Spitzer* Disk Searches

Also during the first cycle of *Spitzer*, two teams independently targeted the most massive white dwarfs to search for infrared excess (Farihi et al. 2008a; Hansen et al. 2006). Two competing hypotheses exist for the origin of white dwarfs with masses larger than roughly $1.0\,\mu\text{m}$; remnants of single, high intermediate-mass stars, or mergers of two white dwarfs (Liebert et al. 2005; Ferrario et al. 2005). In support of the first hypothesis, there is at least one, and possibly up to three massive white dwarfs that descended from single $M \gtrsim 5\,M_{\odot}$ main-sequence stars in the 125 Myr old Pleiades open cluster (Dobbie et al. 2006a). Such young white dwarfs are excellent targets for planets still warm from formation (Farihi et al. 2008a; Baraffe et al. 2003). Evidence for mergers is rather tenuous, but an example is the comoving visual binary LB 9802. The system consists of two white dwarfs where the considerably hotter star is also substantially more massive, in stark contrast with expectations from the coeval evolution of two single stars (Barstow et al. 1995). Models of white dwarf mergers suggest massive disks (and possibly second-generation planets) should form to as a repository of shedded angular momentum Hansen et al. (2006).

The *Spitzer* searches at massive white dwarfs conducted by Hansen et al. (2006) and Farihi et al. (2008a) produced no infrared excess candidates, leaving the question of white dwarf mergers still somewhat open. If mergers occur with the simultaneous formation of a massive disk, it is quite possible they would dissipate rapidly as they are expected to be primarily gaseous, at least initially. Although their composition is expected to be unusual, and composed largely of carbon (and oxygen), they may evolve similarly to the gas-rich, circumstellar disks observed at young stars and dissipate on similar, Myr timescales. The cooling age of a 50,000 K, $1.2\,M_{\odot}$ white dwarf is around 30 Myr (tiny radii make them inefficient radiators) suggesting any disk could have vanished due to a combination of accretion, early phase radiation pressure, and dust/planetesimal formation. It has been suggested that the luminous, post-asymptotic giant R Coronae Borealis stars could be the product of white dwarf mergers (Clayton et al. 2007). These stars are enshrouded in carbon-rich dust (Lambert et al. 2001) and have energetic winds, implying their circumstellar material will not persist on Myr timescales.

5. THE NEXT WAVE OF DISK DISCOVERIES

A wealth of information about disks at white dwarfs emerged from the second, third, and fourth *Spitzer* cycles. Roughly chronologically, the *Spitzer* observations of GD 362 represented the beginning of something akin to a second generation of white dwarf disk discoveries, initially occurring in parallel with the first discoveries. By 2007, all the disk discoveries and

searches had been concentrated at DAZ stars, and this was about to change. In 2006, a weak but definite helium absorption line was detected in a deep and high-resolution optical spectrum of GD 362, demonstrating the star had an atmosphere dominated by helium (Zuckerman et al. 2007). This discovery was announced to the white dwarf community at the biannual European white dwarf workshop held in 2006 at the University of Leicester, and foreshadowed in the paper reporting the *Spitzer* observations of its circumstellar dust.

5.1. The Second Class of Polluted White Dwarfs

The attention paid to DAZ white dwarfs is understandable. Hydrogen-rich atmosphere white dwarfs account for roughly 80% of all white dwarfs at effective temperatures above 12,000 K (Eisenstein et al. 2006). Typical timescales for heavy elements to diffuse below the outer, observable layers of a DA star are a few days for stars between 12,000 and 25,000 K (Koester 2009). In this temperature range, the convection zone or mixing layer of the star is incredibly thin, on the order of 10^{-15} of its total mass. As a DA star cools below 12,000 K, its convection zone increases in depth rapidly and substantially, growing by five orders of magnitude as it reaches 10,000 K, and another three orders of magnitude by 6500 K. The metal sinking timescales grow commensurately, increasing to 100 yr at 10,000 K and 10^4 year by 6500 K (Koester 2009). Hence the existence of all but the coolest DAZ stars implies the recent or ongoing accretion of heavy elements, and circumstellar disks are an obvious suspect.

In contrast, DBZ white dwarfs above 12,000 K have helium atmospheres with only trace hydrogen abundances typically at the lower end of the range $10^{-4} - 10^{-6}$ (Voss et al. 2007). It is thought these stars are the product of very efficient thermal pulses (helium flashes) that expel most of the superficial and primordial hydrogen in the final phases of asymptotic giant mass loss. A white dwarf with a helium-dominated atmosphere is relatively transparent compared to its hydrogen-rich counterparts, facilitating the detection of trace amounts of heavy elements. DB white dwarfs also have significantly larger convection zones than DA stars, roughly 4 to 5 orders of magnitude deeper at all but the coolest temperatures. The size of the convection zone determines the timescales for heavy elements to diffuse downward, and hence metals in DBZ stars can persist for up to 10^6 yr beginning at temperatures of 12,000 K (Koester 2009). Therefore, disk searches initially avoided the DBZ class because their photospheric metals could be traces of long past events.

The potential advantages of searching DBZ white dwarfs for circumstellar dust was highlighted by Jura (2006). He noted that their atmospheric transparency and significantly deep convection zones yielded compelling compositional and mass limits on the polluting material. Based on *IUE* spectroscopic observations of several helium- and metal-rich white

dwarfs (Wolff et al. 2002), Jura (2006) identified three stars with measured or upper limit carbon-to-iron ratios that indicated the accretion of refractory-rich and volatile-poor (i.e. rocky) material: GD 40, Ross 640, and HS 2253+8023. Furthermore, the mass of iron alone in the outer, mixing layers of these three stars ranges between 10^{21} and 10^{24} g; masses comparable to large Solar System asteroids and Ceres.

The SPY and Hamburg Quasar surveys together uncovered more than one dozen DBZ stars including GD 16, a white dwarf with a distinctive DAZ-type optical spectrum remarkably similar to GD 362 (Koester et al. 2005a,b; Friedrich et al. 2000, 1999). Together with previously known white dwarfs in this class (Dufour et al. 2007; Wolff et al. 2002; Dupuis et al. 1993b) and armed with the knowledge that their atmospheric compositions and total heavy element masses suggested the accretion of rocky material, the DBZ stars made their way into *Spitzer* and ground-based searches for dust, alongside the DAZ stars.

5.2. A Highly Successful *Spitzer* Search

Recognizing the helium-rich nature and circumstellar disk of GD 362, Jura et al. (2007a) disregarded basic atmospheric composition and selected a sample of 11 metal-polluted white dwarfs with potential excess flux in their 2MASS K_s -band photometry. On this basis, GD 56 emerged as the strongest candidate for circumstellar dust, having a large apparent K -band excess⁴ All white dwarfs were observed using both IRAC 3–8 μ m and MIPS 24 μ m imaging, and this was the first use of longer wavelength photometry in a survey of white dwarfs. Four strong infrared excesses were identified in the program, at GD 40, GD 56, GD 133, and PG 1015+161 (Figure 15).

The detection of circumstellar dust at GD 40 was excellent confirmation that DBZ white dwarfs held important clues to the nature of their metal-contamination (Jura 2006), in a different yet complimentary way to the DAZ stars. [At the time of writing, GD 362 and GD 40 have revealed more about the nature of the circumstellar debris at metal-contaminated white dwarfs than any other set of stars combined.] Helium atmospheres are not only relatively transparent and thus amenable to the detection of trace abundances of heavy elements, their sizable mixing layers provide a strict lower limit to the total mass of any accreted elements. For stars with circumstellar dust such as GD 40, the minimum, total mass of accreted metals places a lower limit on the mass of the asteroid whose debris now orbits the star. Also, the DBZ stars contain only traces or upper limit hydrogen abundances; this is a sensitive

⁴The selection of GD 56, GD 133, and PG 1015+161 as Cycle 2 *Spitzer* targets was made in early 2005, prior to the publication of their near-infrared spectra (Kilic et al. 2006).

diagnostic for a variety of accretion models.

The three DAZ white dwarfs found to have infrared excess were something of a cautionary tale. For the first time perhaps, it became clear that ground-based observations up to $2.5\,\mu\text{m}$ were sometimes insufficient to confidently identify circumstellar dust. GD 56 displays an unambiguous excess in K -band spectroscopy and photometry, similar to yet stronger than both G29-38 and GD 362, and the IRAC photometry reveals particularly strong emission. While the K -band spectra of GD 133 and PG 1015+161 were inconclusive (Kilic et al. 2006), their IRAC photometry reveals clear excess emission in each case. It is worth remarking that the reason these two white dwarfs lack notable K -band excesses is almost certainly *not* because they lack warm dust, as in the case of G166-58. Rather, the strength of emission from a flat disk depends also on its solid angle with respect to the Sun (Jura 2003).

In fact, the flat disk model is able to reproduce the infrared data at GD 40, GD 133 and PG 1015+161 very well using inner dust temperatures $T = 1000 - 1200\,\text{K}$ and near to where grains should rapidly sublimate (Jura et al. 2007a). However, the strong near-infrared emission at GD 56 cannot be duplicated with a flat disk model, even with dust temperatures above $1200\,\text{K}$. The sharp rise requires more emitting surface than is available in the flat disk model and can be reproduced with a $1000\,\text{K}$ blackbody (Jura et al. 2007a), implying some portion of the disk is warped or flared.

The importance of the MIPS observations lies in the fact that the longer wavelength fluxes constrain the detected disk material to lie well within the Roche limit of the white dwarf, and therefore consistent with a parent body that was tidally destroyed. The publication of these results in 2007 brought the number of white dwarf disks observed at $24\,\mu\text{m}$ to six, with none showing evidence for cool dust. On the contrary the detections and upper limits at this wavelength implied the coolest grains had temperatures of several hundred K and orbited within $1.2\,R_\odot$ (roughly 100 white dwarf radii). If a circumstellar disk is formed by the gravitational capture of interstellar material at the classical Bondi-Hoyle radius, then one might expect to detect cool dust as it approaches from this initial distance of several AU (Koester & Wilken 2006). The MIPS results of Jura et al. (2007a) demonstrated that emission from dust captured at such distances was strictly ruled out, as the predicted emission would be tens to hundreds of times greater than that observed.

5.3. The Detection of Gaseous Debris in a Disk

At roughly the same time period, and to the amazement of the white dwarf community, Gänsicke et al. (2006) reported the discovery of a single, warm DAZ white dwarf with

remarkably strong emission features from both calcium and iron. Like many astronomical discoveries, the identification of metallic emission lines at SDSS J122859.93+104032.9 (hereafter SDSS 1228) was accidental; its spectrum was flagged in a search for weak spectroscopic features due to very low mass (stellar or substellar) companions to apparently single white dwarfs (B. Gänsicke 2010, private communication).

The strongest emission at SDSS 1228 is seen in the calcium triplet centered near 8560Å (Figure 16) and these lines are rotationally broadened in a manner expected from Keplerian disk rotation. While the detected features are directly analogous to hydrogen and helium emission from accretion disks in cataclysmic variables (Horne & Marsh 1986), the spectrum of SDSS 1228 has strong hydrogen Balmer lines seen only in absorption, implying the emitting disk is essentially free of light gases. The full optical spectrum of SDSS 1228 is otherwise fairly typical of a warm DAZ star with a high metal abundance, showing strong magnesium absorption, and similar to the spectrum of G238-44.

Gänsicke et al. (2006) showed that the three calcium features were well-modeled by optically thick emission from a highly inclined disk, which together account for the shape of the central depressions within the emission features. The peak-to-peak velocity broadening of $\pm 630 \text{ km s}^{-1}$ together with the steep outer walls of the feature limit the gas disk to a maximum radius of $1.2 R_{\odot}$. This fact shows that the orbiting material is within the Roche limit of the star, and hence consistent with the tidal destruction of a large asteroid. While disk models had been largely successful in reproducing the observed infrared emission at the white dwarfs with circumstellar dust, and predicted disk radii generally within $1 R_{\odot}$, the gaseous metal emission line profiles were the first *empirical* evidence that circumstellar material at metal-enriched white dwarfs orbits within the Roche limit.

At the time of discovery, SDSS 1228 was the first circumstellar disk identified at a metal-lined white dwarf with $T_{\text{eff}} > 15,000 \text{ K}$. The combined studies of von Hippel et al. (2007) and Kilic et al. (2006) had targeted 11 DAZ white dwarfs warmer than this and speculated that their lack of infrared excess might be due to dust sublimation within the Roche limit of these higher temperature stars. At that time, this hypothesis was consistent with sublimated debris orbiting the 22,000 K white dwarf SDSS 1228 (Gänsicke et al. 2006), but the pattern would soon be broken. The infrared excess discovered at PG 1015+161 was the first to buck the trend, and more examples would follow, including substantial dust at SDSS 1228 itself. Based on this and additional reasons, it is probable that the gaseous debris at SDSS 1228 is the result of collisions rather than sublimation (Melis et al. 2010).

5.4. Dust-Deficiency at DAZ Stars; Collisions?

Based on the work of von Hippel et al. (2007) and Jura et al. (2007a), it became apparent that the DAZ white dwarfs with the highest inferred accretion rates were most likely to harbor circumstellar dust. Previous work had highlighted the correlation of dust disk frequency at DAZ stars with higher calcium-to-hydrogen ratios (Kilic & Redfield 2007; Kilic et al. 2006), but while metal abundance is correlated with its accretion rate, the size of the convection layer also plays a critical role (Koester & Wilken 2006). It makes physical sense that DAZ stars accreting at the highest rates require the most massive reservoirs, and the more massive the supply of heavy elements, the better the chance of its detection in the infrared. At the same time, several DAZ stars requiring relatively high metal accretion rates failed to show an infrared excess between 3 and $8\,\mu\text{m}$, the wavelength range accessible with IRAC photometry. An excellent example of this is G238-44, with one of the highest calcium-to-hydrogen abundances ($\log(\text{Ca}/\text{H}) = -6.7$) known and a diffusion timescale less than a day (Koester & Wilken 2006).

The idea that collisions within an evolving disk can grind dust grains into gaseous debris at white dwarfs was first suggested by Jura et al. (2007a), and can in principle account for a number of polluted white dwarfs where no infrared excess is detected by *Spitzer* out to 8 (and even $24\,\mu\text{m}$). The basic idea is that Keplerian velocities for particles orbiting a few to several tenths of a solar radius from a white dwarf are roughly between 400 and $800\,\text{km s}^{-1}$, and that small (i.e. a few percent) deviations from this can lead to collisions at speeds sufficient to ‘vaporize’ dust grains. Warm particles as small as $0.01\,\mu\text{m}$ are inefficient emitters and absorbers of infrared radiation ($2\pi a/\lambda \ll 1$), while smaller particles are essentially the size of gas molecules.

Farihi et al. (2008b) further showed that mutual collisions should dominate the initial temporal evolution of optically thin dust particles produced in a tidal disruption event. For dust orbiting cool white dwarfs, collisional timescales for disk particles are at least ten times shorter than their PR timescales, implying gaseous debris produce via collisions is plausible. Furthermore, in order to *avoid* the self-erosion of dust in this manner likely requires a high disk surface density so that the particle spacing is comparable to the size of the grains (Farihi et al. 2008b), and collisions are efficiently damped. Such a scenario is consistent the highest accretion rate stars exhibiting the infrared signature of dust most often, and with the (massive) optically thick disk models (Jura et al. 2007a).

Finally, Jura (2008) extended the idea of disk particle collisions to include multiple, smaller tidal disruption events, under the assumption that the mass distribution of a surviving asteroid belt scales similarly to the Solar System and is thus dominated by bodies a few to several km in size. Such a process should more efficiently annihilate solid particles as

an infalling, small asteroid impacts a pre-existing, low mass disk at a nonzero inclination. In systems where multiple, smaller asteroids are destroyed on timescales much shorter than the often inferred 10^5 yr disk lifetimes, the resulting debris should be primarily gaseous. While the focus of this chapter is not theoretical, suffice to say that at this point in time, it is thought that some type of collisional scenario (i.e. vaporized debris) is responsible for the lack of observed mid-infrared excess at a number of metal-polluted white dwarfs, especially those where relatively high metal accretion rates are inferred.

5.5. Expanding Searches to the DBZ Stars

About this time, astronomers widened their gaze, turning to the DBZ stars in earnest and including longer wavelength observations of both classes of polluted white dwarfs. (Kilic et al. 2008) targeted 20 DBZ white dwarfs with the near-infrared spectrograph that had successfully detected excess emission at several DAZ stars, but yielded no candidates within the helium-rich sample. Surprisingly, GD 40 failed to reveal an infrared excess in these observations, despite a potential K_s -band photometric excess in the 2MASS catalog; this was the reason it was selected as a *Spitzer* target by Jura et al. (2007a). The authors tentatively identified the relatively long diffusion timescales in these stars as the reason for the lack of dust, yet persistence of photospheric metals, and estimated that dust disks had typical lifetimes around an order of magnitude shorter than the 10^6 yr required for metals to begin sinking in the bulk of DBZ stars (Koester 2009). At the same time, it became clear that ground-based observations had failed to detect 50% of the known disks by mid 2008 (G166-58, GD 40 GD 133, PG 1015+161). While LTT 8452 has never been observed with K -band spectroscopy, its disk signature is not revealed by the $H = 14.00 \pm 0.06$ mag, $K_s = 14.02 \pm 0.06$ mag photometry available in 2MASS.

Farihi et al. (2009) undertook a *Spitzer* Cycle 3 study comprising new observations as well as an analysis of all available archival data on metal-polluted white dwarfs as of the end of 2008. Targets included 20 white dwarfs composed of roughly equal numbers of DAZ and DBZ types, including MIPS $24\mu\text{m}$ photometry of several stars previously observed only at shorter wavelengths. New disks were detected around GD 16 and PG 1457–086, while a better characterization of the infrared emission from LTT 8452 was enabled by new photometry at both shorter and longer infrared wavelengths. GD 16 is strikingly similar in optical spectral appearance to GD 362, exhibiting a DAZ-type spectrum while actually having a helium-rich atmosphere as evidenced by a very weak absorption features detected at high resolution with VLT / UVES (Koester et al. 2005a). Together with GD 362 and GD 40, the discovery of dust at GD 16 increased the number of disks at DBZ stars by 50%.

The infrared fluxes at GD 16 and LTT 8452 are fairly typical, strong and well modeled by flat disks with inner and outer radii of roughly one and two dozen stellar radii, respectively (Figure 17; Farihi et al. 2009). In contrast, the infrared excess of PG 1457–086 is rather mild in comparison to previously detected disks, with a fractional luminosity, $\tau = L_{\text{IR}}/L = 0.0007$. For comparison, G29-38 and GD 362 have $\tau = 0.03$, roughly 50 times brighter than the excess at PG 1457–086 (Farihi et al. 2009). The observations and model for this star, along with the scientific implications of its existence are discussed in §6.3.

Previous to this point in time, the DBZ stars had been understandably treated rather differently than the DAZ stars. Because the metal sinking timescales are relatively rapid in the DAZ white dwarfs, a steady-state balance between accretion and diffusion is a reasonably safe assumption to make (Koester & Wilken 2006). From this balance and the observed calcium abundance in each star, a total metal accretion rate can be calculated under the assumption that calcium accretes together with other elements in solar proportions but without any hydrogen or helium. This is equivalent to assuming a gas-to-dust ratio of 100:1 in the interstellar medium but that only dust is accreted (Jura et al. 2007a). The analysis of Farihi et al. (2009) attempted to put all metal-contaminated stars on equal footing by calculating time-averaged accretion rates for the DBZ stars in a similar manner. While physically unmotivated due to the long diffusion timescales in DBZ stars (i.e. a steady state cannot be assumed), a time-averaged accretion rate is still a useful diagnostic.

5.6. Additional Disks with Gaseous (and Solid) Debris

SDSS 1228 was the first of three metal-enriched white dwarfs found to have circumstellar, gaseous debris via the detection of emission lines from the calcium triplet by the end of 2008, the subsequent discoveries following in fairly rapid succession. The second single DA white dwarf confirmed to manifest metallic emission was SDSS J104341.53+085558.2 (hereafter SDSS 1043; Gänsicke et al. 2007). At 18,300 K, SDSS 1043 is a cooler star exhibiting the same phenomenon, and its spectrum also displays magnesium absorption indicating atmospheric pollution.

With this second discovery, it was again suggested that the warm temperatures of SDSS 1043 and 1228 were consistent with solid debris becoming sublimated within their stellar Roche limits, and potentially dust-poor analogs of white dwarfs with infrared excess (Gänsicke et al. 2007). However, the dust disks at both PG 1015+161 (Jura et al. 2007a) and 1457–086 (Farihi et al. 2009) orbit stars of 19,300 and 20,400 K, respectively (Koester & Wilken 2006), and the optical spectrum of the former shows no evidence for calcium emission (B. Gänsicke 2010, private communication). Gänsicke et al. (2007) searched

both GD 362 and G238-44 for calcium emission lines, but the former exhibits only lines of absorption in the triplet, while the latter reveals only a stellar continuum.

Importantly, an effort was made to identify additional DA white dwarfs with calcium emission from the vast SDSS DR4 catalog of Eisenstein et al. (2006) and to place some limits on the frequency of these stars. Using an automated routine to select stars with excess flux in the region of the calcium triplet, SDSS 1228 and 1043 emerged as the only two candidates for emission among over 400 DA white dwarfs with $g < 17.5$ mag, while another eight, relatively weak candidates resulted from selecting among 7360 stars with $g < 19.5$ mag. Clearly, the frequency of this phenomenon is less than 1% (Gänsicke et al. 2007).

Gänsicke et al. (2008) expanded their search for calcium emitting white dwarfs in the SDSS DR6 while removing their restriction to DA stars. Among over 15,000 likely white dwarfs and nearly 500 candidates for excess calcium flux, when visually inspected the bulk of spectra were found to suffer from poor night sky line subtraction resulting in an apparent excess in the triplet region. The only stars to pass muster were SDSS 1228, 1043, and SDSS J084539.17+225728.0; a star previously cataloged as Ton 345 and classified as an sdO star in the Palomar Green survey (Green et al. 1986). Ton 345 is a DBZ star with calcium triplet emission and photospheric absorption lines of calcium, magnesium, and silicon (Gänsicke et al. 2008). Remarkably, the emission lines at Ton 345 display a marked asymmetry, suggesting the disk of emitting material is not circular, but has significant nonzero eccentricity in the range 0.2 to 0.4. Additionally, temporal monitoring of this star has revealed variability in the shape of the asymmetric line emission profiles (Figure 18), strongly suggesting disk evolution on roughly yr timescales that appears episodic rather than ongoing (Melis et al. 2010; Gänsicke et al. 2008).

Overall, the white dwarfs with gaseous debris have provided significant insight into the composition, geometry, and evolution of circumstellar disks at white dwarfs. Importantly, all three white dwarfs with gaseous debris also have infrared excess from dust (Melis et al. 2010; Farihi et al. 2010c; Brinkworth et al. 2009) and atmospheres enriched with heavy elements. The solid material is modeled to be spatially coincident with the gas, arguing against sublimation of dust interior to some critical radius. In each case, the calcium triplet line profiles constrain the emitting material to lie within roughly $1 R_{\odot}$, while emission from hydrogen or helium is distinctly absent. Therefore, these stars belong to the same class of white dwarfs polluted by debris from tidally disrupted asteroids.

While this is an evolving field, it appears unlikely that the temperature of the white dwarf plays a role in generating the gas, which is a natural result of collisions among solid particles as in the multiple asteroid scenario of Jura (2008). However, stellar effective temperature dictates how efficiently the circumstellar gas can be heated, and thus detected as

it emits while cooling (Melis et al. 2010).

6. STUDIES AND STATISTICS

Table 2 lists all 18 confirmed and suspected white dwarfs with circumstellar dust with mid-infrared excess as of this writing (early 2010), ordered chronologically by year the infrared excess was published. Also listed are the white dwarf effective temperature, estimated distance from the Earth, apparent K -band magnitude, and the telescope which discovered the infrared excess.

6.1. Spectroscopic Confirmation of Rocky Circumstellar Debris

Near the mid-point of *Spitzer* Cycle 3, there were ten white dwarfs known to have circumstellar dust, but infrared spectra had only been obtained for G29-38 and GD 362. Jura et al. (2009a) used IRS to observe seven of the remaining dusty stars between 5 and 15 μm with the low resolution modules; G166-58 was deemed too problematic for spectroscopy due to its neighboring galaxy (Farihi et al. 2008b). All but one of the IRS targets were detected in the observations; owing to a combination of intrinsic faintness and exposure time restrictions in a high background region of the sky, no signal was obtained at PG 1015+161 (Jura et al. 2009a).

Table 1 lists all the white dwarfs with circumstellar dust targeted by IRS targets. Also listed are representative infrared fluxes and (unbinned) S/N estimations for the region covering the silicate feature at 9 – 11 μm . Despite the groundbreaking sensitivity of *Spitzer*, the bulk of stars have only modest detections, and most were confidently detected only between 8 and 12 μm where the silicate emission peak is typically 20% to 60% stronger than the 6–8 μm thermal continuum (Figure 19). Nonetheless, each of these stars exhibits strong 10 μm emission with a red wing extending to at least 12 μm . The measured features are inconsistent with interstellar silicates (see Figure 10), but are instead typical of glassy (amorphous) silicate dust grains, specifically olivines typically found in the inner Solar System, and in evolved solids associated with planet formation (Lisse et al. 2008).

IRS spectroscopy of all eight circumstellar dust disks reveals no evidence for emission from polycyclic aromatic hydrocarbons. These (carbon-rich) molecular compounds are found in the infrared spectra of the interstellar medium (Draine 2003; Allamandola et al. 1989), some circumstellar environments (Jura et al. 2006; Malfait et al. 1998), and in comets (Bockelée-Morvan et al. 1995), with strong features near 6, 8, and 11 μm . Hence, the dust

at white dwarfs is intrinsically carbon-deficient (Jura et al. 2009a), and similar to the rocky material of the inner Solar System (Lodders 2003). The findings from infrared spectroscopy are consistent with, and almost certainly mirrored by, the carbon-poor atmospheres established at several metal-enriched white dwarfs such as GD 40, GD 61, and HS 2253+8023 (Jura 2008; Desharnais et al. 2008; Zuckerman et al. 2007).

The only white dwarf with circumstellar dust bright enough to be studied spectroscopically with *Spitzer* at wavelengths longer than $15\,\mu\text{m}$ is G29-38. Reach et al. (2009) obtained a second low-resolution IRS spectrum of the prototype dust-polluted white dwarf, this time between 5 and $35\,\mu\text{m}$. The repeat observations over the short wavelength range revealed no change in the shape of the continuum or silicate emission feature, but the longer wavelength data revealed an additional, weaker silicate feature (or combination of features) between 18 and $20\,\mu\text{m}$ (Figure 23). The entire infrared spectrum was reproduced using three physically-distinct models: 1) an optically thin shell, 2) a moderately optically thick and physically thick disk, and 3) an optically thick, physically thin disk with an optically thin layer or outer region.

While the first two models employed by Reach et al. (2009) are attractive as they permit the co-identification of various minerals and water ice with the observed infrared emission, they are in essence optically thin models that invoke no more than 10^{19} g of disk mass. In contrast, the latter model is physically equivalent to the model of Jura et al. (2007b) for GD 362, implying the 10^{19} g of required optically thin material represents only a tiny fraction of the total disk mass. As discussed earlier, the PR timescales for warm, optically thin dust at white dwarfs are very short; 15 yr for $1\,\mu\text{m}$ silicate particles $1\,R_\odot$ distant from G29-38. Thus, for either of the optically thin models proposed by Reach et al. (2009), a mechanism is required to replenish 10^{19} g of material at G29-38 roughly every 15 yr, yet its infrared excess has been present for more than two decades (Zuckerman & Becklin 1987b). A disk whose total mass is orders of magnitude greater can accomplish this readily, and the asteroid-sized masses of heavy elements in DBZ stars such as GD 40 argue strongly for commensurate disk masses. Reach et al. (2009) find the flat disk model with an optically thin layer or outer region can reproduce the entire infrared emission at G29-39, requiring only silicates.

The importance of these observations cannot be overstated. More telling than the atmospheric composition of the metal-contaminated white dwarfs themselves, this is the strongest evidence that circumstellar dust at white dwarfs is derived from rocky planetary bodies (Jura et al. 2009a).

6.2. First Statistics and The Emerging Picture

By the end of 2008, a sufficient number of metal-polluted white dwarfs had been observed with *Spitzer* to merit statistical analysis; 52 stars with IRAC and 31 with MIPS. Because no white dwarf has been detected at $24\,\mu\text{m}$ without a simultaneous and stronger detection at IRAC wavelengths, the IRAC observational statistics better constrain the frequency of dust disks. From these 52 IRAC observations comprising 11 dust disk detections, it was established that that dust disk frequency is correlated with 1) time-averaged accretion rate and 2) cooling age (Figure 20; Farihi et al. 2009). Based on the cumulative *Spitzer* IRAC observations of over 200 white dwarfs, infrared excess from circumstellar dust is only detected at those stars with atmospheric metal contamination (Farihi et al. 2008a; Mullally et al. 2007; Hansen et al. 2006).

Applying the time-averaged metal accretion rate analysis to the IRAC dataset, Farihi et al. (2009) found over 50% of all cool white dwarfs with metal accretion rates $dM/dt \gtrsim 3 \times 10^8 \text{ g s}^{-1}$ have dust disks. Furthermore, when these cool, metal-polluted stars are statistically accounted for as members of larger samples of white dwarfs from which they are drawn, it is found that between 1% and 3% of all white dwarfs with cooling ages less than around 0.5 Gyr have both photospheric metals and circumstellar dust (Farihi et al. 2009). These results signify an underlying population of asteroids that have survived the post-main sequence evolution of their host star, and imply a commensurate fraction of main-sequence A- and F-type stars harbor asteroid belts, and probably build terrestrial planets. Evidence is strong that white dwarfs can be used to study disrupted minor planets.

The MIPS dataset implies that dust is not observed outside the Roche limit of the metal-rich white dwarfs. All white dwarf disks detected at $24\,\mu\text{m}$ have coexisting, strong $3 - 8\,\mu\text{m}$ IRAC excess fluxes, implying the dust is not drifting inward from the interstellar medium (Farihi et al. 2009). Dust grains captured near the Bondi-Hoyle radius of a typical metal-enriched white dwarf should have temperatures below 100 K, warming as they approach the star under PR drag. Both the MIPS detections at white dwarfs with dust, and the nondetections for the remaining metal-rich stars, argue against the influx of interstellar material (Farihi et al. 2009; Jura et al. 2007a). Stars with infrared excess always display decreasing flux towards $24\,\mu\text{m}$, indicating a compact arrangement of dust, consistent with disks created via the tidal disruption of rocky planetesimals.

Successful disk models are vertically optically thick at wavelengths up to $20\,\mu\text{m}$, and geometrically thin (Jura 2003). There are two reasons such models are likely to be accurate. First, particles in an optically thin disk would not survive PR forces for more than a few days to years (Farihi et al. 2008b). Second, the orbital periods of particles within $1 R_\odot$ of a white dwarf can be under 1 hr, implying the disk will relax into a flat configuration on short

timescales. Using this model, the warmest dust has been successfully modeled to lay within the radius at which blackbody grains in an optically thin cloud should sublime rapidly. Generally, the circumstellar disks have inner edges which approach the sublimation region for silicate dust in an optically thick disk; precisely the behavior expected for a dust disk which is feeding heavy elements to the photosphere of its white dwarf host.

The majority of both DAZ and DBZ white dwarfs do not have infrared excesses when viewed with *Spitzer* IRAC and MIPS (Farihi et al. 2009). Circumstellar gas disks are a distinct possibility at dust-poor yet polluted stars with metal accretion rates $dM/dt \gtrsim 3 \times 10^8 \text{ g s}^{-1}$, while fully accreted disks are a possibility for the DBZ stars with metal diffusion timescales near 10^6 yr . It is possible that a critical mass and density must be reached to prevent the dust disk from rapid, collisional self-annihilation, and when this milestone is not reached, a gas disk results.

For $T_{\text{eff}} \lesssim 20,000 \text{ K}$, white dwarfs with younger cooling ages are more likely to be orbited by a dusty disk (Farihi et al. 2009). This observational fact is consistent with a picture where a remnant planetary system gradually resettles post-main sequence (Debes & Sigurdsson 2002). Because an asteroid must be perturbed into a highly eccentric orbit in order to pass within the stellar Roche limit, planets of conventional size are also expected to persist at white dwarfs. The bulk of white dwarfs with dust have cooling ages less than 0.5 Gyr , with only one older than 1 Gyr , suggesting the possibility that surviving minor planet belts tend to become stable or depleted on these timescales.

6.3. Dust-Deficiency at DAZ Stars; Narrow Rings?

During the final cryogenic *Spitzer* Cycle (5), two previously unusual infrared excess stars were found to have counterparts, potentially representing subclasses of circumstellar dust rings at white dwarfs.

6.3.1. Disks with Subtle Infrared Emission

The infrared excess at PG 1457–086 is between 3 and 6σ above the predicted photospheric flux at the three shortest IRAC wavelengths where it is detected, and may not have been recognized without supporting near-infrared photometry that suggested a slight *K*-band excess (Farihi 2009; Farihi et al. 2009). Figure 24 plots the SED of PG 1457–086 together with a very mild infrared excess discovered at HE 0106–3253 again at the $4 - 6\sigma$ level in the IRAC bandpasses (Farihi et al. 2010c). As a benchmark comparison, the IRAC

excess at G29-38 is between 15 and 20σ .

Establishing just how much of the detected flux is excess and how much is photosphere can be a major problem as many white dwarfs are not well-constrained by optical and near-infrared photometry (McCook & Sion 1999). Furthermore, it is probably the case that including IRAC $7.9\mu\text{m}$ photometry in model fits, without the benefit of a MIPS $24\mu\text{m}$ constraint, will bias the outer disk radius towards larger values. This is because the $7.9\mu\text{m}$ bandpass is sufficiently wide to include flux from silicate emission, as clearly occurs for GD 362 and to a lesser degree for G29-38 (see Figure 12). Farihi et al. (2010c) fitted the $2 - 6\mu\text{m}$ SEDs of all white dwarfs with infrared excess in a uniform manner to establish the best fractional infrared luminosity of their disks. Figure 25 plots these values and Table 2 lists these

There are at least three stars whose infrared excesses are sufficiently subtle that flat disk model fits to their IRAC data predict dust rings of radial extent $\Delta r < 0.1 R_\odot$: HE 0106–3253, PG 1457–086, and SDSS 1043 all have $\tau < 10^{-3}$ (Farihi et al. 2010c, 2009). Additional stars which may also have rings this narrow include HE 0307+0746 and PG 1015+161. Since the inclination of these disks is unknown, the radial extent of the rings could be even smaller than predicted for nonzero inclination models. For example, if the disks at HE 0106–3253 or PG 1457–086 are near to face-on ($i = 0^\circ$), their dust rings would have $\Delta r = 0.01 R_\odot$ or roughly an Earth radius and 10 times smaller than the rings of Saturn.

Narrow rings found at a few white dwarfs suggest that asteroid accretion may be relevant to additional and potentially many metal-contaminated stars without an obvious infrared excess (Farihi et al. 2010c). A dust ring of radial extent $0.01 R_\odot$ would be difficult to confirm via infrared photometry above an inclination of $i = 50^\circ$ as it would produce an excess under 2σ for typical IRAC data. At the same time, even such a narrow ring has the potential to harbor over 10^{22}g of dust in an optically thick, flat disk configuration, and supply metals at 10^9gs^{-1} for nearly 10^6yr . Circumstellar disks that produce subtle infrared excesses probably await detection, and may apply to the bulk of all metal-polluted white dwarfs.

6.3.2. Disks with Enlarged Inner Holes

G166-58 displays an infrared excess that becomes obvious only at $5.7\mu\text{m}$, while its shorter wavelength IRAC data are consistent with the stellar continuum (Figure 14 Farihi et al. 2010c, 2008b). As such, it is the only white dwarf with circumstellar dust where the inner disk edge does not coincide with the region where silicate grains rapidly sublime at tem-

peratures near 1200 K (Farihi et al. 2009).

However, in *Spitzer* Cycle 5 PG 1225–079 was found to have a measured excess only at $7.9\,\mu\text{m}$ (Figure 26; Farihi et al. 2010c). Without repeat observations or data at other wavelengths, it is difficult to assign any certainty to the measured excess at PG 1225–079. If real (and confirmed in the future), then this coolmetal-rich white dwarf joins G166-58 in having a dust disk with a relatively large inner region that is dust-poor.

The multiple asteroid model can account for disks with distinct regions dominated by either dust or gas (Jura 2008). Hence it is plausible that the inner regions of dust disks at G166-58 and PG 1225–079 were bombarded by small asteroids that vaporized solids there, but had insufficient mass or orbital energy to destroy all the dust. Additionally, the same model can produce narrow or otherwise attenuated dust disks via impacts that annihilate rocky particles in some, but not all originally dusty regions (Farihi et al. 2010c).

An alternative is that the inner circumstellar regions at these two stars are largely free of matter, having been near to fully accreted from the inside out. This possibility suggests the extant photospheric metals in are residuals from prior infall of disk material. G166-58 is by far the coolest white dwarf with an infrared excess, and the 2000 yr timescale for metals to diffuse below the photosphere is relatively long for a DAZ white dwarf (Koester 2009). PG 1225–079 is a DBZ white dwarf and therefore does not require accretion to be ongoing. An accurate and detailed determination of the lighter and heavier elements polluting these stars may be able to constrain their accretion history.

6.4. The Composition and Masses of Asteroids at GD 362 and GD 40

To date, the polluted stellar and circumstellar environments of two stars have been studied in great detail, facilitated by their relatively transparent, helium-rich atmospheres.

6.4.1. GD 362

Under a several hour exposure with Keck / HIRES, Zuckerman et al. (2007) detected 15 elements heavier than helium in the optical spectrum of GD 362, positively shattering the record for number of metals detected in a cool white dwarf photosphere at any wavelength (Wolff et al. 2002; Friedrich et al. 1999; Sion et al. 1990b). This remarkable star is spectacularly polluted and manifests detectable abundances of strontium and scandium, highly refractory elements that comprise about 1 part in 10^9 of the Sun (Lodders 2003).

The array of ingredients polluting GD 362 is rich in refractory and transitional elements, while relatively poor in volatiles (Zuckerman et al. 2007). There are detectable abundances of six elements with condensation temperatures above 1400 K present in the star; scandium, aluminum, titanium, calcium, strontium, and vanadium. The transitional elements magnesium, silicon, and iron are the most abundant elements in GD 362 by a substantial margin; together with oxygen, these three elements comprise 94% of the bulk Earth (Allègre et al. 1995). In fact, overall the pattern of heavy elements in the white dwarf is most consistent with a combination of the bulk Earth and Moon (Figure 21; Zuckerman et al. 2007).

Jura et al. (2009b) used X-ray observational upper limits to constrain the total mass accretion rate at GD 362, noting that this helium-rich white dwarf has an anomalously high abundance of hydrogen ($\log(\text{H}/\text{He}) = -1.1$; Zuckerman et al. 2007). All together, the mass of heavy elements in the convection zone of GD 362 is 1.8×10^{22} g and comparable to the mass contained in a 240 km diameter Solar System asteroid (e.g. Themis). On the other hand, the mass of hydrogen in its outer layers is 7.0×10^{24} g (Koester 2009) and orders of magnitude larger than for all known helium-rich white dwarfs of comparable temperature except GD 16 (which is also polluted with heavy elements from a circumstellar disk Jura et al. 2009b; Farihi et al. 2009).

One possibility for the atmospheric hydrogen in these two stars is delivery via water-rich planetary bodies. Because surface ices will not survive the giant phases of stellar evolution, any extant water in asteroids at white dwarfs would have to be sufficiently buried. The Solar System objects Ceres and Callisto are thought to have internal water that are roughly 25% and 50% of their total mass, respectively (Thomas et al. 2005; McCord & Sotin 2005; Canup & Ward 2002). One possibility is that GD 362 accreted its hydrogen in the form of water from a few to several hundred large asteroids (unlikely) or an even larger body with internal water. If one supposes the current accretion event is the result of the latter possibility, then all the observed properties of GD 362 can be accounted for – disk, atmospheric pollution, large hydrogen abundance, and X-ray upper limit – by the destruction and subsequent accretion of a parent body with a total mass between that of Callisto and Mars (Jura et al. 2009b).

6.4.2. *GD 40*

In contrast, GD 40 exhibits hydrogen-deficiency typical of DB stars in its temperature range, but is nonetheless interesting. Already known to host magnesium, iron, silicon, and carbon from ultraviolet observations and calcium from optical spectroscopy (Friedrich et al. 1999), the discovery of its disk was in large part motivated by the recognition of its relative

carbon-deficiency and the asteroid-sized mass of metals contained in the star (Jura 2006). Again using Keck / HIRES, Klein et al. (2010) detected an additional four elements and better constrained the abundances of all previously detected elements except carbon via multiple strong lines.

From this optical dataset, seven of the eight heavy elements present in the atmosphere of GD 40 form a subset of those detected in GD 362, with the exception of oxygen. Interestingly, Klein et al. (2010) find that by assuming all of the atmospheric metals were delivered in their common oxides and all the hydrogen was delivered in water, there is an excess of oxygen in the outer layers of the star. A solution to this conundrum is that the photospheric abundances differ from the accreted abundances, and that GD 40 has been accreting for a minimum of a few diffusion timescales. In this picture, the disk has a lifetime greater than 10^6 yr, and the apparent excess of oxygen is due to the fact that heavier elements such as iron sink more rapidly than oxygen (Koester 2009).

The mass of heavy elements currently in the convection zone of GD 40 is 3.6×10^{22} g, already an asteroid-sized mass. However, with the caveat that the star must be in a steady state and has been accreting for at least a few diffusion timescales, the minimum mass of metals in the destroyed parent body grows to 3×10^{23} g (Klein et al. 2010) or about the size of Vesta, the second largest asteroid in the Solar System. In a steady state accretion mode, Klein et al. (2010) find that the water content of the now-destroyed minor planet can be no more than a few percent. Lastly, GD 40 exhibits a silicon-to-magnesium ratio significantly distinct from that found in stars and in the bulk Earth, hinting at the possibility that the parent body polluting GD 40 was at least partially differentiated (Klein et al. 2010).

6.5. A Last Look at the Interstellar Accretion Hypothesis

The totality of published results and works in progress on disks and metal-pollution at white dwarfs circa 2009 strongly argues against interstellar accretion. Yet even as the evidence for circumstellar disks and rocky pollutants began accumulating, and subsequently disseminated at international conferences, the scientific community continued to cite the interstellar medium as a source for accreted metals in cool white dwarfs (Desharnais et al. 2008; Dufour et al. 2007; Koester & Wilken 2006). Given the dearth of circumstellar disk detections at metal-rich white dwarfs cooler than 10,000 K (Farihi et al. 2010c, 2009) and their $10^4 - 10^6$ yr metal diffusion timescales, it is perhaps understandable that some researchers remained skeptical.

The class of stars used most often to argue in favor of interstellar accretion are the

coolest DBZ stars, spectrally classified DZ because helium transitions become difficult to excite below 12,000 K (Voss et al. 2007; Wesemael et al. 1993). Because detectable metals can persist in DZ white dwarfs for a few to several Myr, it is conceivable that these stars are now located up to a few hundred pc from a region in which they became polluted by interstellar matter. Classically, the glaring problem with this picture is the lack of accreted hydrogen in these stars, as the interstellar medium (cosmic or solar abundance) is 91% hydrogen and 0.01% elements heavier than neon by number (Däppen 2000; Aannestad et al. 1993). Calcium-to-hydrogen abundances in DZ stars are typically super-Solar, despite the fact that calcium continually sinks in their atmospheres (Farihi et al. 2010a).

Farihi et al. (2010a) used 146 DZ stars from the SDSS DR4 and with stellar parameters modeled by Dufour et al. (2007) to evaluate the interstellar accretion hypothesis by calculating several diagnostics. No correlation is found between calcium abundance and tangential speed as expected if the stars were accreting at Bondi-Hoyle, fluid rates necessary to produce the observed pollution (Koester & Wilken 2006; Dupuis et al. 1993a). More than half the sample white dwarfs are currently situated above the ± 100 pc thick gas and dust layer of the Galaxy, with nearly one fifth of the stars located over 200 pc above the plane. Furthermore, roughly half the sample are now moving back into the disk of the Galaxy rather than away, implying they have been out of the interstellar medium for several to tens of Myr (Farihi et al. 2010a).

Comparing a commensurate number of cool, helium-rich SDSS white dwarfs with and without detected photospheric metals also is a problem for instellar accretion. The two classes of stars appear to belong to the same population of disk stars in temperature, atmospheric composition, Galactic positions and velocities. Among all these helium-rich white dwarfs, there are pairs within several pc of one another where: 1) only one star is metal-rich yet the pair share similar space velocities, and 2) both stars are polluted yet their space velocities differ dramatically.

Perhaps the strongest evidence against interstellar accretion in these stars actually comes from the same mechanism that permits the metals to reside for Myr timescales; their relatively deep convection zones (Koester 2009; Paquette et al. 1986). Because any atmospheric metals are thoroughly mixed in the convective layers of the star, the measured abundances can be translated into masses by knowing the mass of the convective envelope. Figure 22 plots the mass of calcium detected in the 146 SDSS DZ stars as a function of effective temperature, revealing these masses are typical of large Solar System asteroids. Moreover, because metals in the interstellar medium are locked up in dust grains, they will not be captured by a passing white dwarf at the fluid rate, but at a rate around 10 times the Eddington accretion rate (Alcock & Illarionov 1980). The calcium masses plotted in Figure 22 cannot

be accounted for by the accretion of interstellar dust grains, even assuming Myr passages within the densest of environments (Farihi et al. 2010a).

At present, there is no observational evidence in favor of interstellar accretion onto white dwarfs, yet plentiful and compelling data supporting the accretion of rocky planetary material. Given the existing observational data on metal-enriched white dwarfs, the interstellar accretion hypothesis is no longer viable.

6.6. Evidence for Water in Debris Orbiting White Dwarfs

Starting from a default position that white dwarf atmospheric pollutants are delivered via planetary system remnants, some well-established observational properties then require reexamination. Perhaps most intriguing is the trace hydrogen seen in helium-rich white dwarfs.

In short, if DB white dwarfs accreted interstellar hydrogen at the fluid rate, they would quickly become DA white dwarfs and therefore this does not occur (Wesemael 1979; Koester 1976). Convective mixing can dredge-up helium in DA stars with $T_{\text{eff}} < 12,000$ K, resulting in a helium-dominated atmosphere with traces of hydrogen Tremblay & Bergeron (2008), but hydrogen is found in DB and DBZ stars at warmer temperatures as well (Voss et al. 2007). Lastly, trace hydrogen in helium-rich white dwarfs can be either primordial or accreted from interstellar space at rates comparable to the Eddington rate (i.e. direct impact). However, if helium atmosphere white dwarfs obtain trace metals and hydrogen from independent sources, then stars exhibiting both should be less frequent than stars exhibiting either. This is not supported by the observations, suggesting that helium atmosphere white dwarfs with both metals and hydrogen are polluted by water-rich asteroids (Farihi et al. 2010a).

Of the four DBZ white dwarfs with circumstellar dust, GD 16 and GD 362 have more than 10^{24} g of atmospheric hydrogen, while GD 40 and Ton 345 have abundances and upper limits four orders of magnitude lower (Jura et al. 2009b). These stark differences are not due to sensitivity, as trace hydrogen is detectable in DBZ white dwarfs typically down to 1 part in 10^5 with moderate-resolution optical spectra (Voss et al. 2007; Dufour et al. 2007). The hydrogen-poor atmospheres of the latter two stars are fairly typical of DB white dwarfs, while the hydrogen contents of the former two stars are rather remarkable.

One possibility is these four stars represent extremes of water content in planetary bodies post-main sequence. Oxygen has yet to be detected in either GD 16 or GD 362, but as both stars have $T_{\text{eff}} < 12,000$ K and only optical spectra to date, this is not really surprising. It takes enormous oxygen abundances to produce detectable, optical absorption lines in cool

white dwarfs (Gänsicke et al. 2010). Sensitive searches for photospheric oxygen in these two stars via ultraviolet spectroscopy will be able to further constrain scenarios of pollution by parent bodies with internal water.

Interestingly, there are currently two warm DBZ stars with marked oxygen detections made in the far-ultraviolet; GD 61 and GD 378 (Desharnais et al. 2008). Jura & Xu (2010) recognized the significance of these data, noting that both atmospheres had $O/C > 1$ and trace hydrogen in a temperature range where convection could not transform a DA into a DB. Their carbon-deficiency rules out pollution by interstellar matter, and accounting for their multiple atmospheric metals as oxides leaves an excess of oxygen in both stars (Jura & Xu 2010). Because the heavy element diffusion timescales in these DBZ white dwarfs are of the order 10^5 yr, it remains uncertain what fraction of the excess oxygen can be attributed to mineral oxides common to rocky planetary bodies, but whose metal components have sunk more rapidly than the oxygen. Under some reasonable assumptions about their accretion history, Jura & Xu (2010) finds that GD 378 was likely polluted by a water-rich asteroid, while the case for water at GD 61 is less compelling but still possible⁵.

The near future will probably hold some confirmations of water in the circumstellar debris that orbits white dwarfs.

7. RELATED OBJECTS

The discussion in this chapter has been focussed on apparently single, cool and metal-enriched white dwarfs because only these stars are observed to have circumstellar dust. Additionally, all stars in this class require external sources of pollution, for which circumstellar matter is currently the strongest candidate. It has already been mentioned that *Spitzer* observations have not identified infrared excess at over 150 white dwarfs without photospheric metals, but this needs some qualification. Below is a brief discussion of white dwarfs that are (potentially) related to the stars of this chapter.

7.1. White Dwarfs Polluted by Companions?

Zuckerman et al. (2003) identified several DAZ stars among white dwarfs with low mass stellar companions, M dwarfs, in suspected or confirmed short period orbits. The orbital separations of these systems are either established by radial velocity studies or constrained by

⁵mention *Nature* result here?

direct imaging, and consistent with detached, post-common envelope binaries (Hoard et al. 2007; Farihi et al. 2005a; Schultz et al. 1996). Although these stars are not interacting in the conventional sense of Roche lobe overflow, the relatively high frequency of photospheric metal detections in their white dwarf components indicates that these DAZ stars are capturing material from a stellar wind (Debes 2006; Zuckerman et al. 2003). Recent high-resolution imaging with the *Hubble Space Telescope* (*HST*) has strengthened this interpretation by finding all the DA+dM systems are visual pairs, while the DAZ+dM systems are typically spatially unresolved (Farihi et al. 2010b).

These observational results strengthened the hypothesis that apparently single, metal-enriched white dwarfs may be polluted by unseen companions (Dobbie et al. 2005; Holberg et al. 1997). However, any such companions would have to be sufficiently low in both mass and temperature that they are not detected in large near-infrared surveys such as 2MASS (Hoard et al. 2007). Five years of *Spitzer* IRAC studies have laid this hypothesis firmly to rest; the infrared SEDs of metal-rich white dwarfs fail to reveal the expected signature of low mass companions down to $25 M_J$, according to substellar cooling models (Farihi et al. 2009, 2008a; Baraffe et al. 2003; Burrows et al. 2003). Therefore, metal-rich white dwarfs are not polluted by mass transfer or wind capture from unseen, substellar companions.

Interestingly, two of the five known brown dwarf companions to white dwarfs are in close orbits analogous to the DAZ+dM systems found by Zuckerman et al. (2003); GD 1400B and WD 0137–049B (Maxted et al. 2006; Farihi & Christopher 2004). Neither of the two cool white dwarfs in these systems show signs of atmospheric metal pollution from their close substellar secondaries, despite both stars having a large number of co-added, high-resolution spectra taken with VLT / UVES (R. Napiwotzki 2009, private communication). Thus, it appears that the mid- to late-L dwarfs in these systems do not generate winds comparable to their higher mass, M dwarf counterparts.

7.2. Dust in The Helix?

Su et al. (2007) reported a strong infrared excess at the location of the central star of the Helix Nebula (NGC 7293), detected at 24 and $70 \mu\text{m}$ with *Spitzer* MIPS (Figure 27). An analysis of the excess emission using photometry at all IRAC and MIPS wavelengths, together with high-resolution IRS spectroscopy between 10 and $35 \mu\text{m}$, reveals a 100 K continuum. Su et al. (2007) attribute this emission to cold dust grains at several tens of AU from the star, which evolutionarily may be best described as a pre-white dwarf (Napiwotzki 1999).

The 24μ flux source was reported to be partly spatially-resolved but potentially due

to imperfect subtraction of the diffuse nebular emission, which is nonuniform and contains both continuum and emission components (Su et al. 2007). Assuming the detected excess is indeed point-like, the $6''$ size of the MIPS $24\mu\text{m}$ PSF only limits the physical size of the emitting region to 1300 AU and herein lies one difficulty in the interpretation of the detected excess. Additionally, the nebular emission is spatially complex and contains dust condensed within the expelled and cooling envelope of the giant star progenitor of the pre-white dwarf. This outflowing dust emits in the infrared and is a significant component of the overall emission in the Helix Nebula (Su et al. 2007).

A distinct alternative to cold dust analogous to that detected at main-sequence stars is dust captured by a companion star and heated by the pre-white dwarf. Bilikova et al. (2009) reported the results of a *Spitzer* survey for additional $24\mu\text{m}$ excesses at 72 hot and pre-white dwarfs, about half of which are in planetary nebulae. They find 12 new cases of strong excess, all of which are associated with planetary nebulae, and at least two of which have binary central stars. Given that (asymmetric) planetary nebulae are likely to be intimately connected with binary star evolution (de Marco 2009), and in light of the findings of Bilikova et al. (2009), it seems plausible the infrared excess in the Helix is not associated with a circumstellar dust disk at the pre-white dwarf.

8. SUMMARY AND OUTLOOK

8.1. Remnant Planetary Systems

The current picture painted by the observations of circumstellar dust at white dwarfs, and the consequent atmospheric pollution, is of a surviving planetary system. The asteroid analogs currently favored by the data could be either primitive bodies and analogous to member of the Main Belt in the Solar System, or they might be fragments of a larger parent body such as a moon or major planet. Regardless, the inferred masses and elemental abundance patterns of the observed debris is consistent with material condensed within the near environment of a main-sequence star and so far similar to the constitution of the terrestrial planets and their building blocks, the minor planets (Klein et al. 2010; Farihi et al. 2010a; Jura et al. 2009b; Zuckerman et al. 2007; Jura 2006).

In order for an asteroid to pass within the Roche limit of a white dwarf, it must be in a highly eccentric orbit requiring substantial gravitational perturbation. Thus, major planets almost certainly exist in metal-polluted white dwarf systems, especially in those with circumstellar dust disks. Furthermore, it is energetically difficult to deposit the entire mass of an asteroid in close orbit around a white dwarf. This can potentially be achieved

over many orbits as collisions and viscous stirring, especially if significant amounts of gas are produced during a tidal disruption event. Alternatively, a large but intact fragment of the shattered parent body might carry away most of the orbital energy and continue to interact with the evolving disk with each orbital pass.

Evidence for such interactions may already exist. The aforementioned change in the eccentricity of the gaseous debris at Ton 345, as well as the eccentricity itself are most easily induced by gravitational forces (Melis et al. 2010; Gänsicke et al. 2008). Strong infrared continuum emission from stars like GD 56 and GD 362 cannot be accounted for by flat disks alone, implying some portion of their disks is warped or flared (Jura et al. 2009a, 2007a). Again, these deviations from a fully relaxed disk require the injection of energy that can be provided by large bodies such as (Saturnian) ring-moon analogs near or within the disk, or major planets further out.

The inferred masses of circumstellar dust, supported by the observed heavy element masses within the polluted stars, should typically be only a fraction of the total mass of terrestrial bodies within these systems (Zuckerman et al. 2010). If extrasolar planetesimal belts scale similarly to the Solar System, then smaller asteroids will be injected into the inner system relatively often but may result in a disk composed primarily of gaseous debris (Jura 2008). More rarely, a large asteroid will approach a white dwarf and become tidally destroyed. With sufficient mass it can overcome sputtering within any pre-existing, gas-dominated disks and self-annihilation via particulate collisions, resulting in an infrared excess (Jura 2008; Farihi et al. 2008b). A combination of injection events may give rise to a diverse family of dust rings at white dwarfs, including narrow or tenuous rings, and dusty disks large inner holes (Farihi et al. 2010c).

Given the correlation of dust disk frequency with cooling age, it seems reasonable that dynamical resettling in planetary systems post-main sequence is driving the injection of minor planets into the inner regions of white dwarf systems (Farihi et al. 2009). This picture is strengthened by recent results indicating higher metal accretion for warmer white dwarfs (Zuckerman et al. 2010), and predicts that rocky planetary bodies are destroyed within the Roche limit of hotter white dwarfs more often than those observed at cool white dwarfs. High-resolution ultraviolet spectra of hot DA white dwarfs with photospheric metals has revealed velocity-shifted, circumstellar (and distinctly not interstellar), heavy element absorption features in several stars (Bannister et al. 2003). At $T_{\text{eff}} \geq 30,000$ K, white dwarfs will sublime even the most refractory materials within their Roche limits, suggesting the possibility that hotter white dwarfs may host disks composed only of gaseous heavy elements (von Hippel et al. 2007).

Tentative evidence points to dust disks that are relatively long-lived and ultimately

dissipated via accretion onto the white dwarf. In this picture, the lifetime of a given dust disk may be largely determined by its initial mass. Viscous spreading among solids and PR drag are orders of magnitude insufficient to generate the inferred metal accretion rates at DAZ stars, and it is likely that gas viscosity from sublimated particles at the inner dust disk edge drives these rates (Farihi et al. 2010c; Jura 2008; Farihi et al. 2008b; von Hippel et al. 2007). Forces such as PR drag and radiation pressure are unable to significantly influence the lifetime of optically thick circumstellar dust at $T_{\text{eff}} \lesssim 20,000$ K white dwarfs. Optically thin material necessary to account for the observed silicate emission features at white dwarfs with circumstellar dust is naturally supplied by an (optically thick) disk that is orders of magnitude more massive (Jura et al. 2009a).

The frequency of metal-polluted white dwarfs likely reflects the frequency of rocky planetary systems at main-sequence, A- and F-type stars that are progenitors of the current population of white dwarfs. Very conservatively, the minimum frequency of remnant planetary systems at white dwarfs is around 3% from those displaying both atmospheric metals and circumstellar dust (Farihi et al. 2009). However, evidence is growing that most if not all metal-contaminated white dwarfs are the result of the accretion of rocky planetesimals (Farihi et al. 2010a). In this more liberal and likely more accurate view, the fraction of intermediate mass stars with terrestrial planetary systems that have survived partly intact into the white dwarf phase is 20 – 30% (Zuckerman et al. 2010, 2003). It appears likely that some fraction of A- and F-type stars build planetary systems replete with water-rich asteroids, the building blocks of habitable planets and potentially analogous to the parent bodies that supplied the bulk of water in Earth’s oceans (Morbidelli et al. 2000).

8.2. The Present and Near Future

At the time of writing, *Spitzer* IRAC is still operating at 3.6 and 4.5 μm with Cycle 7 observations beginning in the latter part of this year (2010), with an eighth cycle is planned. Observing at mid-infrared wavelengths similar to cryogenic *Spitzer*, the *Wide Field Infrared Survey Explorer* (*WISE*) has just completed its coverage of the entire sky. While not as sensitive as pointed observations with *Spitzer* IRAC, *WISE* has the capability to detect bright (1 mJy), warm dust disks at white dwarfs not yet known to be metal-polluted and hence not yet targeted by *Spitzer* or ground-based searches for infrared excess.

Herschel is currently observing in the far-infrared and soliciting the first open round of proposals from the scientific community, but may not be sufficiently sensitive for dust studies at white dwarfs. The mid-infrared excesses observed by *Spitzer* are typically tens to hundreds of μJy and falling towards longer wavelengths, while *Herschel* reports 5 to

10 mJy detection limits. Unless white dwarfs harbor especially prominent excesses from cold dust, around 1 – 10 times their peak optical fluxes, *Herschel* will not detect dust in many white dwarf systems. At somewhat longer wavelengths, the Atacama Large Millimeter Array (ALMA) is set to begin science operations (next year) in 2011. ALMA should have both μ Jy sensitivity and sub-arcsecond spatial resolution, making it a promising tool for direct imaging of spatially-resolved, cold debris at white dwarfs.

Further in the future, *JWST* will operate in the near- and mid-infrared with sensitivity superior to *Spitzer*. There are two leaps forward that can be envisioned with such capacity. First, better quality mid-infrared spectra of warm dust at white dwarfs will enable a more detailed analysis of its temperature, location, geometry, and composition. Second, infrared spectroscopy may reveal very subtle infrared excesses at metal-rich white dwarfs where *Spitzer* IRAC photometry does not. This technique was successfully employed at main-sequence stars with *Spitzer* IRS, where high S/N spectroscopy revealed at least two cases of spectacular yet subtle, warm dust emission (Lisse et al. 2007; Beichman et al. 2006, 2005).

On the other end of the electromagnetic spectrum, the recently-installed ultraviolet Cosmic Origins Spectrograph (COS) on the *HST* promises to be a useful instrument with which to study the elemental abundances of polluted white dwarfs. Optimized for the far-ultraviolet, COS will function best for metal-rich white dwarfs warmer than 16,000 K, but near-ultraviolet observations are possible with lower efficiency for all but the coolest white dwarfs with metals. The science enabled by instruments like COS is really at the core of circumstellar dust studies at white dwarfs. The stellar atmosphere distills the accreted debris, providing the bulk chemical composition destroyed parent body. In this manner, circumstellar dust studies at white dwarfs have the potential to reveal more about the anatomy of extrasolar, terrestrial planetary bodies than any other technique.

I would like to thank my colleagues and collaborators for many years of helpful discussions and interesting projects, and the editor D. W. Hoard for the opportunity to contribute to this book. The published and online⁶ versions of the white dwarf catalog assembled by G. McCook & E. M. Sion have been an invaluable resource over the years and the white dwarf community owes the authors and caretakers an enormous debt of gratitude for their effort. I also thank D. Koester for making available the white dwarf atmosphere models used in this chapter. Many of the plots and figures used here include data from the various sources: the *Galaxy Evolution Explorer* (*GALEX*), the Sloan Digital Sky Survey (SDSS), the Two

⁶<http://www.astronomy.villanova.edu/WDCatalog/index.html>

Micron All Sky Survey (2MASS), and the *Spitzer Space Telescope*. *GALEX* is operated for NASA by the California Institute of Technology under NASA contract NAS5-98034. The SDSS is managed by the Astrophysical Research Consortium for the Participating Institutions (<http://www.sdss.org/>). 2MASS is a joint project of the University of Massachusetts and the Infrared Processing and Analysis Center / California Institute of Technology, funded by NASA and the National Science Foundation. The *Spitzer Space Telescope*, is operated by the Jet Propulsion Laboratory, California Institute of Technology under a contract with NASA

REFERENCES

- Aannestad, P. A., Kenyon, S. J., Hammond, G. L., & Sion, E. M. 1993, *AJ*, 105, 1033
- Alcock, C., Fristrom, C. C., & Siegelman, R. 1986, *ApJ*, 302, 462
- Alcock, C., & Illarionov, A. 1980, *ApJ*, 235, 534
- Allamandola, L. J., Tielens, A. G. G. M., & Barker, J. R. 1989, *ApJS*, 71, 733
- Allegre, C. J., Poirier, J. P., Humler, E., & Hofmann, A.W. 1995, *Earth Planetary Sci. Letters*, 4, 515
- Bannister, N. P., Barstow, M. A., Holberg, J. A., & Bruhweiler, F. C. 2003, *MNRAS*, 341, 477
- Baraffe, I., Chabrier, G., Barman, T. S., Allard, F., & Hauschildt, P. H. 2003, *A&A*, 402, 701
- Barstow, M. A., Jordan, S., O’ Donoghue, Burleigh, M. R., Napiwotzki, R., & Harrop-Allin, M. K. 1995, *MNRAS*, 277, 971
- Becklin, E. E., Farihi, J., Jura, M., Song, I., Weinberger, A. J., & Zuckerman, B. 2005, *ApJ*, 632, L119
- Beichman, C. A., et al. 2005, *ApJ*, 626, 1061
- Beichman, C. A., et al. 2006, *ApJ*, 639, 1166
- Bilikova, J., Chu, Y. H., Su, K., Gruendl, R., Rauch, T., De Marco, O., & Volk, K. 2009, *JPhCS*, 172, 012055

- Binzel, R. P., Hanner, M. S., & Steel, D. I. 2000, in *Allen’s Astrophysical Quantities*, ed. Cox, A. N. (4th ed.; New York: AIP Press; Springer), 315
- Bockelée-Morvan, D., Brooke, T. Y., & Crovisier, J. 1995, *Icarus*, 116, 18
- Brinkworth, C. S., Gänsicke, B. T., Marsh, T. R., Hoard, D. W., & Tappert, C. 2009, *ApJ*, 696, 1402
- Barnbaum, C., & Zuckerman, B. 1992, *ApJ*, 396, L31
- Burrows, A., Sudarsky, D., & Lunine, J. I. 2003, *ApJ*, 596, 587
- Canup, R. M., & Ward, W. R. 2002, *AJ*, 124, 3404
- Chary, R., Zuckerman, B., & Becklin, E. E. 1999, in *the Universe as Seen by ISO*, ed. P. Cox & M. F. Kessler (Noordwijk: ESA/ESTEC), 289
- Chayer, P., Fontaine, G., & Wesemael, F. 1995, *ApJS*, 99, 189
- Clayton, G. C., Geballe, T. R., Herwig, F., Fryer, C., & Asplund, M. 2007, *ApJ*, 662, 1220C
- Däppen, W. 2000, in *Allen’s Astrophysical Quantities*, ed. Cox, A. N. (4th ed.; New York: AIP Press; Springer), 315
- Davidsson, B. J. R. 1999, *Icarus*, 142, 525
- Debes, J. H., & Sigurdsson, S. 2002, *ApJ*, 572, 556
- Debes, J. H., Sigurdsson, S. & Hansen, B. 2007, *AJ*, 134, 1662
- Debes, J. H. 2006, *ApJ*, 652, 636
- de Marco, O. 2009, *PASP*, 121, 316
- Desharnais, S., Wesemael, F., Chayer, P., Kruk, J. W., & Saffer, R. A. 2008, *ApJ*, 672, 540
- Dobbie, P. D., Burleigh, M. R., Levan, A. J., Barstow, M. A., Napiwotzki, R., Holberg, J. B., Hubeny, I., & Howell, S. B. 2005, *MNRAS*, 357, 1049
- Dobbie, P. D., Napiwotzki, R., Lodieu, N., Burleigh, M. R., Barstow, M. A., & Jameson, R. F. 2006a, *MNRAS*, 373, L45
- Draine, B. T. 2003, *ARA&A*, 41, 241
- Dufour P., et al. 2007, *ApJ*, 663, 1291

- Dupuis, J., Fontaine, G., Pelletier, C., & Wesemael, F. 1992, *ApJS*, 82, 505
- Dupuis, J., Fontaine, G., Pelletier, C., & Wesemael, F. 1993a, *ApJS*, 84, 73
- Dupuis, J., Fontaine, G., & Wesemael, F. 1993b, *ApJS*, 87, 345
- Eisenstein, D. J., et al. 2006, *AJ*, 132, 676
- Farihi, J. 2009, *MNRAS*, 398, 2091
- Farihi, J., Barstow, M. A., Redfield, S., Dufour, P., & Hambly, N. C. 2010a, *MNRAS*, 404, 2123
- Farihi, J., Becklin, E. E., & Zuckerman, B. 2005a, *ApJS*, 161, 394
- Farihi, J., Becklin, E. E., & Zuckerman, B. 2008a, *ApJ*, 681, 1470
- Farihi, J., & Christopher, M. 2004, *AJ*, 128, 1868
- Farihi, J., Hoard, D. W., & Wachter, S. 2010b, *ApJS*, submitted
- Farihi, J., Jura, M., Zuckerman, B. 2009, *ApJ*, 694, 805
- Farihi, J., Jura, M., Lee, J. E., & Zuckerman, B. 2010c, *ApJ*, 714, 1386
- Farihi, J., Zuckerman, B., & Becklin, E. E. 2008b, *ApJ*, 674, 431
- Fazio, G. G., et al. 2004a, *ApJS*, 154, 10
- Ferrario, L., Wickramasinghe, D. T., Liebert, J., & Williams, K. A. 2005, *MNRAS*, 361, 1131
- Fontaine, G., & Michaud, G. 1979, *ApJ*, 231, 826
- Friedrich, S., Koester, D., Christlieb, N., Reimers, D., & Wisotzki, L. 2000, *A&A*, 363, 1040
- Friedrich, S., Koester, D., Heber, U., Jeffery, C. S., & Reimers, D. 1999, *A&A*, 350, 865
- Gänsicke, B. T., Koester, D., Girven, J., Marsh, T. R., & Steeghs, D. 2010, *Science*, 327, 188
- Gänsicke, B. T., Koester, D., Marsh, T. R., Rebassa-Mansergas, A., & Southworth J. 2008, *MNRAS*, 391, L103
- Gänsicke, B. T., Marsh, T. R., & Southworth, J. 2007, *MNRAS*, 380, L35

- Gänsicke, B. T., Marsh, T. R., Southworth, J., & Rebassa-Mansergas, A. 2006, *Science*, 314, 1908
- Gianninas, A., Dufour, P., & Bergeron, P. 2004, *ApJ*, 617, L57
- Glasse, A. C., Atad-Ettdedgui, E. I., & Harris, J. W. 1997, *Proc. SPIE*, 2871, 1197
- Graham, J. R., Matthews, K., Neugebauer, G., & Soifer, B. T. 1990, *ApJ*, 357, 216
- Green, P. J., Ali, B., & Napiwotzki, R. 2000, *A&A*, 540, 992
- Green, R. F., Schmidt, M., & Liebert, J. 1986, *ApJS*, 61, 305
- Hansen, B. M. S., Kulkarni, S., & Wiktorowicz, S. 2006, *AJ*, 131, 1106
- Hoard, D. W., Wachter, S., Sturch, L. K., Widhalm, A. M., Weiler, K. P., Pretorius, M. L., Wellhouse, J. W., & Gibiansky, M. 2007, *AJ*, 134, 26
- Hodapp, K. W., et al. 2003, *PASP*, 115, 1388
- Holberg, J. B., Barstow, M. A., & Green, E. M. 1997, *ApJ*, 474, L127
- Horne, K., & Marsh, T. R. 1986, *MNRAS*, 218, 761
- Houck, J. R., et al. 2004, *ApJS*, 154, 18
- Jura, M. 2003, *ApJ*, 584, L91
- Jura, M. 2006, *ApJ*, 653, 613
- Jura, M., et al. 2006, *ApJ*, 637, L45
- Jura, M. 2008, *AJ*, 135, 1785
- Jura, M., Farihi, J., & Zuckerman, B. 2007a, *ApJ*, 663, 1285
- Jura, M., Farihi, J., & Zuckerman, B. 2009a, *AJ*, 137, 3191
- Jura, M., Munro, M., Farihi, J., & Zuckerman, B. 2009b, *ApJ*, 699, 1473
- Jura, M., Farihi, J., Zuckerman, B., & Becklin, E. E. 2007b, *AJ*, 133, 1927
- Jura, M., & Xu, S. 2010, *AJ*, in press
- Kilic, M., Farihi, J., Nitta, A., & Leggett, S. K. 2008, *AJ*, 136, 111
- Kilic, M., & Redfield, S. 2007, *ApJ*, 660, 641

- Kilic, M., von Hippel, T., Leggett, S. K., & Winget, D. E. 2005, *ApJ*, 632, L115
- Kilic, M., von Hippel, T., Leggett, S. K., & Winget, D. E. 2006, *ApJ*, 646, 474
- Klein, B., Jura, M., Koester, D., Zuckerman, B., & Melis C. 2010, *ApJ*, 709, 950
- Kleinman, S. J. 1994, *ApJ*, 436, 875
- Koester D. 1976, *A&A*, 52, 415
- Koester, D. 2009a, *A&A*, 498, 517
- Koester, D., Napiwotzki, R., Voss, B., Homeier, D., & Reimers, D. 2005a, *A&A*, 439, 317
- Koester, D., Provencal, J., & Shipman, H. L. 1997, *A&A*, 230, L57
- Koester, D., Rollenhagen, K., Napiwotzki, R., Voss, B., Christlieb, N., Homeier, D., & Reimers, D. 2005b, *A&A*, 432, 1025
- Koester, D., & Wilken, D. 2006, *A&A*, 453, 1051
- Lacombe, P., Wesemael, F., Fontaine, G., & Liebert, J. 1983, *ApJ*, 272, 660
- Lambert, D. L., Rao, N. K., Pandey, G., & Ivans, I. I. 2001, *ApJ*, 555, 925
- Liebert, J., Bergeron, P., & Holberg, J. B. 2005, *ApJS*, 156, 47
- Lisse, C. M., Beichman, C. A., Bryden, G., & Wyatt, M. C. 2007, *ApJ*, 658, 584
- Lisse, C. M., Chen, C. H., Wyatt, M. C., & Morlok, A. 2008, *ApJ*, 673, 1106
- Lisse, C. M., et al. 2006, *Science*, 313, 635
- Lodders, K. 2003, *ApJ*, 591, 1220
- Malfait, K., Waelkens, C., Waters, L. B. F. M., Vandenbussche, B., Huygen, E., & de Graauw, M. S. 1998, *A&A*, 332, L25
- Maxted, P. F. L., Napiwotzki, R., Dobbie, P. D., & Burleigh, M. R. 2006, *Nature*, 442, 543
- Mclean, I. S. 1997, in *Electronic Imaging in Astronomy*; (West Sussex: Wiley)
- McCook, G. P., & Sion, E. M. 1999, *ApJS*, 121, 1
- McCord, T. B., & Sotin, C. 2005, *JGRE*, 110, E05009
- Melis, C., Jura, M., Albert, L., Klein, B., & Zuckerman, B. 2009, *ApJ*, in press

- Morbidelli, A., Chambers, J., Lunine, J. I., Petit, J. M., Robert, F., Valsecchi, G. B., & Cyr, K. E. 2000, *M&PS*, 35, 1309
- Mullally, F., Kilic, M., Reach, W. T., Kuchner, M., von Hippel, T., Burrows, A., & Winget, D. E. 2007, *ApJS*, 171, 206
- Napiwotzki, R. 1999, *A&A*, 350, 101
- Napiwotzki, R., et al. 2003, *Msngr*, 112, 25
- Paquette, C., Pelletier, C., Fontaine, G., & Michaud, G. 1986, *ApJS* 61, 197
- Patterson, J., Zuckerman, B., Becklin, E. E., Tholen, D. J., & Hawarden, T. 1991, *ApJ*, 374, 330
- Probst, R. 1981, Ph.D. Thesis, University of Virginia
- Probst, R. 1983, *ApJS*, 53, 335
- Probst, R. G., & O’Connell, R. W. 1982, *ApJ*, 252, L69
- Rayner, J. T., Toomey, D. W., Onaka, P. M., Denault, A. J., Stahlberger, W. E., Vacca, W. D., Cushing, M. C., & Wang S. 2003, *PASP*, 115, 362
- Reach, W. T., Kuchner, M. J., von Hippel, T., Burrows, A., Mulally, F., Kilic, M., & Winget, D. E. 2005a, *ApJ*, 635, L161
- Reach, W. T., Lisse, C., von Hippel, T., & Mullally, F. 2009, *ApJ*, 693, 697
- Rieke, G., et al. 2004, *ApJS*, 154, 25
- Schultz, G., Zuckerman, B., & Becklin E. E. 1996, *ApJ*, 460, 402
- Shipman, H. L. 1986, in *Astrophysics of Brown Dwarfs*, eds. M. C. Kafatos, R. S. Harrington, & S. P. Maran, (Cambridge; New York: Cambridge University Press), 71
- Sion, E. M., Hammond, G. L., Wagner, R. M., Starrfield, S. G., & Liebert, J. 1990a, *ApJ*, 362, 691
- Sion, E. M., Kenyon, S. J., Aannestad, P. A 1990b, *ApJS*, 72, 707
- Skrutskie, M. F., et al. 2006, *AJ*, 131, 1163
- Song, I., Zuckerman, B., Weinberger, A. J., & Becklin, E. E. 2005, *Nature*, 436, 363

- Su, K. Y. L., et al. 2007, *ApJ*, 657, L41
- Telesco, C. M., Joy, M., & Sisk, C. 1990, *ApJ*, 358, L21
- Thomas, P. C., Parker, J. W., McFadden, L. A., Russell, C. T., Stern, S. A., Sykes, M. V., & Young, E. F. 2005, *Nature*, 437, 224
- Tokunaga, A. T., Becklin, E. E., & Zuckerman, B. 1990, *ApJ*, 358, L17
- Tokunaga, A. T., Hodapp, K. W., Becklin, E. E., Cruikshank, D. P., Rigler, M., Toomey, D. W., Brown, R. H., & Zuckerman, B. 1988, *ApJ*, 332, L71
- Tremblay, P. E., & Bergeron, P. 2008, *ApJ*, 672, 1144
- van Maanen, A. 1917, *PASP*, 29, 258
- van Maanen, A. 1919, *PASP*, 31, 42
- von Hippel, T., Kuchner, M. J., Kilic, M., Mullaly, F., & Reach, W. T. 2007, *ApJ*, 662, 544
- Vauclair, G., Vauclair, S., & Greenstein, J. L. 1979, *A&A*, 80, 79
- Voss, B., Koester, D., Napiwotzki, R., Christlieb, N., & Reimers, D. 2007, *A&A*, 470, 1079
- Wachter, S., Hoard, D. W., Hansen, K. H., Wilcox, R. E., Taylor, H. M., & Finkelstein, S. L. 2003, *ApJ*, 586, 1356
- Wegner, G. 1972, *ApJ*, 172, 451
- Wehrse, R. 1975, *A&A*, 39, 169
- Weidemann, V. 1960, *ApJ*, 131, 638
- Welsh B. Y., Craig N., Vedder P. W., & Vallergera J. V. 1994, *ApJ*, 437, 638
- Welsh B. Y., Sfeir D. M., Sirk M. M., & Lallement R. 1999, *A&A*, 352, 308
- Werner, M. W., et al. 2004, *ApJS*, 154, 1
- Wesemael F. 1979, *A&A*, 72, 104
- Wesemael, F., Greenstein, J. L., Liebert, J., Lamontagne, R., Fontaine, G., Bergeron, P., & Glaspey, J. W. 1993, *PASP*, 105, 761
- Wolff, B., Koester, D., & Liebert, J. 2002, *A&A*, 385, 995

Zuckerman B. 2001, ARA&A, 39, 549

Zuckerman, B., & Becklin, E. E. 1987b, Nature, 330, 138

Zuckerman, B., & Becklin, E. E. 1992, ApJ, 386, 260

Zuckerman, B., Koester, D., Melis, C., Hansen, B. M. S., & Jura, M. 2007, ApJ, 671, 872

Zuckerman, B., Koester, D., Reid, I. N., & Hünsch, M. 2003, ApJ, 596, 477

Zuckerman, B., Melis, C., Klein, B., Koester, D., & Jura, M. 2010, ApJ, in press

Zuckerman, B., & Reid, I. N. 1998, ApJ, 505, L143

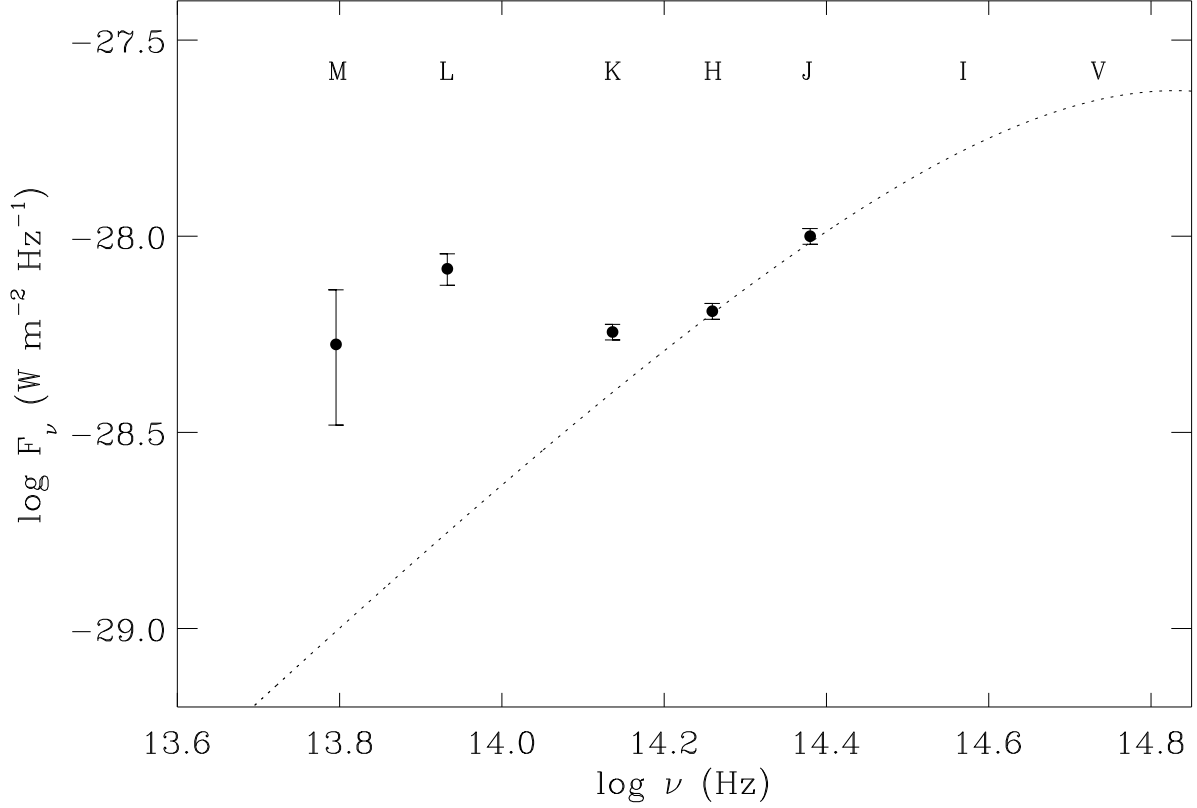


Fig. 1.— The discovery of infrared excess emission from the white dwarf G29-38 made at the IRTF. The plot is a reproduction of the figure presented in Zuckerman & Becklin (1987b) and shows their measurements with errors in five infrared bandpasses labelled in the figure *J* ($1.25 \mu\text{m}$), *H* ($1.65 \mu\text{m}$), *K* ($2.2 \mu\text{m}$), *L* ($3.5 \mu\text{m}$), and *M* ($4.8 \mu\text{m}$). The dotted line is a blackbody plotted through the two shortest wavelength fluxes, consistent with the stellar photosphere.

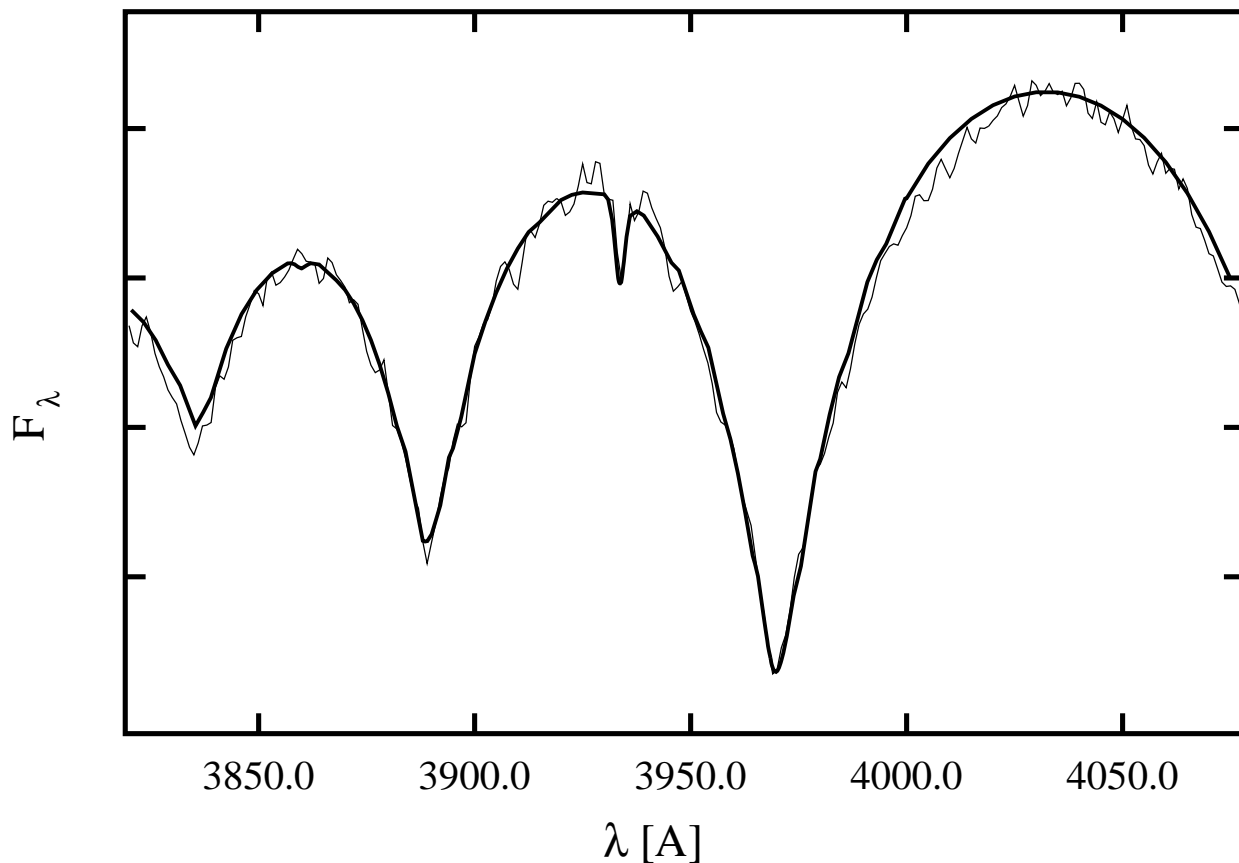


Fig. 2.— The discovery of photospheric calcium in the optical spectrum of G29-38 (Koester et al. 1997), at the same atomic transition that is strongest in the Sun (the Fraunhofer K line). The thin line is the actual data while the thick line is the best model fit. It is noteworthy that the absorption line is quite weak despite the large calcium abundance ($\log(\text{Ca}/\text{H}) = -6.8$; Zuckerman et al. 2003), and is due to the relatively high opacity of hydrogen-rich white dwarf atmospheres. All else being equal, a similar calcium abundance produces a line equivalent width roughly 100 times greater in a helium-dominated atmosphere (see Figure 3).

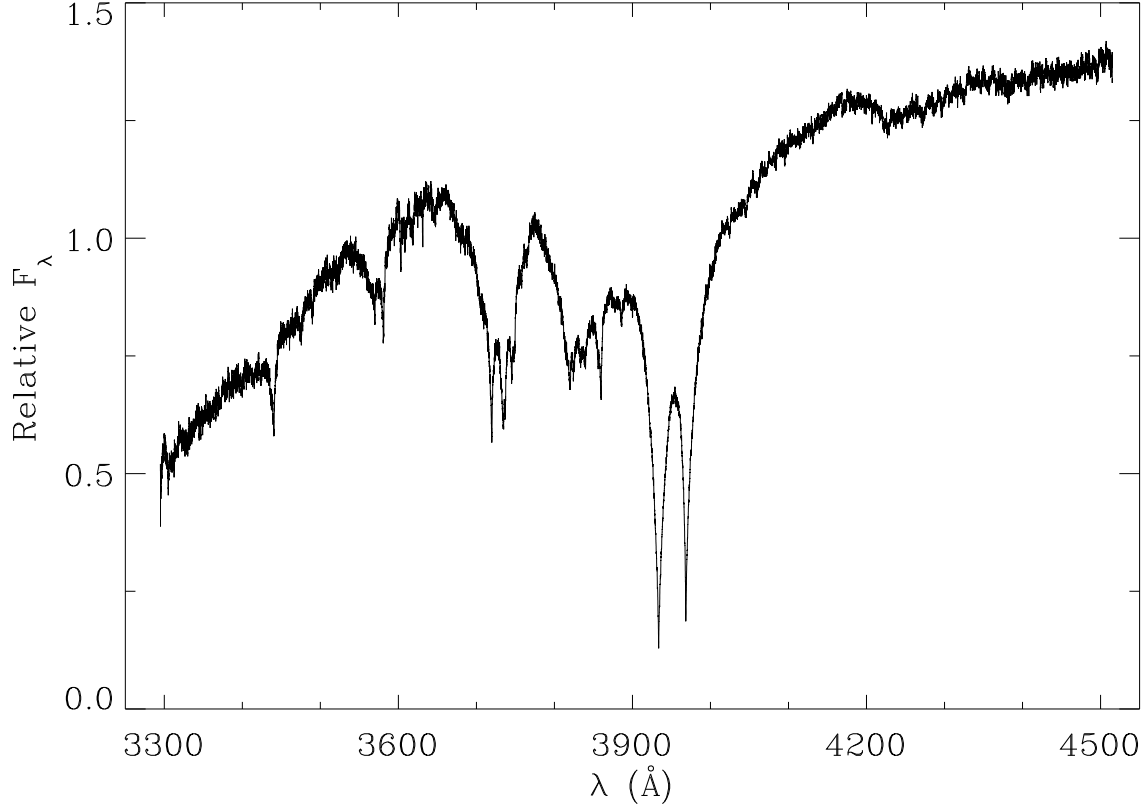


Fig. 3.— The prototype metal-lined white dwarf vMa2 (van Maanen’s star; van Maanen 1917). In contrast to hydrogen-rich atmospheres, metal absorption features in helium-rich stars can be quite prominent, and often dominate their optical spectra as in this case. Plotted is an unpublished spectrum taken with the UVES spectrograph on the Very Large Telescope for the SPY program (PI: R. Napiwotzki). All salient features are absorption due to iron, magnesium, or calcium.

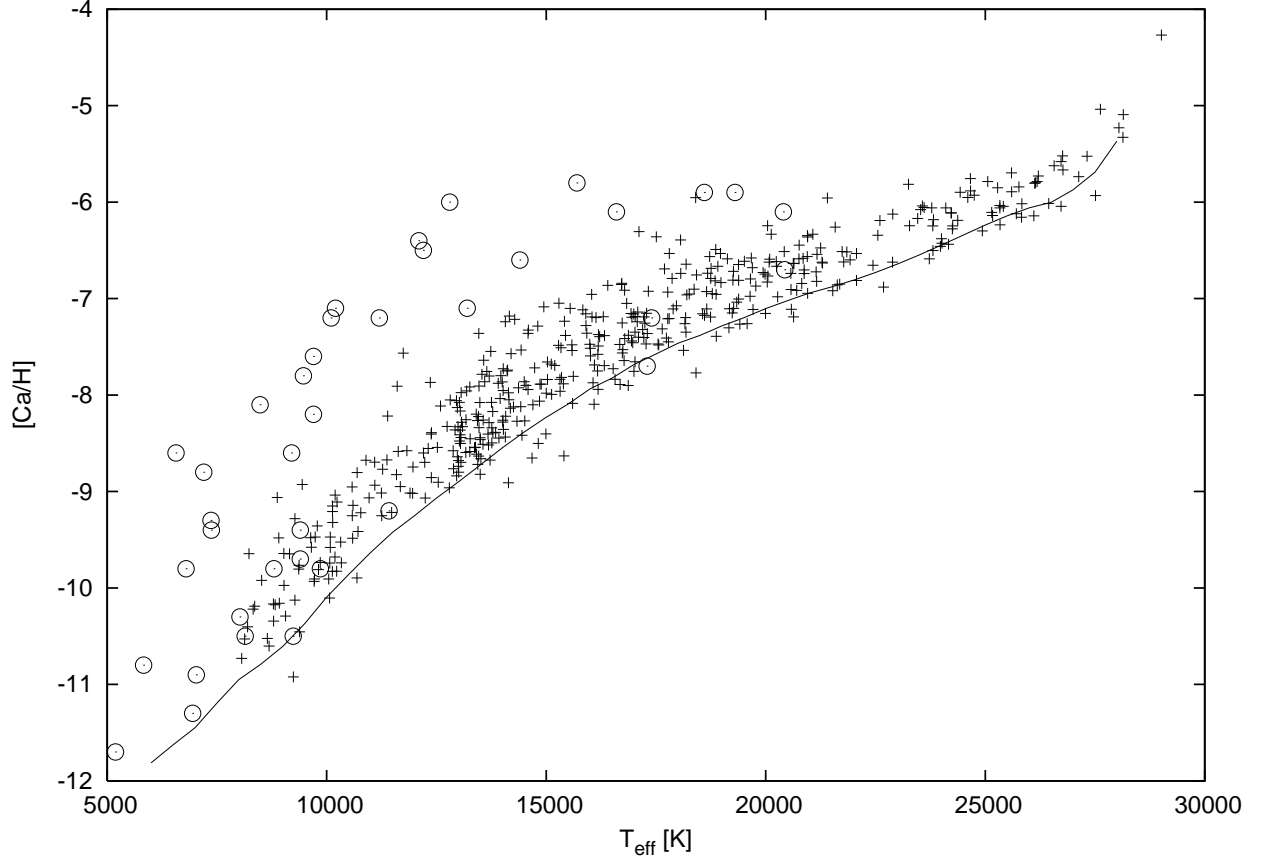


Fig. 4.— Calcium-to-hydrogen abundances (circles) and upper limits (plus symbols) for over 550 DA white dwarfs from the surveys of Koester et al. (2005b) and Zuckerman et al. (2003). The plot demonstrates the observational bias precluding the detection of modest metal abundances in warmer white dwarfs. The solid line represents an equivalent width detection limit of 15 mÅ (Koester & Wilken 2006).

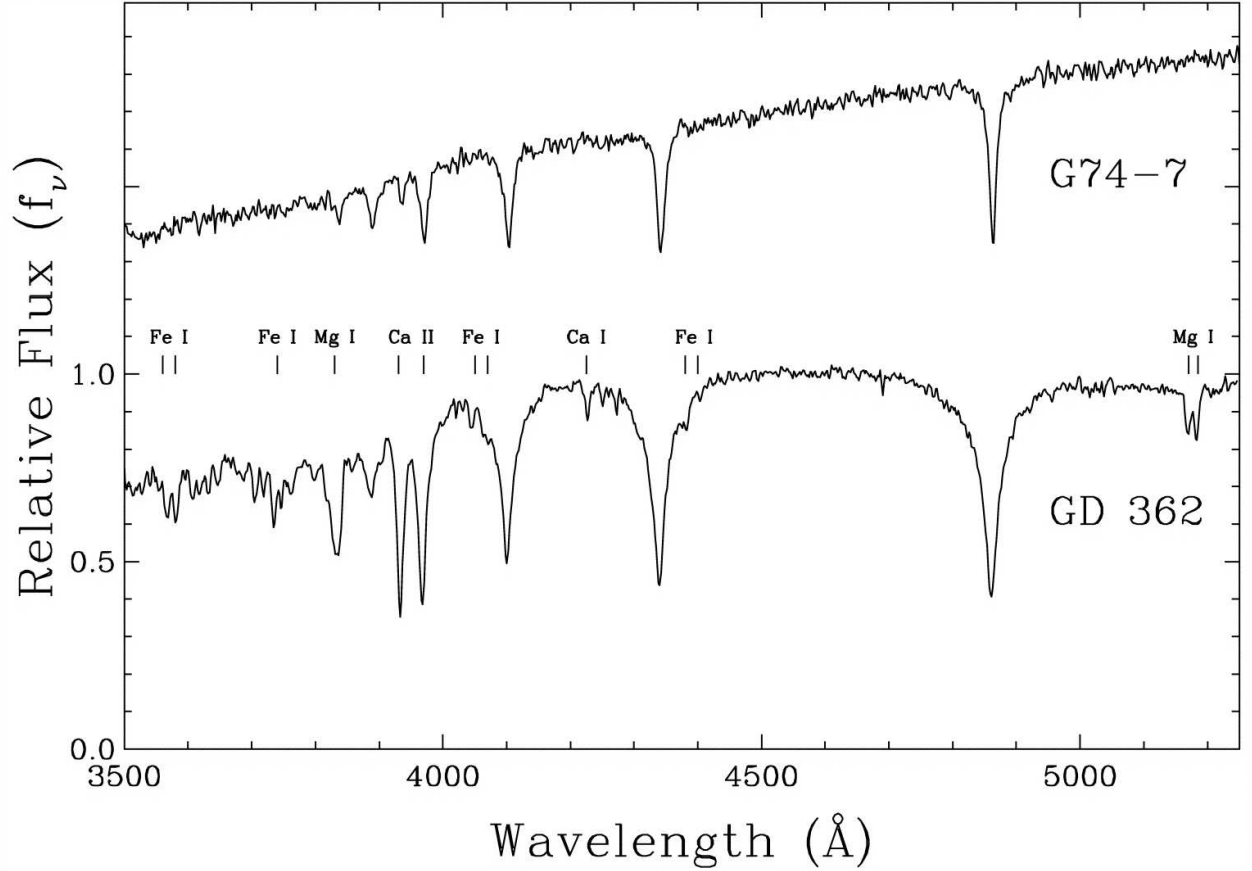


Fig. 5.— The highly metal-rich optical spectrum of GD 362 exhibits strong lines of calcium, magnesium, and iron in addition to hydrogen Balmer lines, thus appearing as a DAZ-type star (Gianninas et al. 2004). As it turns out, this spectacularly polluted star has an atmosphere dominated by helium rather than hydrogen (Zuckerman et al. 2007). Notably, the calcium H line is sufficiently strong that it overwhelms H ϵ . Shown for comparison is G74-7, the prototype DAZ white dwarf.

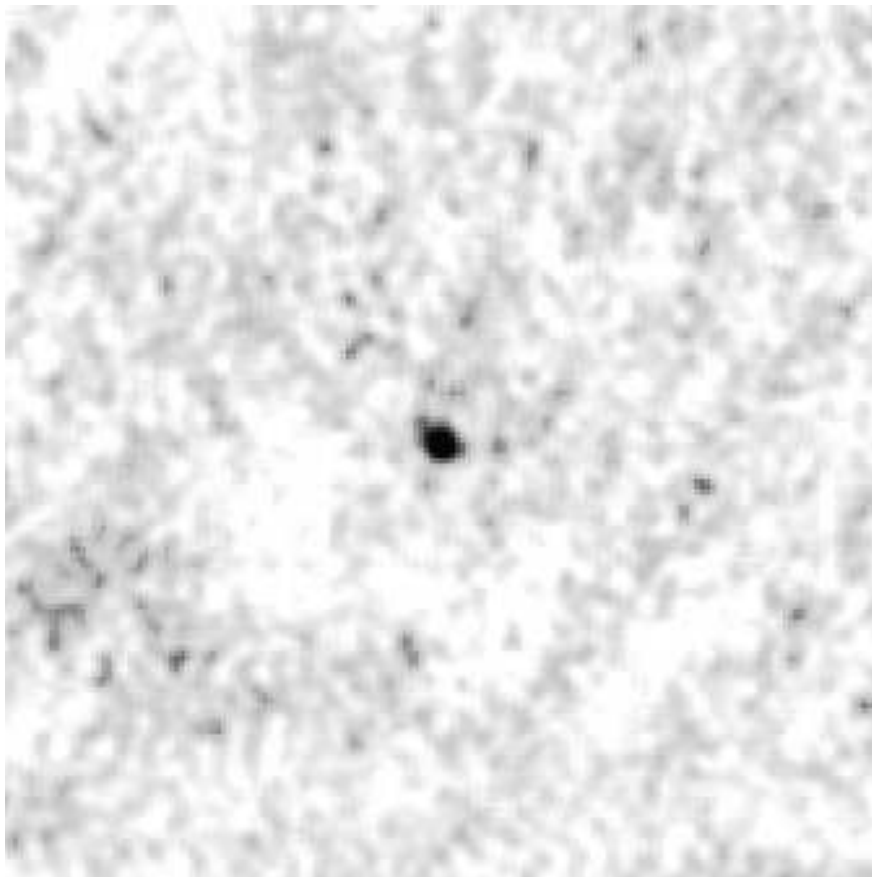


Fig. 6.— The N' -band ($11.3\,\mu\text{m}$) imaging discovery of unresolved infrared excess at GD 362, acquired with MICHELLE (Glasse et al. 1997) on Gemini North (Becklin et al. 2005). This image has been processed and is somewhat historic as it represents a remarkable ground-based detection of $1.4\,\text{mJy}$ (4.5σ), representing less than 1 hour on source. Contrast this with the multi-hour exposures necessary to detect the $11\,\text{mJy}$ flux from G29-38 at a similar wavelength with earlier instruments (Telesco et al. 1990; Tokunaga et al. 1990; Graham et al. 1990)

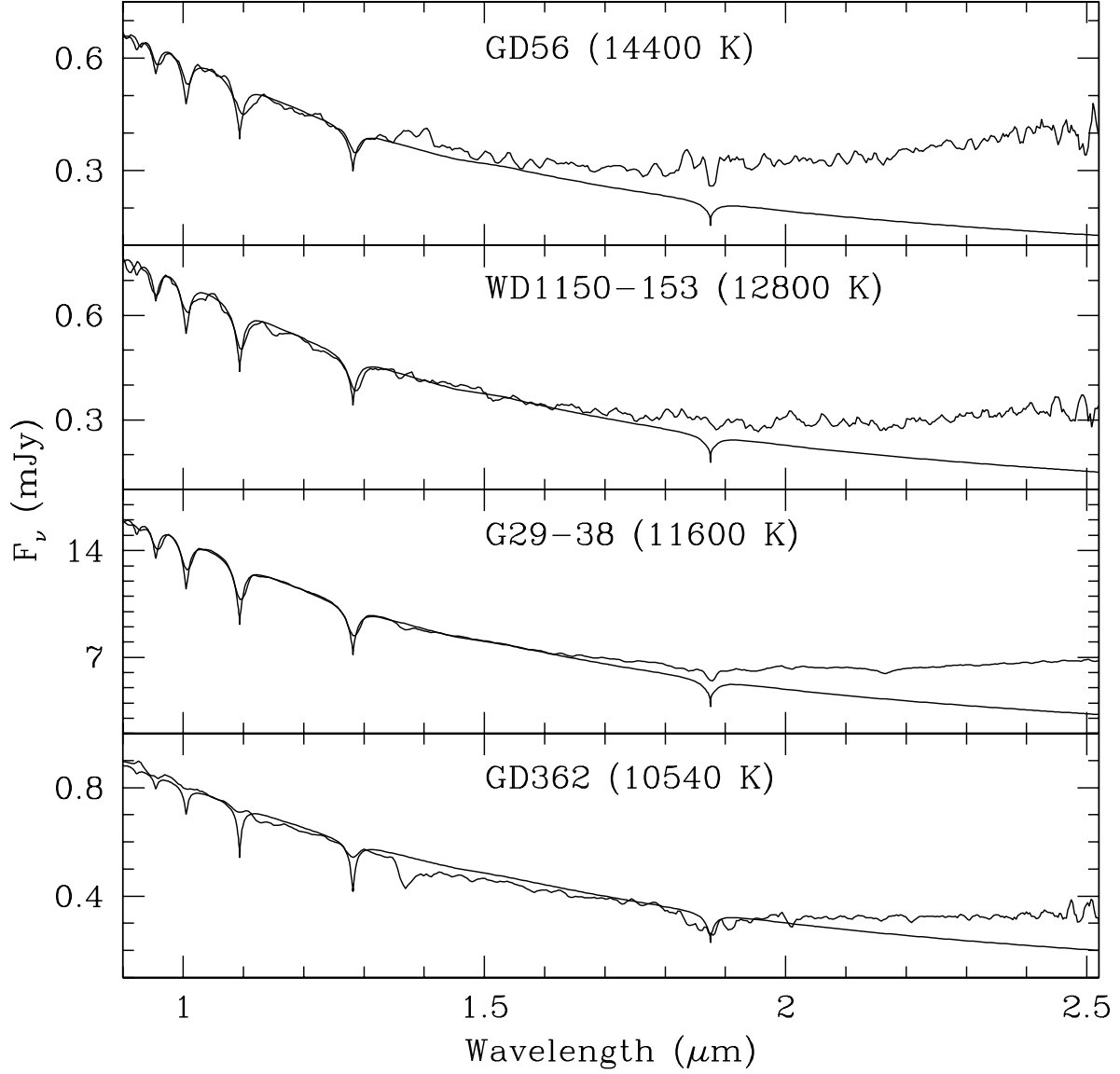


Fig. 7.— Low-resolution, near-infrared spectra of four metal-rich white dwarfs with circumstellar dust (Kilic & Redfield 2007; Kilic et al. 2006, 2005) taken with the SpeX spectrograph (Rayner et al. 2003) and plotted against model stellar atmospheres. Though the measured spectra vary somewhat in slope and strength, the inner dust temperature at all of these stars is likely to be essentially the same, as the excess emission is largely a function of the emitting solid angle as seen from Earth. The H -band excess at GD 56 is perhaps unique among white dwarfs with dust and may be due to a warp in the inner disk region.

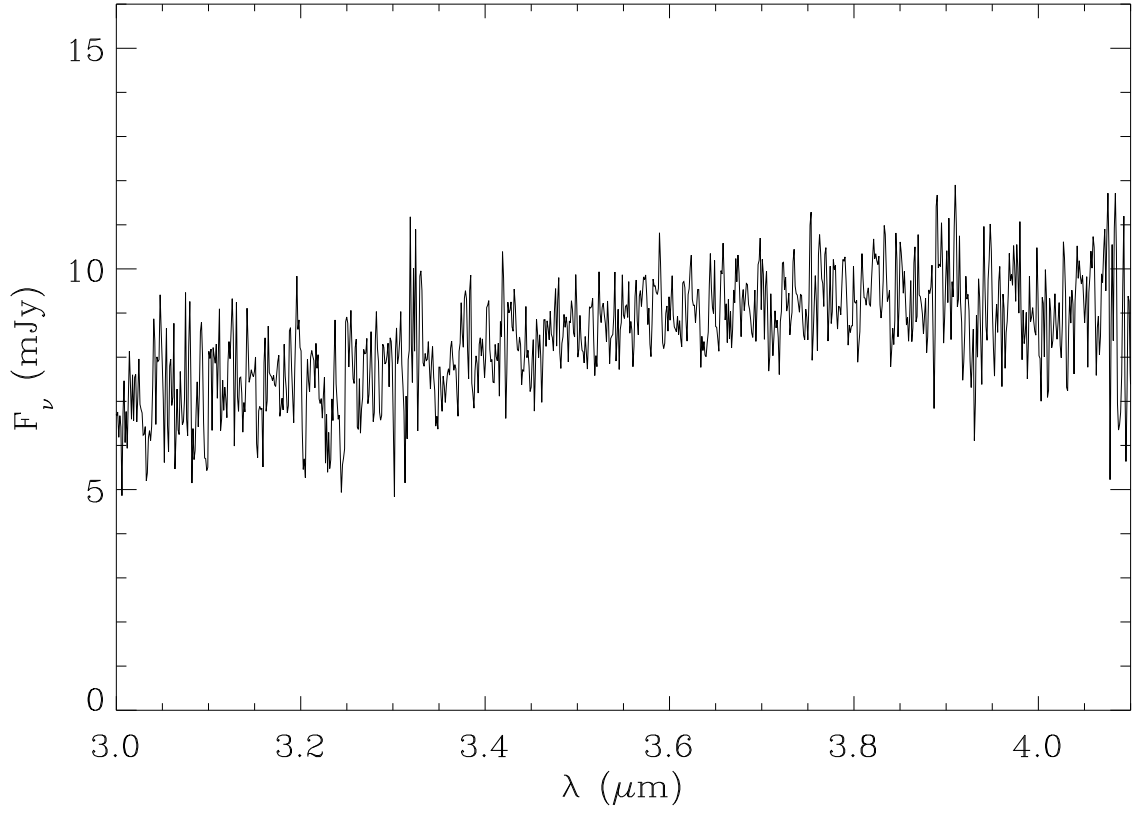


Fig. 8.— L' -band grism, $R \approx 500$ spectrum of G29-38 obtained using NIRI (Hodapp et al. 2003) on the Gemini North 8 m telescope in approximately 2 hr of exposure time. The S/N of the featureless spectrum is a strong function of wavelength due to varying atmospheric transparency, but is typically around 10 (Farihi et al. 2008b).

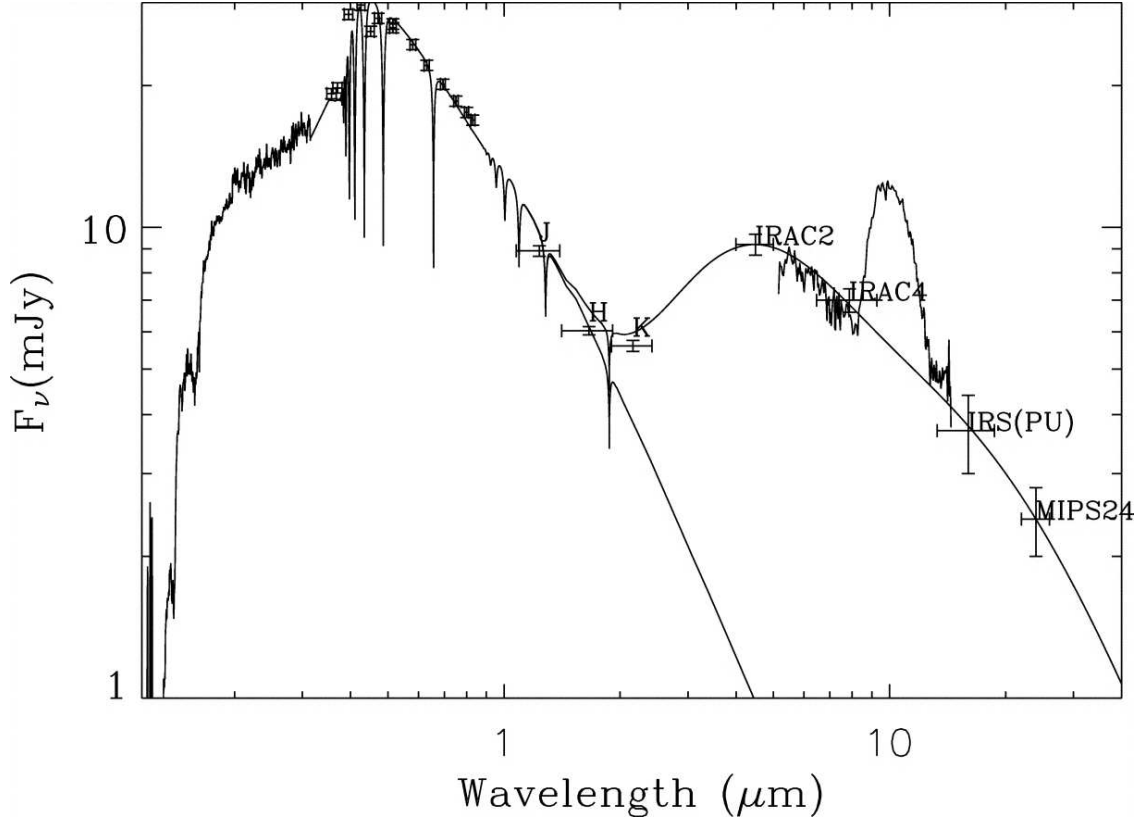


Fig. 9.— The ultraviolet through mid-infrared spectral energy distribution (SED) of G29-38, including *Spitzer* photometric and spectroscopic observations (Reach et al. 2005a). Photometric data are shown as error bars, while solid lines plot an *International Ultraviolet Explorer* (IUE) spectrum, a stellar atmosphere model from the ultraviolet through infrared, a model for the thermal continuum, and the measured mid-infrared spectrum. The *Spitzer* data reveal $T \approx 900$ K dust emission and a strong silicate emission feature at $9 - 11 \mu\text{m}$ consistent with micron-sized olivines (Reach et al. 2005a).

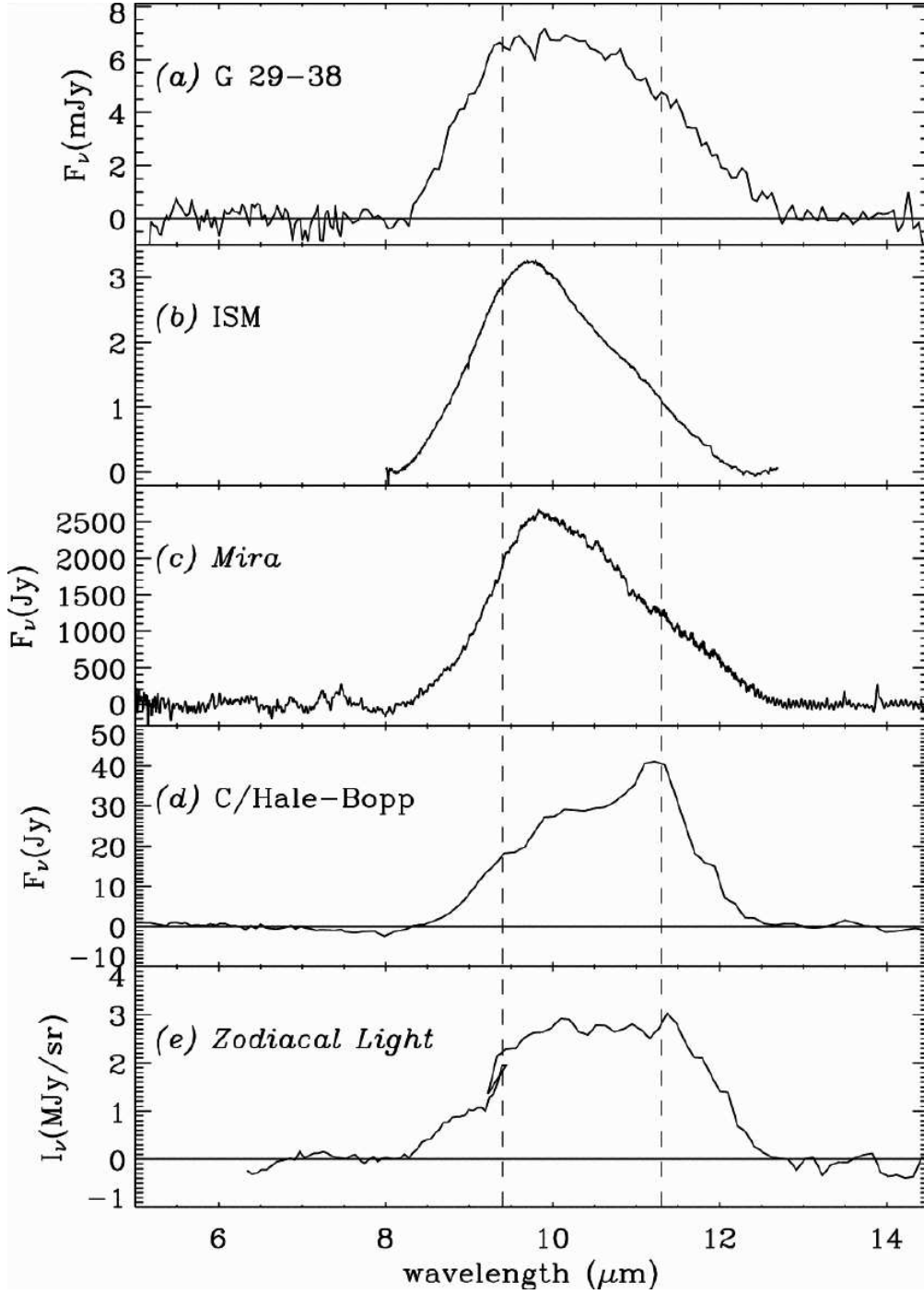


Fig. 10.— Comparison of the high S/N, continuum-subtracted, silicate emission feature observed at G29-38 compared to various astronomical silicates. The feature at G29-38 has a red wing distinct from interstellar silicates and most similar to the dust in the zodiacal cloud of the Solar System (Reach et al. 2005a).

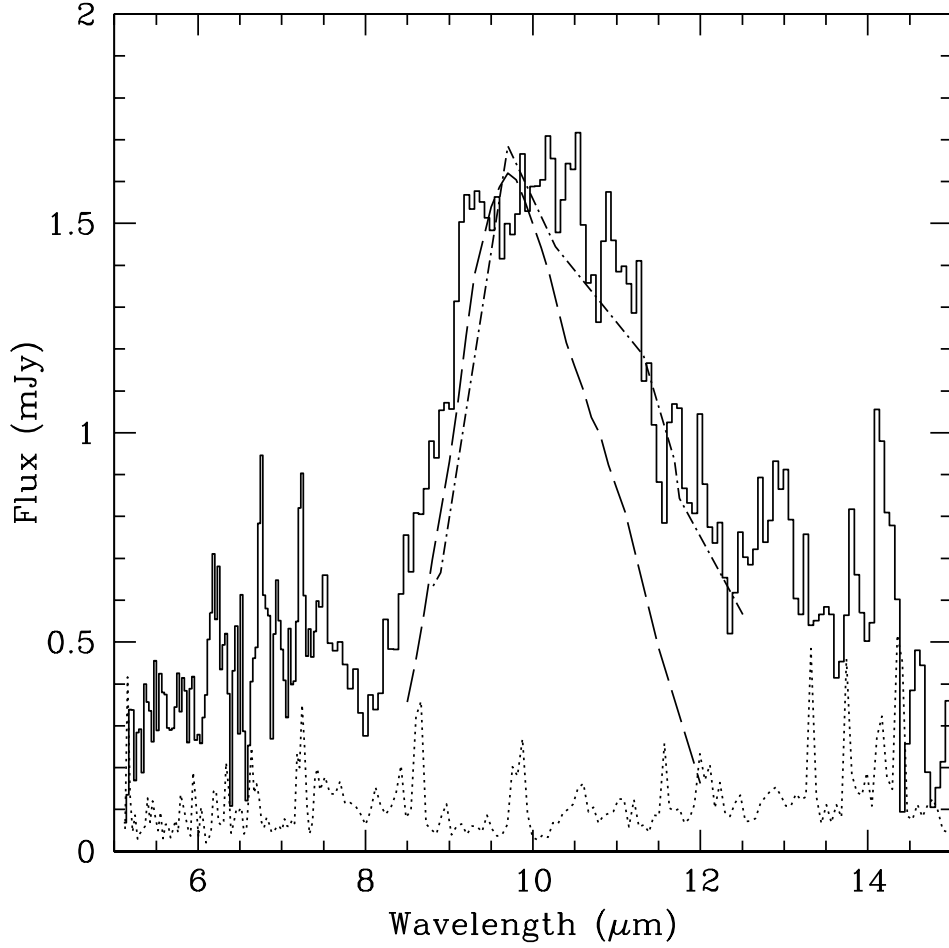


Fig. 11.— *Spitzer* IRS low-resolution spectrum of GD 362 revealing a very strong silicate feature with a red wing extending to nearly $12\,\mu\text{m}$ (Jura et al. 2007b). The solid line is the data while the dotted line represents the errors. Overplotted with dashed and dashed-dotted lines are the emission profiles of interstellar silicates and from planetesimal dust at the main-sequence star BD +20 307 (Song et al. 2005), respectively. The exceptionally strong emission feature at GD 362 reprocesses 1% of the stellar luminosity.

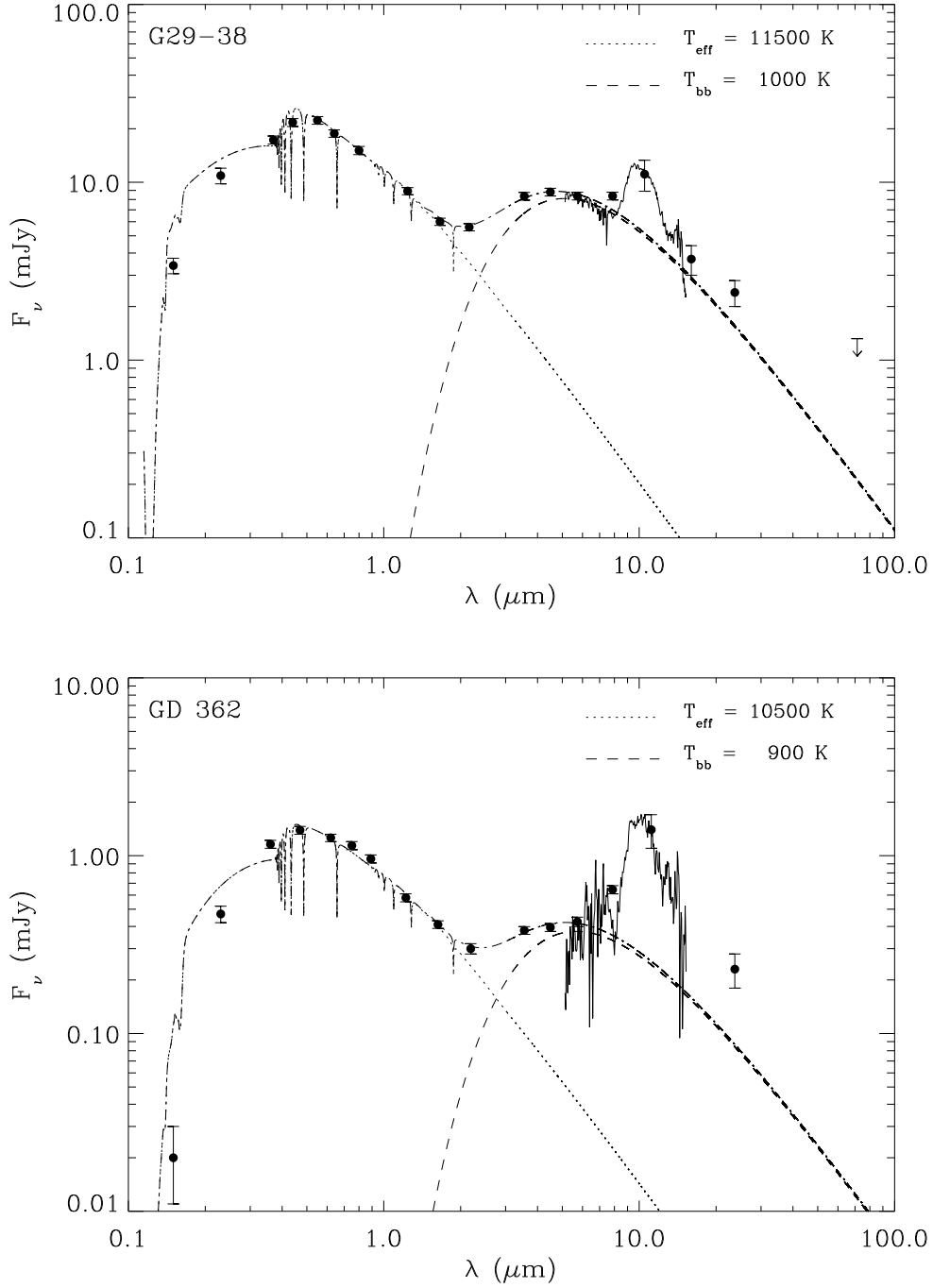


Fig. 12.— A side-by-side look at the full SEDs of G29-38 and GD 362. Available short wavelength data are shown together with *Spitzer* photometry and spectra (described in the text), plus 10 μm (*N*- or *N'*-band) photometry from the ground. Also shown is an upper limit to the flux of G29-38 at 70 μm from MIPS imaging. Stellar atmosphere models are plotted as dotted lines, while simple blackbodies fitted to the near-infrared continua are shown as dashed lines. The strength of the silicate emission at GD 362 is plain in this figure, and its 24 μm flux also appears strong relative to that at G29-38.

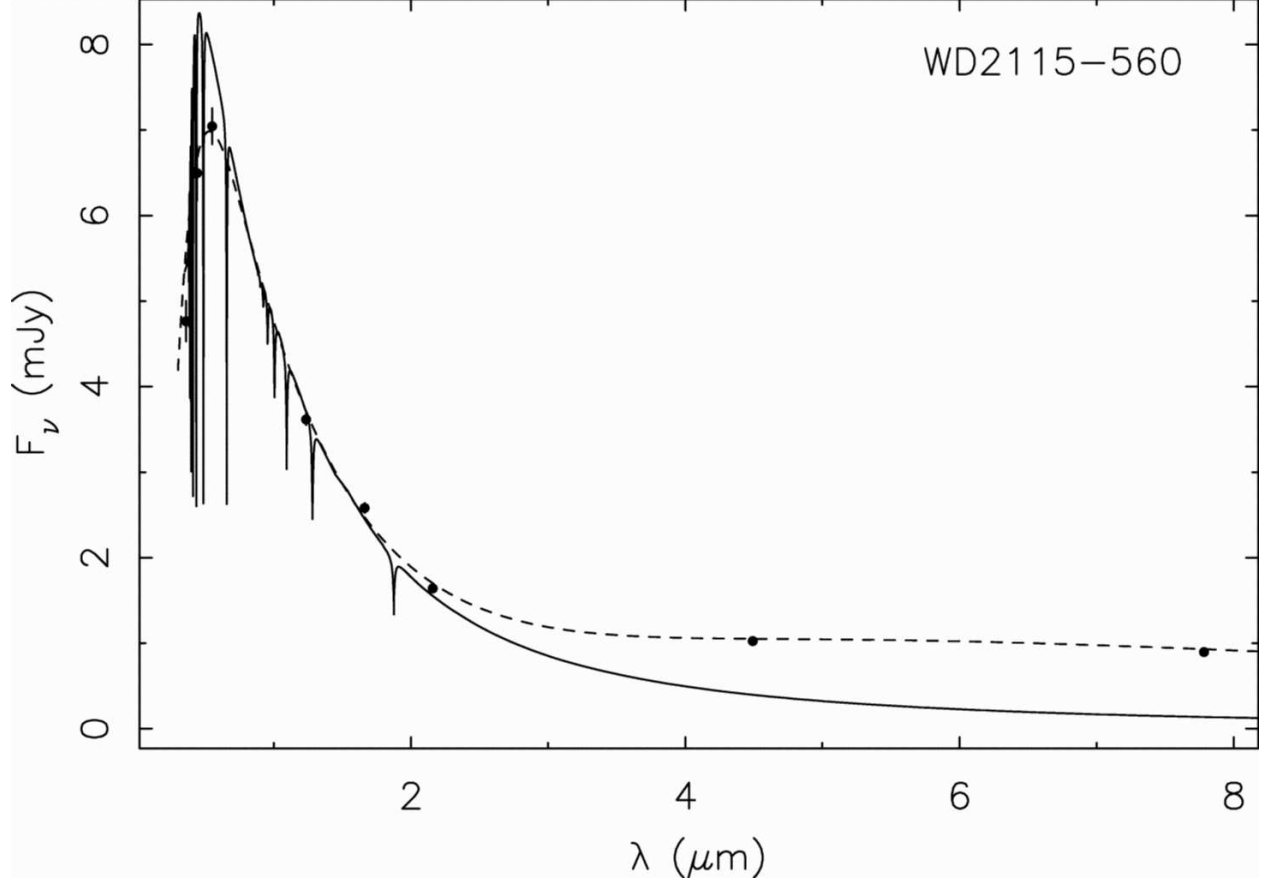


Fig. 13.— Infrared excess at the DAZ white dwarf LTT 8452 as measured by *Spitzer* IRAC. Short wavelength photometry from the literature and IRAC fluxes are shown as dots with (small) error bars. The solid line is a stellar atmosphere model, while the dashed line represents the addition of an optically thick, flat disk model for the circumstellar dust (von Hippel et al. 2007).

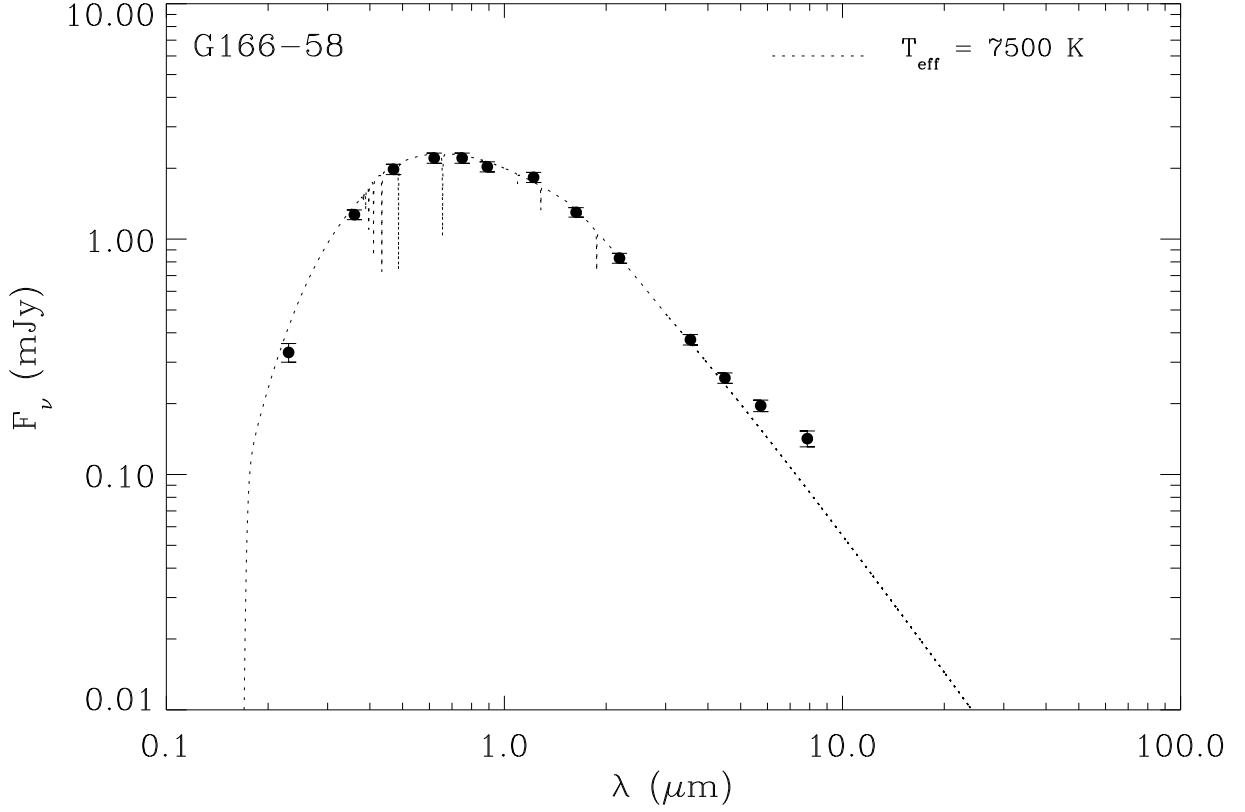


Fig. 14.— G166-58 was the first white dwarf found to have an infrared excess at mid- but not near-infrared wavelengths (Farihi et al. 2008b), and it remained anomalous among the first dozen disks found at white dwarfs over a period of several years. Available short wavelength data are shown together with IRAC photometry and a stellar atmosphere model. The warmest dust at G166-58 is only 400 – 500 K compared to 1000 – 1200 K in other circumstellar disks at white dwarfs.

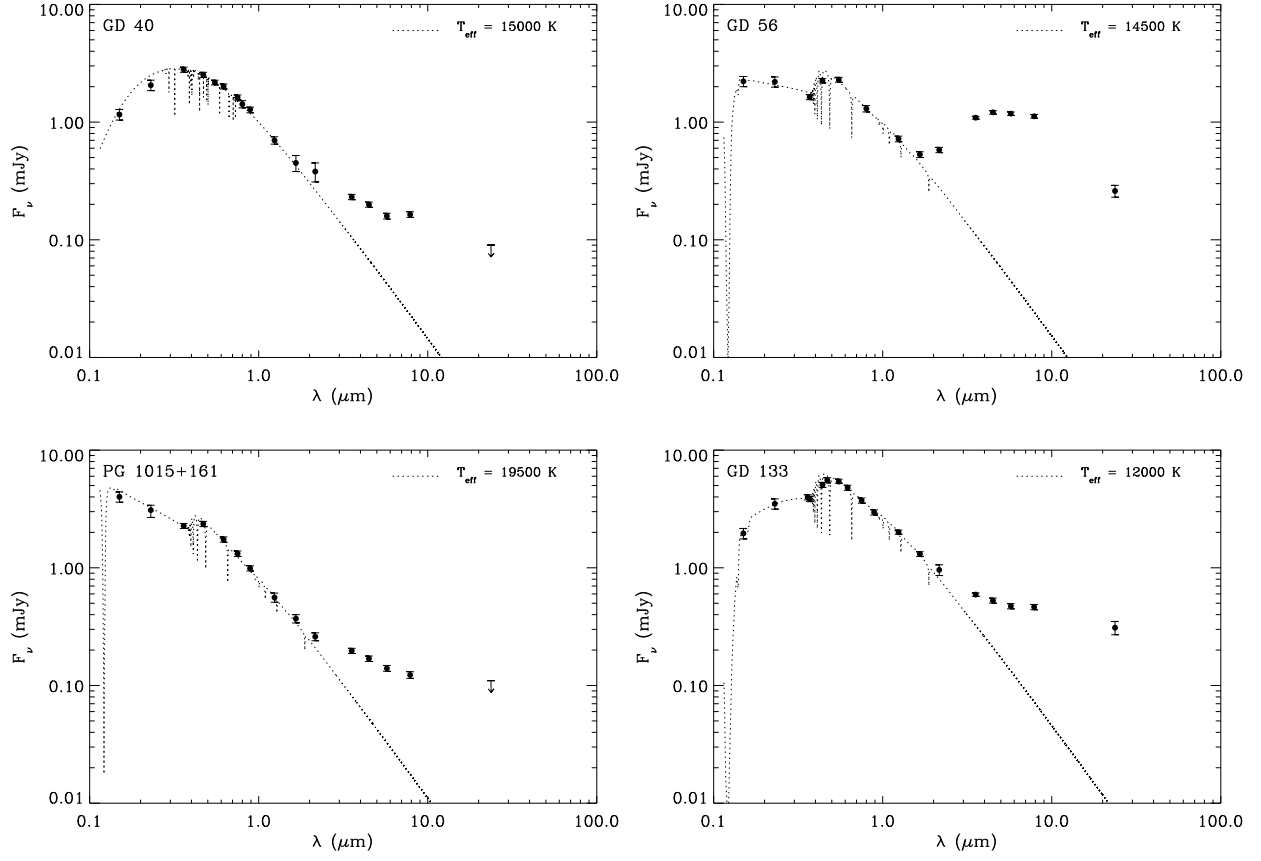


Fig. 15.— Infrared excesses detected at GD 40, GD 56, GD 133, and PG 1015+161 with *Spitzer* IRAC and MIPS. Short wavelength photometric data from the literature are shown together with appropriate stellar atmosphere models. The downward arrows are 3σ upper limits for non-detections.

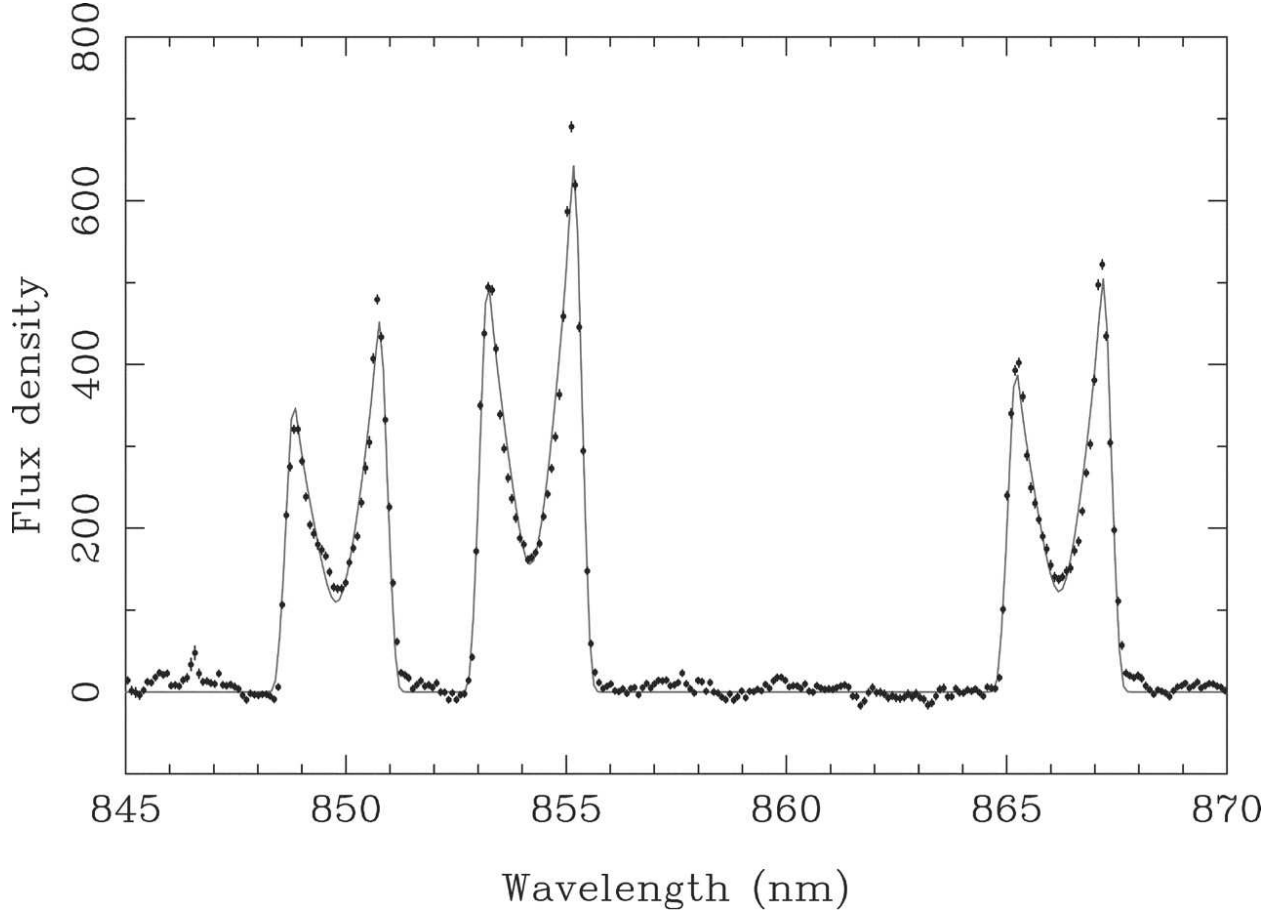


Fig. 16.— Calcium emission in the optical spectrum of SDSS 1228 measured taken at the William Herschel Telescope with the ISIS spectrograph (Gänsicke et al. 2006). The data are shown as points with (small) error bars while the model for the emission is shown as a solid line. The overall shape of the emission features is consistent with a high inclination (i.e. close to face on) and a gas disk radius no more than $1.2 R_{\odot}$ (Gänsicke et al. 2006). The asymmetry in the line profiles indicate a slightly elliptical orbit with $e = 0.02$.

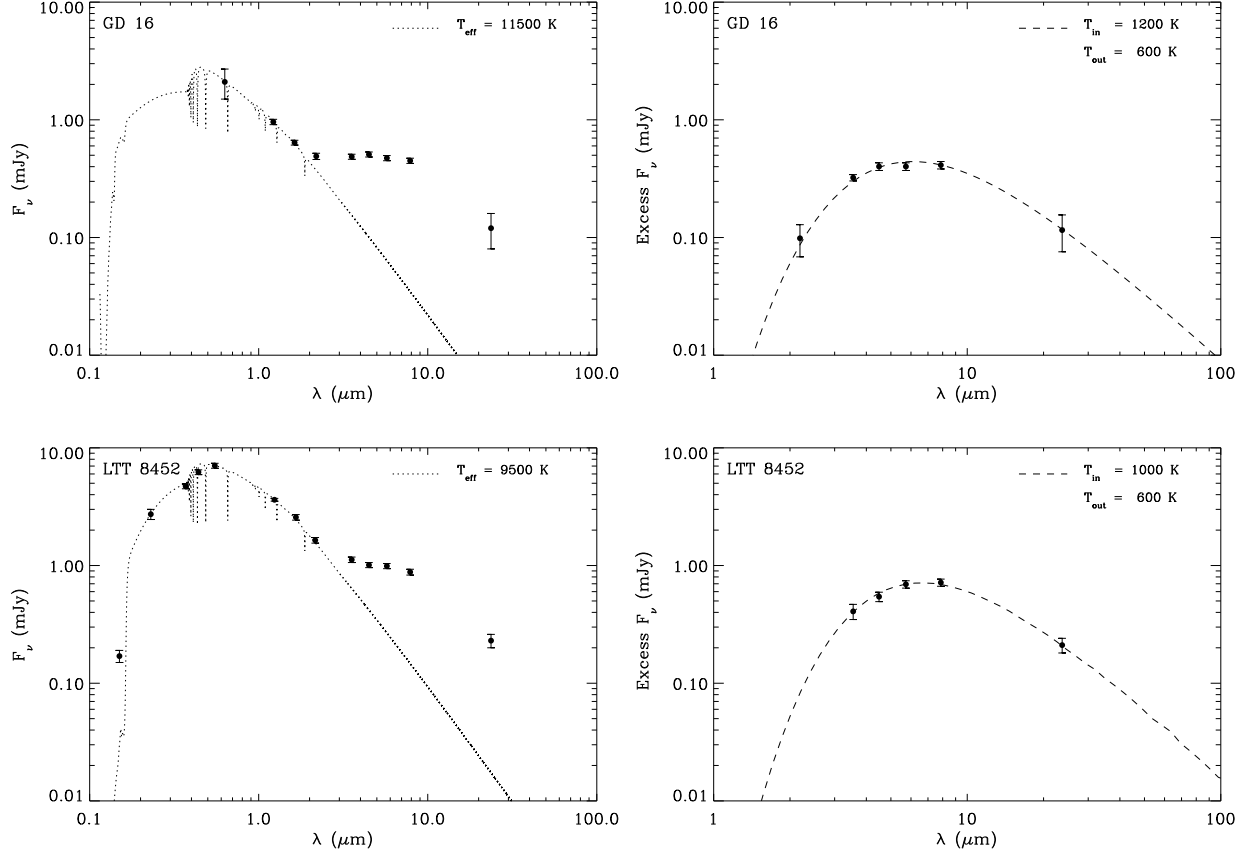


Fig. 17.— *Spitzer* IRAC and MIPS 3 – 24 μm photometry for GD 16 and LTT 8452. The left hand panels show available short wavelength photometry together with the *Spitzer* data and reveal strong infrared excesses compared to photospheric models. The right hand panels show the excess fluxes are well fitted by optically thick, flat disk models placing the warm dust within $0.5 R_\odot$ of the white dwarf (Farihi et al. 2009).

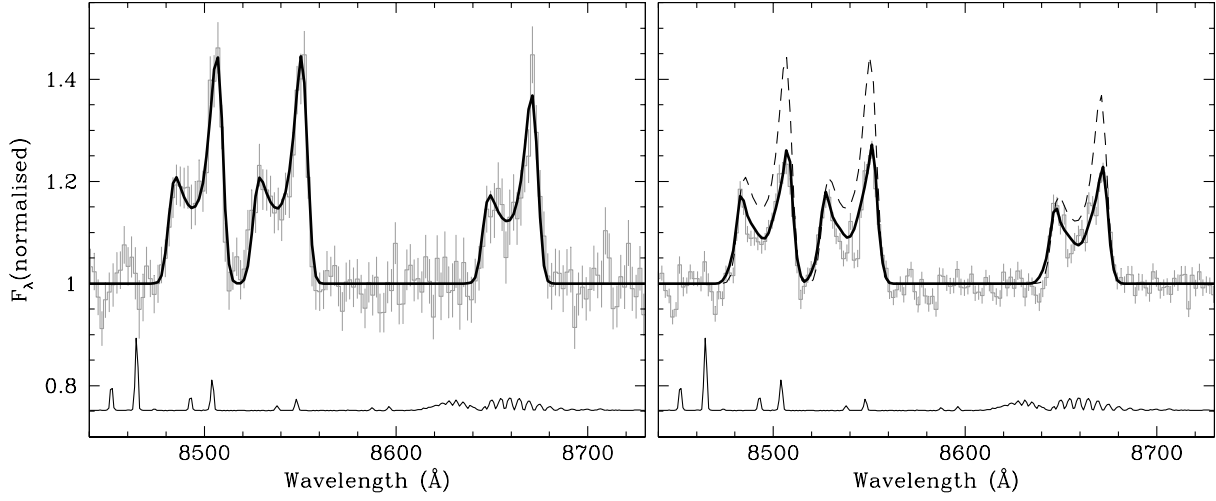


Fig. 18.— Varying, asymmetric line profiles of the calcium emission from Ton 345 (Gänsicke et al. 2008). The observed changes imply a shift in disk eccentricity from 0.4 (left panel, 2004 December) and 0.2 (right panel, 2008 January). Interestingly, no further changes to the line profile were observed in 2008 February and November (Melis et al. 2010).

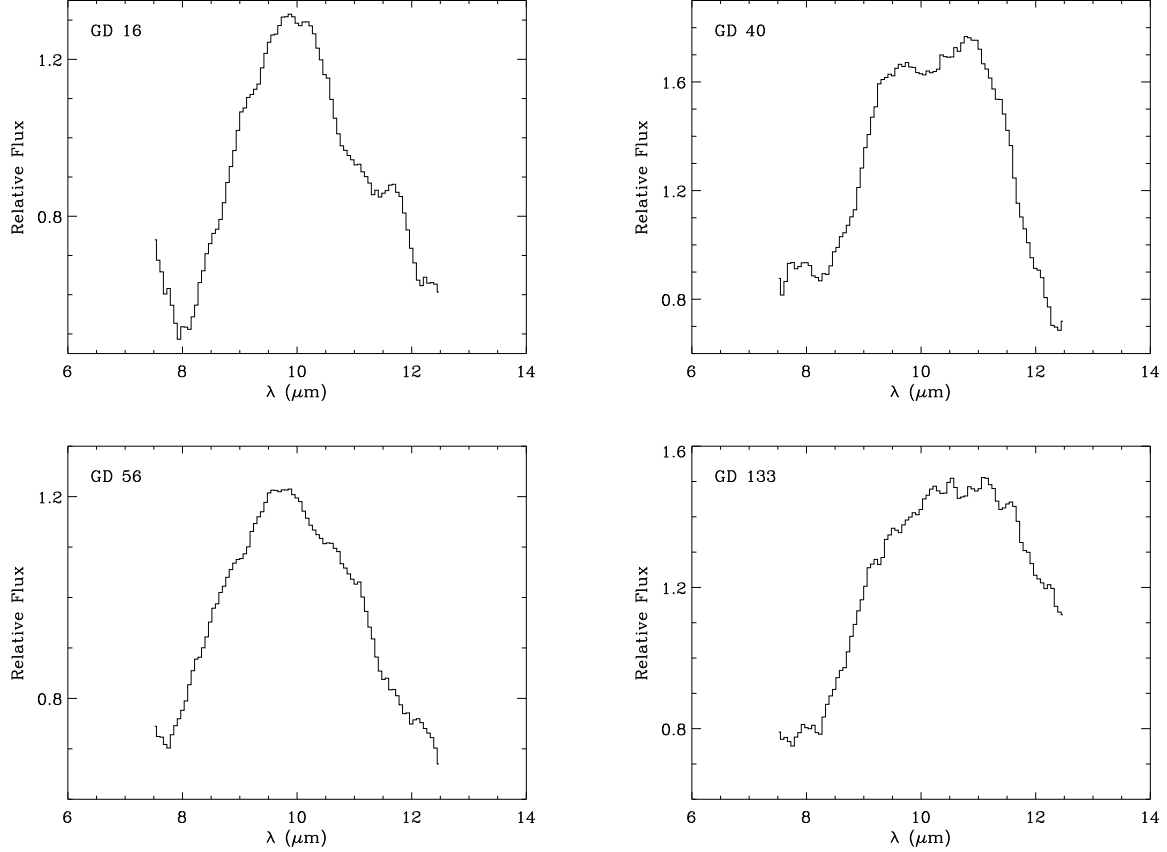


Fig. 19a.— Silicate emission features detected in all existing *Spitzer* IRS low-resolution observations of metal-rich white dwarfs with infrared excess. Each spectrum has been normalized to the average of the 5.7 and 7.9 μm IRAC fluxes, and smoothed by 15 pixels (0.8 μm). The binned data points are highly correlated and structures within the broad silicate feature are probably not real. The detections are modest in most cases, and the data below 8 μm are not shown as this region is typically noise-dominated. Despite the low S/N in most cases, the binned data clearly show the features are broad, with red wings extending to 12 μm and typical of minerals associated with planet formation (Jura et al. 2009a). Note the strength of the feature at GD 362 dwarfs all other detections.

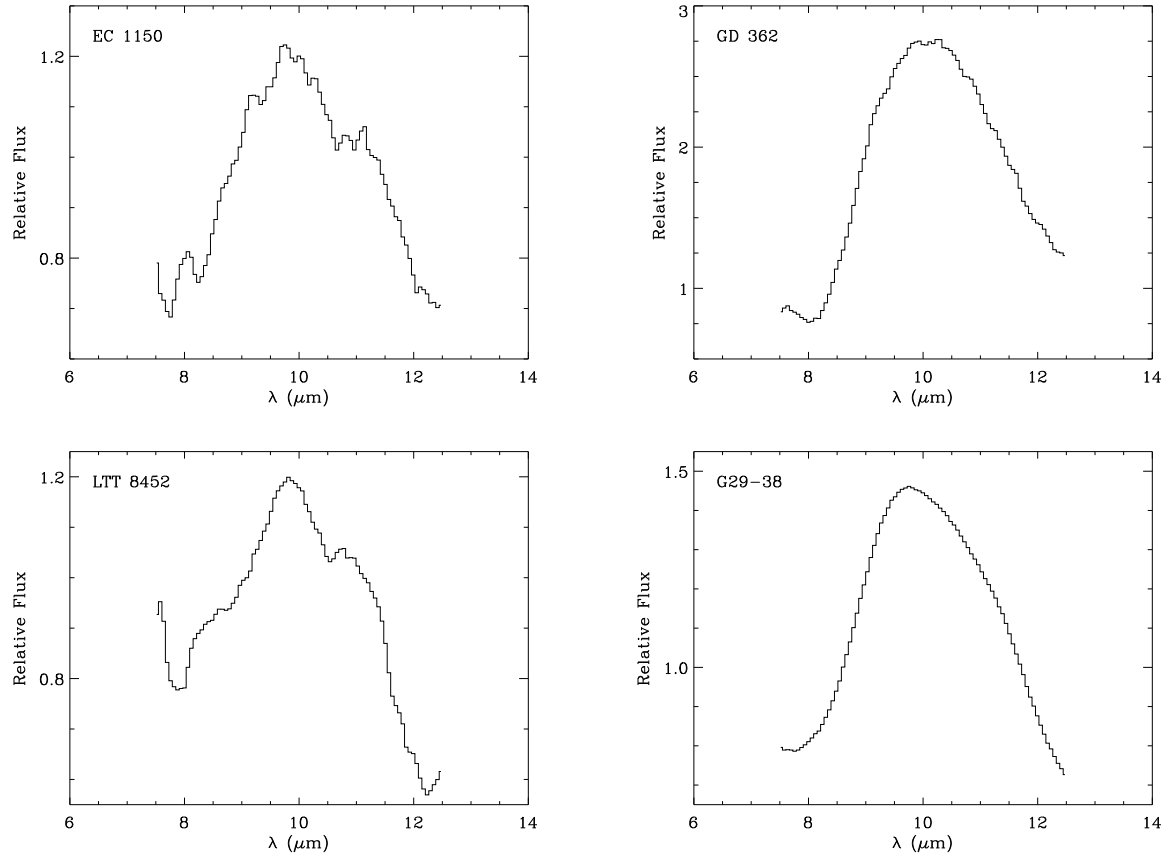


Fig. 19b.— *Continued*

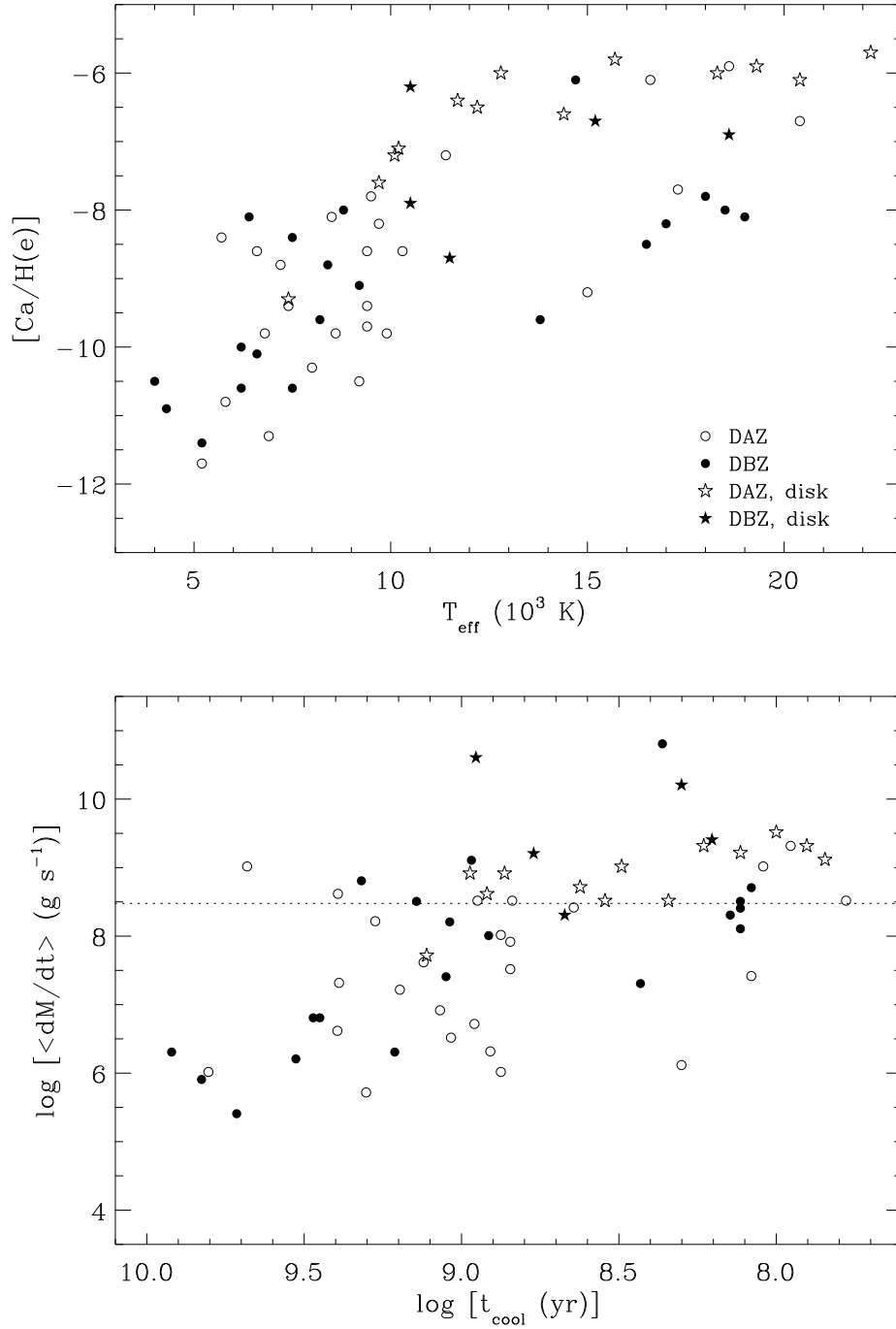


Fig. 20.— Dust disk frequency among all 61 metal-rich white dwarfs observed by *Spitzer* IRAC (Farihi et al. 2010c). The upper panel uses a purely observational approach plotting both disk detections and non-detections versus calcium abundance and effective temperature. The lower panel employs more physics by calculating the time-averaged metal accretion rate and cooling age for each star. The dotted line in the lower panel corresponds to $3 \times 10^8 \text{ g s}^{-1}$. G166-58 is the only star with a disk that is located significantly below this accretion rate benchmark, and with a cooling age beyond 1 Gyr.

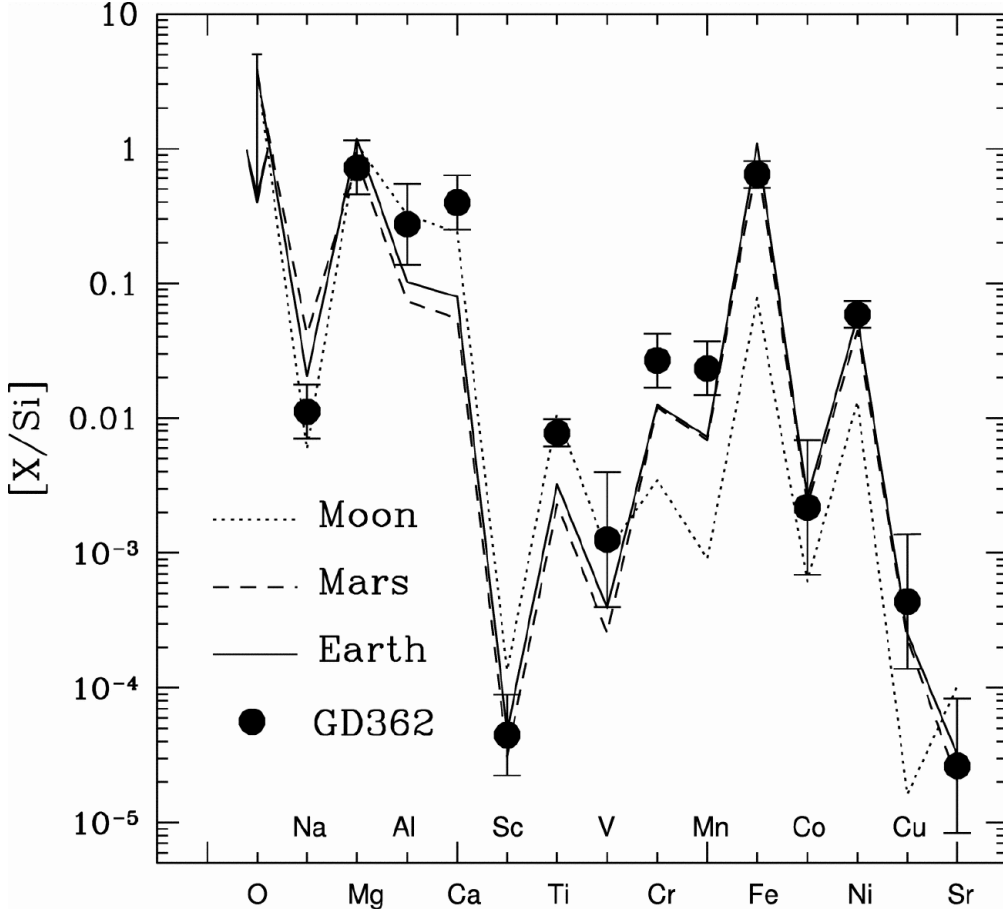


Fig. 21.— The remarkable heavy element abundances in the atmosphere of GD 362 (Zuckerman et al. 2007). Plotted are the measured abundances for 14 detected metals (and an upper limit for oxygen) relative to silicon, together with the bulk composition of the Earth, Moon, and Mars . The best overall fit is achieved with a combination of the Earth and Moon.

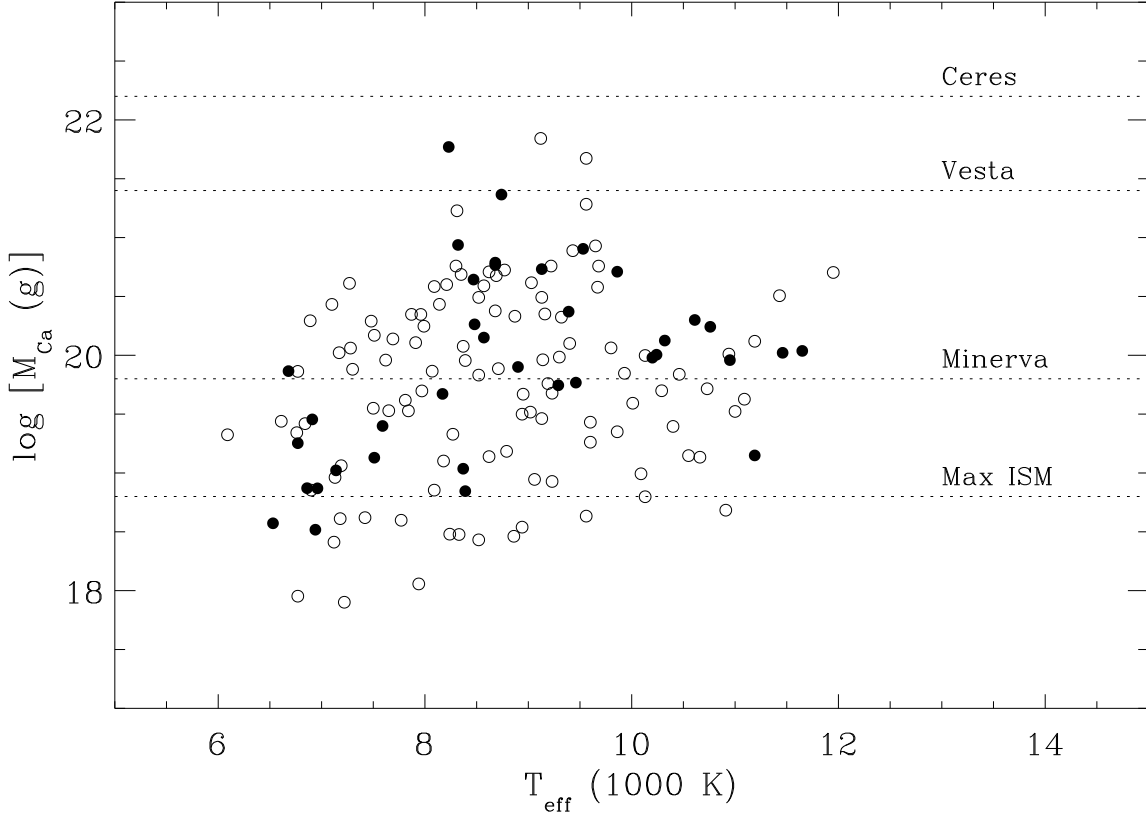


Fig. 22.— Calcium masses in the convective envelopes of 146 cool and metal-polluted white dwarfs with helium atmospheres from the SDSS (Farihi et al. 2010a). The open and filled circles represent stars with trace hydrogen abundance upper limits and detections, respectively. The top three dotted lines represent the mass of calcium contained in the two largest Solar System asteroids Ceres and Vesta, and the 150 km diameter asteroid Minerva, assuming calcium is 1.6% by mass as in the bulk Earth (Allègre et al. 1995). The dotted line at the bottom is the maximum mass of calcium that can be accreted from interstellar dust by a 50 km s^{-1} cool white dwarf in a $\rho = 1000 \text{ cm}^{-3}$ interstellar cloud over 10^6 yr (Farihi et al. 2010a).

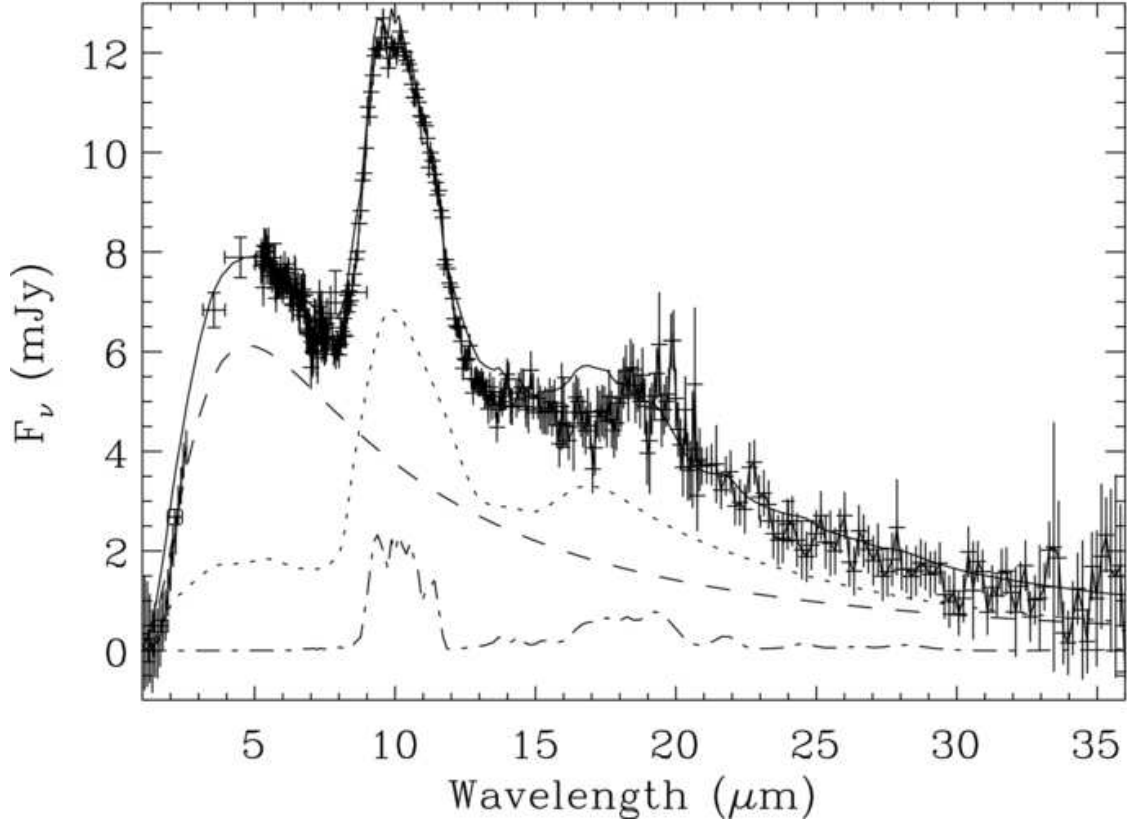


Fig. 23.— *Spitzer* IRS 5 – 35 μm spectrum of the circumstellar dust at G29-38 (Reach et al. 2009). Data are represented by crosses while the best fitting, flat disk plus optically thin layer, model is shown as a solid line. The dashed line is the contribution of the optically thick, flat disk, while the emission from silicates is shown as dotted (olivine) and dash-dotted (pyroxene) lines. Multiple model fits to the data produce equally good agreement (Reach et al. 2009) but the model shown here is the most physically plausible.

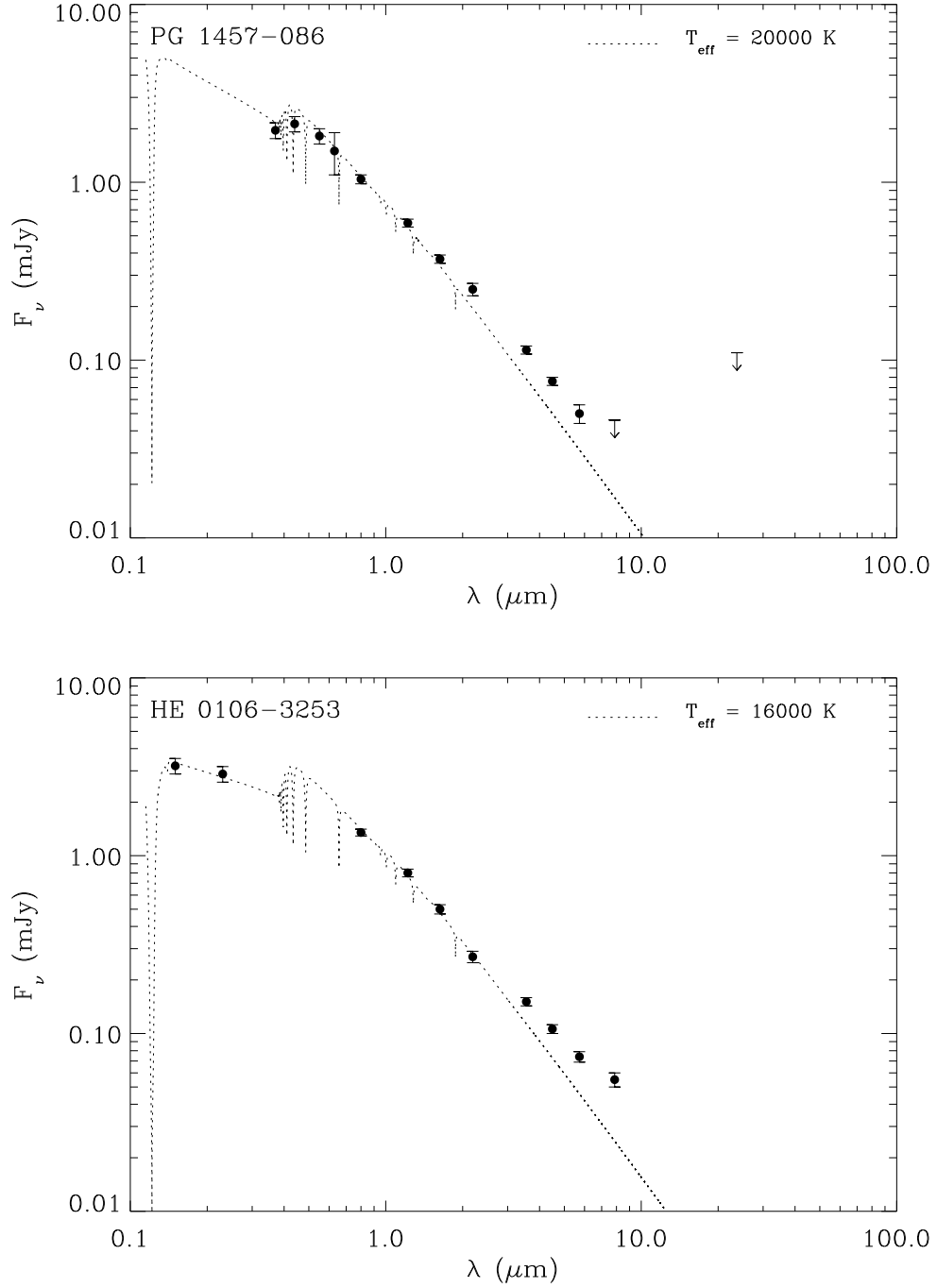


Fig. 24.— The two most subtle infrared excesses detected from narrow, circumstellar dust rings (Farihi et al. 2010c, 2009). In each case, dedicated near-infrared *JHK* photometry was instrumental in the recognition of the mid-infrared excess. Flat disk models predict radial widths $\Delta r < 0.1 R_\odot$ at modest inclinations, while for zero inclination (i.e. face-on) these rings shrink to only $0.01 R_\odot$ (Farihi et al. 2010c).

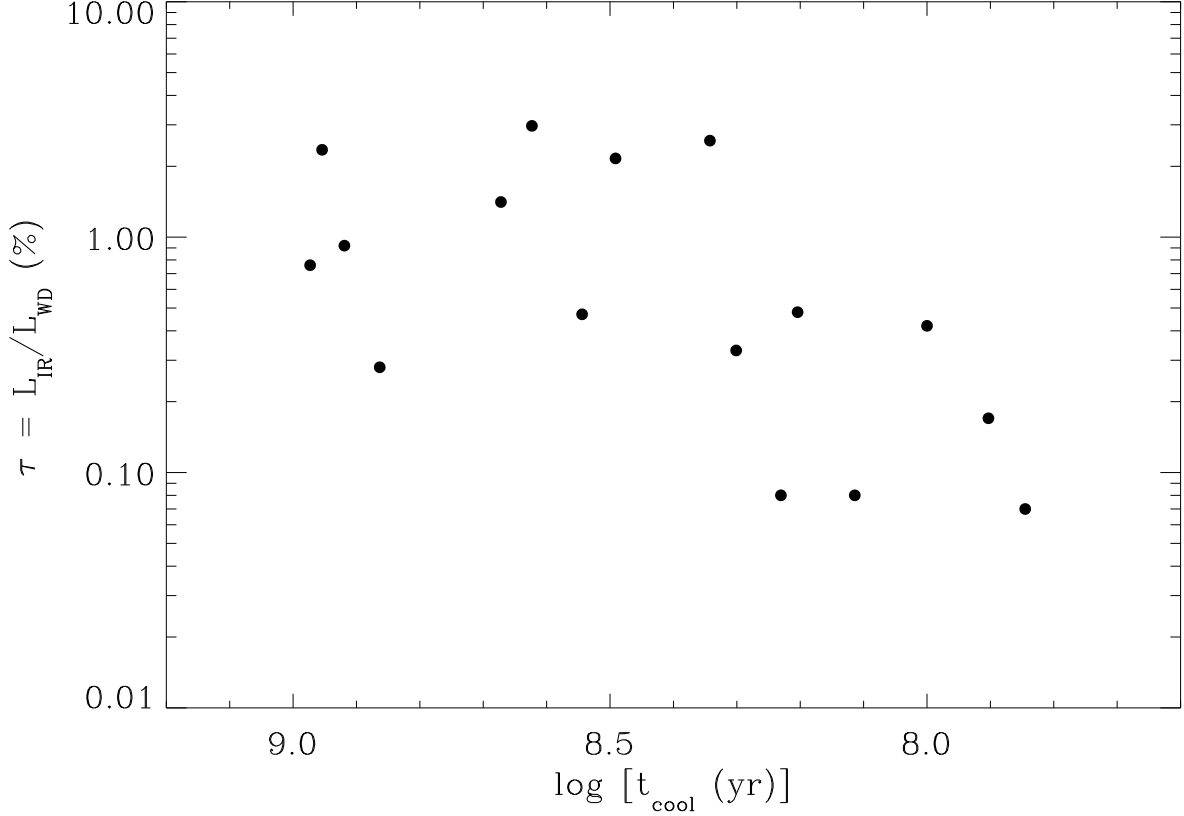


Fig. 25.— Fractional infrared luminosity from the thermal continuum (see Table 3 of circumstellar dust disks at white dwarfs plotted versus cooling age. There is insufficient data to confidently identify a trend, but it appears the narrowest rings are found at younger systems, while rings comparable to those at Saturn occur in more evolved systems. If the trend is real, possible explanations include viscous spreading over long timescales (Farihi et al. 2008b; von Hippel et al. 2007) or a decrease over time in the frequency of additional asteroid impacts during disk evolution (Jura 2008).

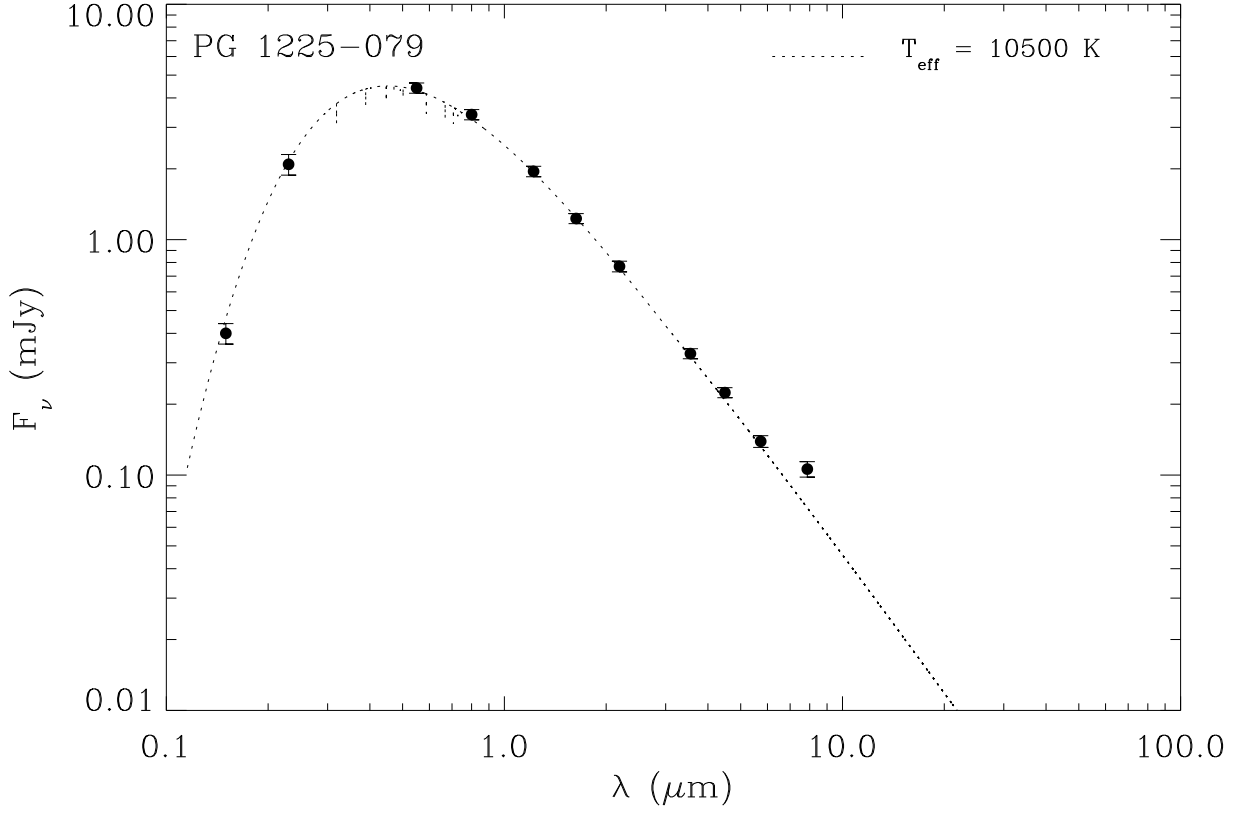


Fig. 26.— SED of PG 1225–079 with *Spitzer* IRAC flux measurements (Farihi et al. 2010c). All available photometric data are of sufficient quality to be confident of the measured excess at $7.9\,\mu\text{m}$, but without corroborating observations the single data point is somewhat uncertain.

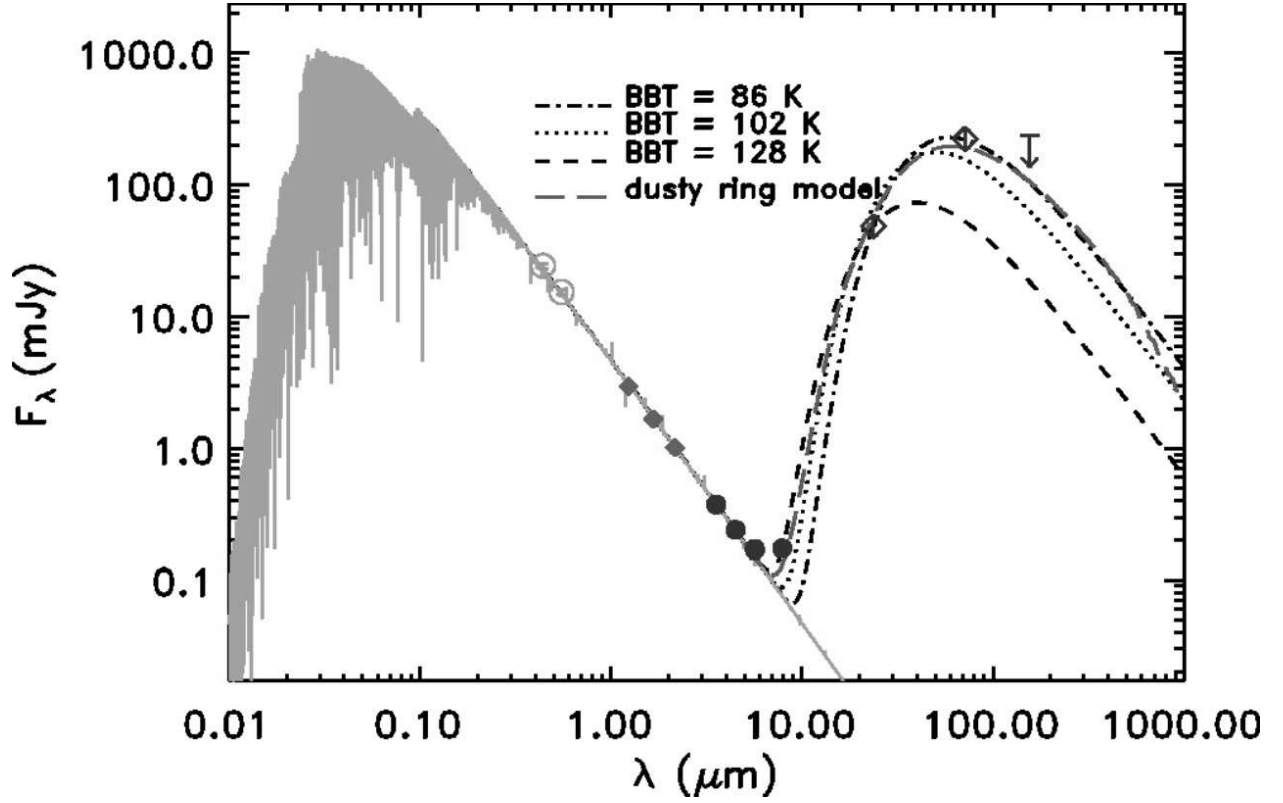


Fig. 27.— The strong infrared excess detected by *Spitzer* at the location of the central star in the Helix Nebula (Su et al. 2007). The combination of multiple, known emission sources within the nebula and the low spatial resolution of MIPS beam makes the interpretation of the excess ambiguous. A cold debris disk is one possibility but scenarios involving a companion star are perhaps more plausible (Bilikova et al. 2009).

Table 1. Metal-Rich White Dwarfs Observed by *Spitzer* IRS at $5 - 15 \mu\text{m}$

WD	Name	$F_{2.2\mu\text{m}}$ (μJy)	$F_{7.9\mu\text{m}}$ (μJy)	Raw S/N
0146+187	GD 16	0.49	0.45	3.4
0300–013	GD 40	0.38	0.16	4.7
0408–041	GD 56	0.58	1.12	8.0
1015+161	PG	0.26	0.12	...
1116+026	GD 133	0.96	0.46	6.0
1150–153	EC	0.37	0.61	3.7
1729+371	GD 362	0.30	0.64	6.8
2115–560	LTT 8452	1.64	0.88	5.5
2326+049	G29-38	5.59	8.37	22

Table 2. The First 18^a White Dwarfs with Circumstellar Dust Disks

WD	Name	SpT	T_{eff} (K)	d (pc)	K (mag)	Publication Year	Discovery Telescope	Reference
2326+049	G29-38	DAZ	11700	14	12.7	1987	IRTF	1
1729+371	GD 362	DBZ	10500	57	15.9	2005	IRTF/Gemini	2,3
0408−041	GD 56	DAZ	14400	72	15.1	2006	IRTF	4
1150−153	EC 11507−1519	DAZ	12800	76	15.8	2007	IRTF	5
2115−560	LTT 8452	DAZ	9700	22	14.0	2007	<i>Spitzer</i>	6
0300−013	GD 40	DBZ	15200	74	15.8	2007	<i>Spitzer</i>	7
1015+161	PG	DAZ	19300	91	16.0	2007	<i>Spitzer</i>	7
1116+026	GD 133	DAZ	12200	38	14.6	2007	<i>Spitzer</i>	7
1455+298	G166-58	DAZ	7400	29	14.7	2008	<i>Spitzer</i>	8
0146+187	GD 16	DBZ	11500	48	15.3	2009	<i>Spitzer</i>	9
1457−086	PG	DAZ	20400	110	16.0	2009	<i>Spitzer</i>	9
1226+109	SDSS 1228	DAZ	22200	142	16.4	2009	<i>Spitzer</i>	10
0106−328	HE 0106−3253	DAZ	15700	69	15.9	2010	<i>Spitzer</i>	11
0307+077	HS 0307+0746	DAZ	10200	77	16.3	2010	<i>Spitzer</i>	11
0842+231	Ton 345	DBZ	18600	120	15.9	2008	<i>AKARI</i>	11
1225−079	PG	DBZ	10500	34	14.8	2010	<i>Spitzer</i>	11
2221−165	HE 2221−1630	DAZ	10100	70	15.6	2010	<i>Spitzer</i>	11
1041+091	SDSS 1043	DAZ	18300	224	17.7	2010	CFHT/Gemini	12

^a1225−079 is listed tentatively as the 18th discovery

References. — (1) Zuckerman & Becklin 1987b (2) Becklin et al. 2005; (3) Kilic et al. 2005; (4) Kilic et al. 2006; (6) Kilic & Redfield 2007; (6) von Hippel et al. 2007; (7) Jura et al. 2007a; (8) Farihi et al. 2008b; (9) Farihi et al. 2009; (10) Brinkworth et al. 2009; (11) Farihi et al. 2010c; (12) Melis et al. 2010

Table 3. Thermal Continuum Excess at White Dwarfs with Dust

WD	Name	Stellar Model T_{WD} (K)	2 – 6 μm Blackbody ^a T_{IR} (K)	$\tau = L_{\text{IR}}/L_{\text{WD}}$
0106–328	HE 0106–3253	16 000	1400	0.0008
0146+187	GD 16	11 500	1000	0.0141
0300–013	GD 40	15 000	1200	0.0033
0408–041	GD 56	14 500	1000	0.0257
0307+077	HS 0307+0746	10 500	1200	0.0028
0842+231	Ton 345	18 500	1300	0.0048
1015+161	PG	19 500	1200	0.0017
1041+091	SDSS 1043	18 500	1500	0.0008
1116+026	GD 133	12 000	1000	0.0047
1150–153	EC 11507–1519	12 500	900	0.0216
1226+110	SDSS 1228	22 000	1000	0.0042
1225–079:	PG	10 500	300:	0.0005:
1455+298	G166-58	7500	500	0.0015
1457–086	PG	20 000	1800	0.0007
1729+371	GD 362	10 500	900	0.0235
2115–560	LTT 8452	9500	900	0.0092
2221–165	HE 2221–1630	10 100	1000	0.0076
2326+049	G29-38	11 500	1000	0.0297

Note. — Measured infrared excess from thermal continuum emission between 2 and 6 μm , as most stars lack spectroscopic data on any potential silicate emission in the 8 – 12 μm region.

^aThis single temperature is a zeroth order approximation of the true disk SED.